INTRODUCTION TO THE IONOSHPERE AND GEOMAGNETISM

OCT 1964

SEL-64-111

INTRODUCTION TO THE IONOSPHERE AND GEOMAGNETISM

by

H. Rishbeth and O. K. Garriott

October 1964

Technical Report No. 8

Prepared under
National Aeronautics and Space Administration
Grant NsG 30-60

Radioscience Laboratory
Stanford Electronics Laboratories
Stanford University Stanford, California

CONTENTS

TABLES

ILLUSTRATIONS

I. THE NEUTRAL ATMOSPHERE

1. Atmospheric Nomenclature

The scientific study of the upper atmosphere has become known as aeronomy. As generally happens in the study of a complex natural system, nomenclature has been developed to describe the different parts of the atmosphere (Chapman, 1950). The description may be based on chemical composition or on temperature or on the dominant physical processes. For each of these alternatives there exists a series of words terminating in "-sphere," each using some property to characterize the atmosphere within a certain range of altitude. The upper boundary of any "-sphere" may be denoted by a similar word ending in "-pause"; thus, the "tropopause" is the upper bound of the troposphere. Sometimes these levels can be defined to within a few kilometers, but in other cases, the "-pause" nomenclature is inappropriate because the divisions can only be specified within tens or hundreds of kilometers. Figure 1 contains all the "-sphere" terms that occur in this review.

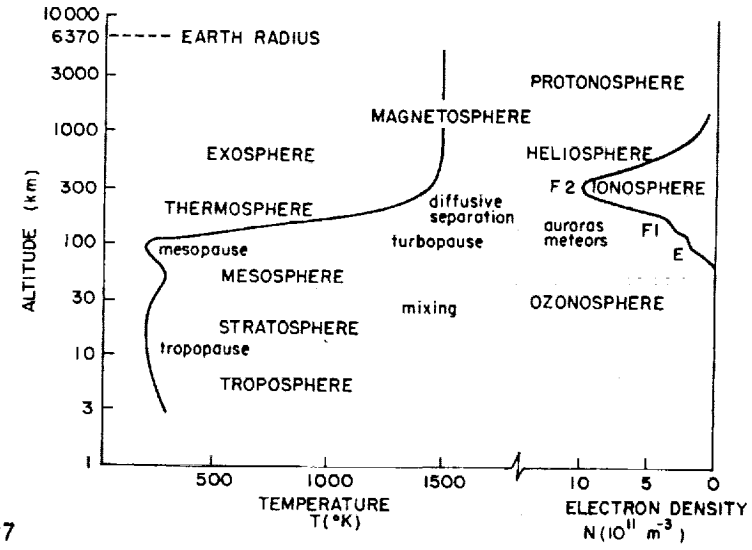

FIG. 1. REGIONS OF THE ATMOSPHERE, SHOWING CONVENTIONAL NAMES DESCRIPTIVE OF LEVELS, PHYSICAL REGIMES, AND CHARACTERISTIC CONSTITUENTS. The temperature profile is taken from the U.S. Standard Atmosphere and the electron density profile represents average daytime conditions for middle latitudes, high solar activity.

The lowest layer is the troposphere, in which the composition is uniform and the temperature generally decreases upward. The emission and absorption of infrared radiation by molecules such as water vapor, carbon dioxide and ozone provides the most efficient transfer of heat between different levels in this region. If we solve simplified equations for radiative transfer, we find that the equilibrium temperature in the lower atmosphere decreases approximately linearly with the partial pressure of these constituents. At low heights, this would lead to a "lapse rate" (negative temperature gradient) exceeding the "dry adiabatic lapse rate," which is about 10 °K/km. Such a situation is unstable and the lapse rate is maintained by turbulence and water vapor condensation at a somewhat smaller value, about 7 °K/km, throughout the troposphere. Under certain conditions, particularly at night, "inversions" may be set up in which the temperature gradient near the ground is positive.

Until the turn of the century, it was supposed that the temperature continues to decrease upward and that the atmosphere terminates at about 50 km, there merging into cold interplanetary space. However, experiments with kiteborne thermometers revealed a nearly isothermal region beginning at an altitude of about 11 km in mid-latitudes at a temperature of about 220 °K which has since been named the stratosphere. Its base, named the tropopause, is somewhat higher, and the stratospheric temperature is about 20 °K cooler at the equator than in the polar regions. Uniformity of temperature is maintained principally by radiation exchange in the infrared part of the spectrum between the minor constituents of the atmosphere.

The existence of a temperature inversion or positive temperature gradient above the stratosphere was suggested by observations of sound propagation over distances of 100 km or more, which seemed to result from the refraction of sound waves in the upper atmosphere. We now know that such an inversion results from the presence of a trace of ozone in the atmosphere. Although it is a very minor constituent, only contributing a few millionths of the total ground level pressure, the presence of ozone is very important. It absorbs all solar ultraviolet radiation of wavelength less than 2900 Å, and partially absorbs wavelengths between 2900 Å and 3600 Å. The atmosphere is heated by this absorption and the earth's

surface is shielded from the otherwise lethal radiation. This region of elevated temperature is known as the mesosphere. It does not seem to have a well-defined lower boundary (stratopause) but its upper boundary (mesopause) lies at 80 to 85 km, and is the coldest level in the entire atmosphere (about 180 °K). Heat flows toward this level by conduction, from above and below, and can only be removed by radiation which is primarily in the infrared, such as the 63μ line of atomic oxygen. The existence of the temperature minimum arises from the lack of any strong heating mechanism at this height. Ozone cannot exist in appreciable quantities at this level or higher, being rapidly destroyed by photochemical reactions.

The shorter UV radiations are absorbed at greater heights, in the thermosphere, and are responsible for the high temperatures existing there. Most of the heat liberated in the thermosphere is removed by downward conduction, so that the temperature increases upward. Finally, the heat conductivity becomes so good that the region of the upper thermosphere is maintained nearly isothermal at a relatively high temperature (about 1000 °K). In the exosphere, collisions between molecules are so infrequent that neutral particles move in ballistic orbits subject only to gravity, whereas the ionized particles are constrained by the magnetic field. No more will be said about this region now, since a later section (I-6) is devoted to it.

The foregoing description is closely linked to the vertical temperature profile, which is shown in Fig. 2. Parallel to this, a classification in terms of composition can be made. The term, ozonosphere, may be principally associated with the mesosphere, but is not too well defined because appreciable concentrations of ozone exist in the stratosphere. The vertical distribution of ozone extends, roughly, between 5 and 60 km. The peak of concentration lies at about 30 km, though on occasions two peaks have been detected, the lower at 10 - 15 km. The "median" of the ozone distribution is at about 25 km. The maximum rate of heat production occurs higher up, at about 45 km, near the level of unit optical depth for the incident solar radiation.

The ionosphere may be defined as the part of the earth's upper atmosphere where ions and electrons are present in quantities sufficient to

affect the propagation of radio waves. It extends down to perhaps 50 km and thus overlaps the ozonosphere. It has no well-defined upper boundary, but merges into (or may be extended to include) the heliosphere, where neutral and ionized helium are important constituents, and the protonosphere, which is composed principally of ionized hydrogen. The latter "-spheres" are still poorly defined in extent.

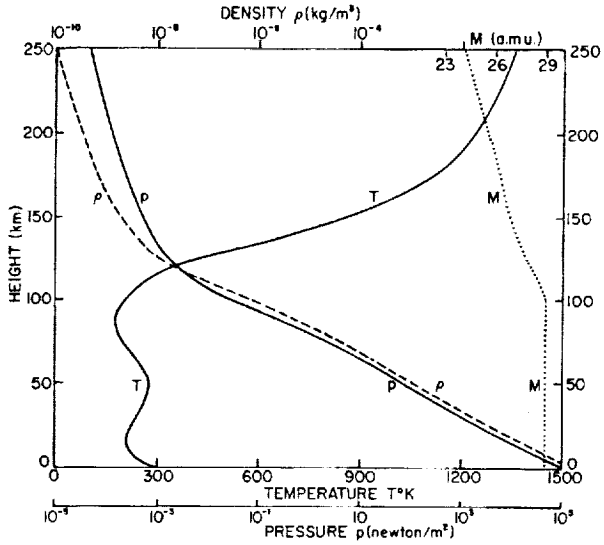

30952

FIG. 2. U.S. STANDARD ATMOSPHERE (Government Printing Office, Washington, D.C., 1962). Vertical distribution of pressure p, density ρ, temperature T and mean molecular mass M to 250 km. The composition is assumed constant up to 100 km.

The remaining terms used in Fig. 1 refer to the physical regimes at different levels in the atmosphere. Up to about 100 km, the atmosphere is well mixed by turbulence. The relative abundances of major constituents may be assumed independent of height, except at the highest heights. The abundances of chemically active constituents, such as ozone, are of course subject to variation, as are constituents such as water vapor and contaminants in the troposphere. In the lower thermosphere, the composition can be modified by photochemical reactions, such as dissociation of molecular gases.

The level at which turbulence ceases may be called the turbopause; it is rather sharply defined, and lies at about 100 km. Probably this depends on the increase of viscosity with height. At greater heights, the lack of turbulence enables a condition of diffusive separation to be established, in which the vertical distribution of each neutral gas depends on its molecular weight. The distribution of chemically active gases may however be influenced to some extent by photochemical reactions as well as by diffusion. This is especially true of the ionization, which attains a diffusely controlled distribution only at heights above 400 km.

Finally, there is the term magnetosphere, denoting the region in which the earth's magnetic field controls the dynamics of the atmosphere. It is difficult to define a lower limit since the movement of ionization is geomagnetically controlled at all heights above about 150 km (or even less), but the magnetosphere certainly includes the whole atmosphere above the level at which ionized constituents predominate over neutral, probably at about 1500 km. Because of this magnetic control, the earth's atmosphere may be said to terminate at the magnetopause, the boundary of the geomagnetic field which lies at 10 to 20 earth radii (see Sec. VII).

2. Evolution of the Earth's Atmosphere

It would be very surprising, indeed, if the atmosphere as we know it today had remained relatively unchanged in the several thousand million years in which our planet has been in existence. There has naturally been much study directed toward understanding the sequence of events which have combined to produce our nitrogen-oxygen environment and a variety of theories have been developed to explain it. The origin of the atmosphere must be closely linked to the development of the solid earth, but geologists are not in agreement concerning the earliest history of the planet. Most theories may be considered within a "molten globe hypothesis" or an "accretion hypothesis" (Chamberlin, 1949). In the former, the globe was originally molten and developed a crust as it cooled, while in the latter, the planet was accumulated by the gradual collection of small masses of solid material.

In either event, the relative abundance of the various elements in the solid earth and in the atmosphere may be compared with the "cosmic abundance" of the elements as estimated from meteorites and solar studies. When this comparison is made (cf. Kuiper, 1949), the lighter elements and particularly the rare gases of the earth are found to be less abundant by five to ten orders of magnitude. Oxygen is the first exception which appears with near normal cosmic abundance. This would suggest that any gases present early in our planet's history must have escaped and that in some way the oxygen was retained, perhaps in the rocks.

The present atmosphere may then be one primarily established by volcanic emissions. Water vapor and carbon dioxide are the main gases liberated while nitrogen concentrations are also important. Photosynthetic action by plants would seem to provide an adequate explanation for the conversion of CO_2 to oxygen (Chamberlin, 1949) accompanied by the deposition of carbon in plant material.

Berkner and Marshall (1963) argue very forcefully that the primordial atmosphere must have been one in which molecular oxygen was very scarce, at no more than 0.1 percent of its present atmospheric level. The oxygen produced by the photodissociation of water vapor would lead to production of O_3 (thereby shielding the water vapor from further dissociation) and would also react with surface materials to form oxides. Concentrations of O_2 substantially greater than 0.1 percent would appear to require the generation of oxygen from biological sources.

The work of Hoering and Abelson (1961) places the beginnings of photosynthesis at more than 2.7×10^9 years ago and from this point the equilibrium levels of oxygen abundance may have begun their slow increase. As a convincing illustration of the importance of photosynthesis and respiration to our present oxygen levels (Rabinowitch, 1951), it is found that all the carbon dioxide in the atmosphere is exchanged within about 400 years, all the oxygen in about 2000 years and all the waters in the oceans may have participated in the biological process within about two million years.

However, it was only in the much more recent Cambrian period (600 million years ago) that higher forms of life, leaving fossil remains,

came into existence. With oxygen levels at perhaps 1 percent of their present amount, it was possible for organisms to exist near the surface of the oceans without being destroyed by the intense ultraviolet radiation from the sun. Over the course of the next two hundred million years, Berkner and Marshall suggest that the oxygen content rose to about 10 percent of present levels, at which time the ozone shielding was adequate to permit oxygen-breathing organisms to live on land. They identify these two "critical levels" at which life could first exist near the water's surface and then on the land, with the interrelated rise of oxygen abundance and ultraviolet absorption by ozone. It is interesting to observe that current models of the Martian atmosphere, in which nitrogen and carbon dioxide are considered to be the principal constituents, may be characteristic of the earth's primitive atmosphere.

3. Structure of the Atmosphere

The distribution with height h of a neutral atmospheric gas may be assumed to be subject to the perfect gas law

$$\rho = nkT \qquad \text{(I-1)}$$

and the hydrostatic or barometric equation

$$-\frac{dp}{dh} = nmg \qquad \text{(I-2)}$$

The symbols p, ρ, and n are used to denote pressure, density, and concentration. If it is necessary to specify any particular gas, the chemical symbol is appended in square brackets, e.g., $n[N_2]$. T denotes absolute temperature and g the acceleration due to gravity. Molecular mass is denoted by M (in atomic units) and m (in conventional units) so that $\rho = nm$. The ratio M/m is denoted by N, which is 6×10^{23} per gram-mole (Avogadro's number), but takes the value 6×10^{26} per kilogram-mole in mks units. If R stands for the molar gas constant and k for Boltzmann's constant, then

$$\frac{R}{k} = \frac{M}{m} = N \qquad (I\text{-}3)$$

By combining these equations, we find that

$$-\frac{1}{p}\frac{dp}{dh} = \frac{Mg}{RT} \equiv \frac{1}{H} \qquad (I\text{-}4)$$

These equations provide two alternative definitions of the scale height H (more precisely, the pressure scale height). For each individual gas, these definitions are consistent at a level where diffusive separation exists and where the distribution is determined solely by the balance of the partial pressure gradient against gravity. They are also valid for a gas in a completely mixed atmosphere, in which processes such as turbulence are strong enough to cause each gas to conform to the scale height of the mixture as a whole. The masses M and m then refer not to the individual gas, but to the "composite" gas, air.

It is sometimes convenient to measure altitude in units of the scale height H, from some reference height h_o. The reduced height z, measured in this way, is defined by the equations

$$z \equiv \int_{h_o}^{h} \frac{dh}{H} = \frac{h - h_o}{H} \qquad (I\text{-}5)$$

The second equality applies if H is independent of height, but in any case, the vertical pressure distribution is given by $p/p_o = e^{-z}$. This relation is valid for the partial pressure of any constituent which obeys the hydrostatic equation, as well as for the whole atmosphere, provided that the proper scale height is used in the equation for z.

Also, we see that if the whole atmosphere above any arbitrary level z = 0 were compressed to a uniform pressure p_o, its vertical extent would be the scale height H_o at z = 0, wherever this level is chosen. The total number of particles above this level is $n_o H_o$, as can be deduced from the gas law and the definitions of H and z. Since $n = p/kT = p/mgH$, we have

$$\int_{h_o}^{\infty} n\, dh = \int_{0}^{\infty} nH\, dz = \frac{p_o}{mg} \int_{0}^{\infty} e^{-z}\, dz = n_o H_o \qquad (I\text{-}6)$$

We emphasize that these equations assume m and g to be independent of height, and thus apply to a single gas in hydrostatic equilibrium. In this case, gradients of H arise only from gradients of T, so that $dH/H = dT/T$. By taking logarithms and differentiating the gas law, we obtain the useful relations

$$-dz = -\frac{dh}{H} = \frac{dp}{p} = \frac{dn}{n} + \frac{dH}{H} \qquad (I\text{-}7)$$

Although many authors do not use the concept of reduced height, we shall find it useful in subsequent discussions. For example, let us examine the changes which occur when a column of air is heated. Each small volume of thickness δh will be called a "cell." If there is no horizontal flow of air, the weight of air above any cell does not change; therefore, the pressure within the cell remains constant and so does its reduced height z. If we assume that the column of air is initially at a uniform temperature T, and is then heated to a uniform temperature τT, the gas concentration with each cell is reduced from n to n/τ and its thickness expands to $\tau\delta h$. Since the scale height has increased from H to τH, the real altitude, h, measured from the ground $(z = 0)$ is increased in the same ratio: that is, from zH to $z\tau H$. If n_o is the initial concentration at $z = 0$, then the concentration at a distance h above $z = 0$ is $n_o e^{-z}$, or $n_o \exp(-h/H)$. After the heating, the vertical distribution is given by

$$n(h) = \left(\frac{n_o}{\tau}\right) \exp\left(-\frac{h}{\tau H}\right) \qquad (I\text{-}8)$$

H being the <u>original</u> scale height. For small values of h, this equation shows that the concentration n is <u>decreased</u> by the heating. But at greater heights n is increased because the reduction of the exponent in

the equation more than compensates for the factor $1/\tau$. At some intermediate level, therefore, n is unchanged, and for small changes of temperature ($\tau \approx 1$) this may be shown to be just one scale height above z = 0. This is known in meteorology as the isopycnic level. Obviously, the total integrated concentration throughout the atmosphere, $\int n\, dh$, is unaffected by the heating, in the absence of horizontal flow.

Although the above discussion relates to a case of an isothermal air column in contact with the ground, it can easily be generalized to apply to the diurnal temperature variations in the thermosphere. There are three important differences, which complicate the analysis but do not affect the principle of the discussion.

First, the part of the atmosphere subject to the heating does not extend to the ground, but is bounded by the temperature minimum (mesopause) at about 80 km. Secondly, the temperature in the thermosphere is not uniform but varies with height. Thirdly, the atmosphere at this height is subject to diffusive separation. Consequently, the hydrostatic equation must be solved for each constituent separately with the appropriate scale height being inserted for each. When the composition at the lower boundary of the heated region is kept constant, it is found that at any fixed pressure-level the relative concentrations of all the gases are unaffected by the heating (Garriott and Rishbeth, 1963).

In detailed calculations of atmospheric parameters, it must be remembered that the acceleration due to gravity decreases upward, in accordance with the inverse square law

$$g(h) = \frac{GM_E}{r^2} = g(0)\,\frac{r_E^2}{(r_E + h)^2} \qquad \text{(I-9)}$$

where G is the gravitational constant, M_E and r_E are the earth's mass and radius, $r = r_E + h$ is radial geocentric distance and $g(0)$ is the sea-level value of g. This variation may be included in the equation for the scale height, Eq. (I-4). Sometimes, a "geopotential height" is used, which may be defined in various ways. The simplest definition is that in

which the work done in raising unit mass to height h, e.g., $\int g(h)\, dh$, is equated to the geopotential height h^* multiplied by the sea-level value, $g(0)$. In addition, centrifugal force may become appreciable in problems involving the exosphere.

Various "standard" model atmospheres have been proposed. They present detailed distributions of pressure, density and temperature which are based upon observations and computed with the aid of the equations given above. At heights where the mean molecular weight is independent of height, knowledge of the vertical distribution of one of the basic parameters, plus boundary assumptions, enables the others to be computed from Eqs. (I-1) and (I-2). This is not true in the thermosphere above 200 km where the molecular weight varies with height. Here the best determined parameter is density, as determined from satellite drag data. But even if the complete density distribution $\rho(h)$ is available, further information is required in order to compute the temperature profile and gas concentrations. The calculations which have been published generally start from an assumed chemical composition at a lower boundary level (variously taken as 100 to 150 km). If diffusive separation is assumed to exist above this level, the variation of mean molecular weight with reduced height, z, can be found at once by applying the equation $p/p_o = e^{-z}$ to the partial pressure of each individual gas. But conversion of reduced height z to real height h involves knowledge of the temperature profile $T(h)$. In some published models, this is found by a trial-and-error fitting of the model to the observed density profile $\rho(h)$ (e.g., Yonezawa, 1960) or by detailed solution of the heat-conduction equations (e.g., Nicolet, 1959). In the very detailed models of Harris and Priester (1962a,b), the time-varying conduction equations are solved for the temperature distribution $T(h,t)$, for different heat inputs corresponding to several different levels of solar activity. Moreover, none of the models so far published takes account of possible variations of composition at the lower boundary, nor of horizontal transport of air, which might have an important influence on thermospheric structure.

Figure 2 gives the vertical distribution of temperature, pressure, and density from 0 to 250 km, as tabulated in the U.S. Standard Atmosphere

(Champion and Minzner, 1963). Some typical data for higher heights is given in Fig. 3. In a later section, we consider methods of obtaining the experimental data on which such models are based.

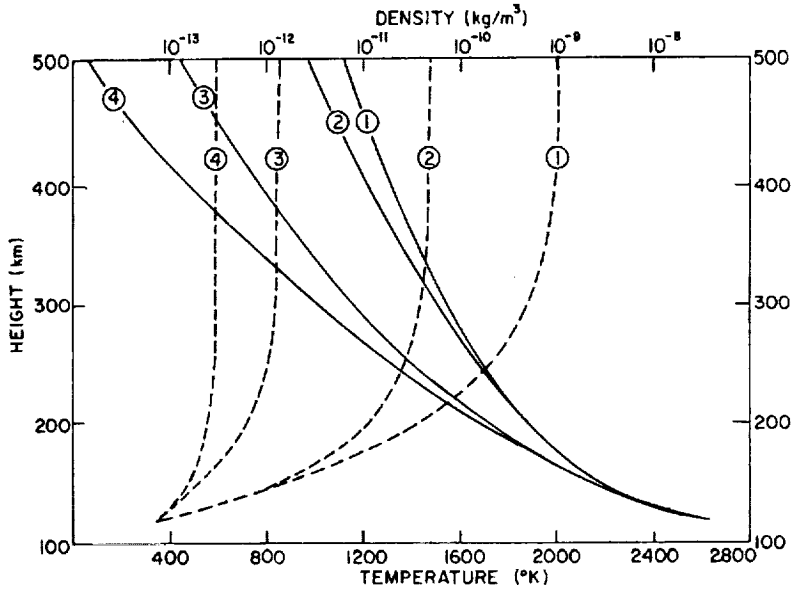

FIG. 3. THEORETICAL MODELS OF HARRIS AND PRIESTER (1962a,b). Vertical distribution of density and temperature for high solar activity (10 cm solar flux, S = 250) at noon (1) and midnight (2); and for low solar activity (S = 70) at noon (3) and midnight (4). These models assume the pressure, composition, and temperature at 120 km to be invariant.

4. Dissociation and Diffusive Separation

Above the mesopause the composition of the neutral atmosphere varies with height. This is associated with the dissociation of molecular oxygen and the occurrence of diffusive separation above the turbopause.

The dissociation of oxygen has been studied in detail by Nicolet and Mange (1963). They point out that even though O_2 molecules are dissociated by radiation in the Schumann-Runge continuum (wavelength < 1750 Å), the lifetime of an O_2 molecule above 100 km is of order days, the actual lifetime being very dependent on the intensity of the solar radiation. However, the O_2 concentration in the thermosphere is replenished by

diffusion in a time shorter than this, so that the vertical distribution of O_2 should more closely correspond to the hydrostatic equation (I-2) than to a condition of photochemical equilibrium.

The N_2 molecule, unlike O_2, has a very small cross-section for photodissociation and most of the nitrogen in the upper atmosphere is thought to be in molecular form. Such atomic nitrogen as does exist is produced by other photochemical processes, such as those involved in the production of ionization. Its abundance is linked with that of oxides of nitrogen. We may note in passing that nitric oxide, NO, is thought to exist in small quantities in the mesosphere and lower thermosphere. Probably at no level does NO represent more than one part in 10^{10} of the total concentration, yet its presence may be significant for the formation of the D region (Nicolet and Aikin, 1960).

The question of diffusive separation of atmospheric gases has been of interest ever since the composite nature of air was recognized in the eighteenth century. It was once thought that diffusion separation would take effect just above the ground, but it is now clear that major constituents are well mixed up to at least 100 km. Evidence is accumulating that diffusive separation begins near this altitude.

From observations with rocket-borne mass spectrometers, Meadows and Townsend (1958) found molecular nitrogen and argon to be diffusively separated at heights above 115 km. The situation concerning the gases N_2, O_2, and O remained obscure, partly because the chemical activity of atomic oxygen creates difficulties in mass-spectrometer sampling. The loss of atomic oxygen by chemical reactions within the apparatus and contamination by gases from the vehicle have been major problems. Some measurements have been published which show only a slow upward decrease of the $[N_2]/[O]$ ratio at heights up to 210 km (Pokhunkov, 1963). However, the results of Schaefer and Brown (1964) have found a rapid upward decrease of the $[O_2]/[O]$ ratio above 100 km, which indicates the existence of diffusive equilibrium even at this altitude. Recent measurements by Nier et al (1964), shown in Fig. 4, also indicate that diffusive separation of O, O_2 and N_2 occurs as low as 110 km.

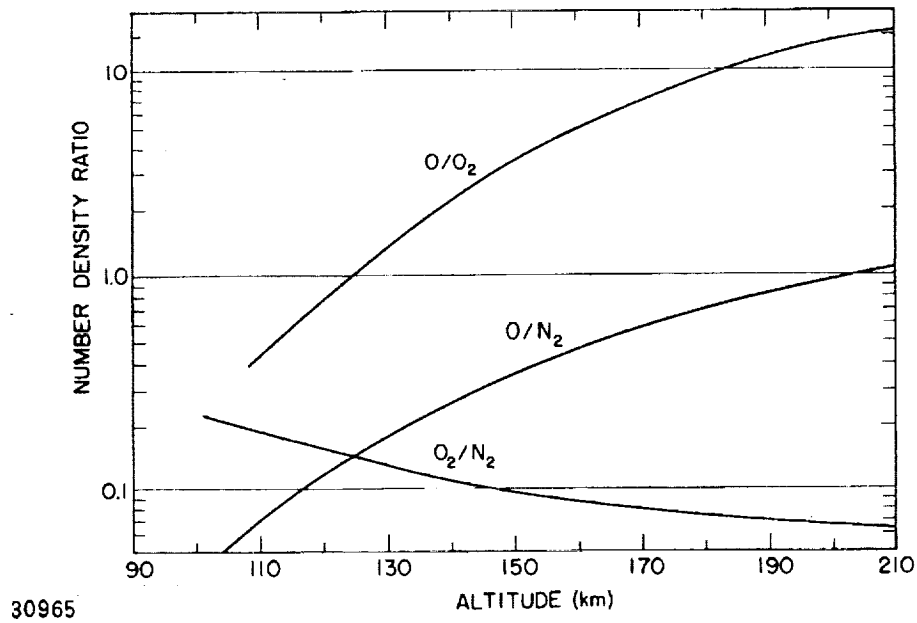

FIG. 4. RATIOS OF THE CONCENTRATIONS OF THE MAJOR NEUTRAL CONSTITUENTS OF THE UPPER ATMOSPHERE (after Nier et al, 1964).

We note that according to these data the level at which the concentrations of O and N_2 are equal is near 200 km. Further measurements such as these should eventually resolve the discrepancies between existing models. For instance, Harris and Priester (1962) place this level at 190 - 300 km (depending on temperature) although Norton, Van Zandt and Denison (1963) place it at 130 km.

The neutral composition can also be determined from observations of the solar spectrum at a series of heights, such as those of Hinteregger and Watanabe (1962). It is necessary to know the ultraviolet absorption cross-sections, as a function of wavelength, for each gas. This is essentially a trial-and-error method and has been applied by Norton, Van Zandt and Denison (1963) although their ratio of $[N_2]/[O]$ is considerably smaller than that measured by Nier et al, as we have noted.

The question of diffusive separation is linked to that of turbulence, which is believed to be absent at heights above about 100 km. Blamont and de Jager (1961) observed the rate of expansion of sodium vapor trails released from rockets. Below 102 km the trails were rapidly distorted by turbulence, but above this level they expanded more slowly, at a rate

consistent with molecular diffusion. A similar result was found by Rosenberg (1963) whose results place the turbopause at 110 to 115 km.

The theory of mixing and diffusive separation is incomplete. A number of different approaches have been compared by Mange (1957). Most of these define a "criterion" for estimating the time taken for a minor constituent to attain a diffusive equilibrium, starting from an initial nonequilibrium (or mixed) condition. This time is in general of order (scale height)^2/(diffusion coefficient). If it is less than some time-constant characteristic of the process responsible for mixing, then mixing will not be maintained. Naturally, the problem is more complicated if photochemical processes are operative as well as diffusion.

More recently, Hines (1963) discusses the problem of mixing of major constituents, with special reference to turbulence. If mixing were suddenly to cease, the gases would separate with a relative velocity which is found by balancing the resistance to motion, due to collisions, against the "buoyancy" forces which tend to separate the gases. The power dissipation of the collisional forces can than be found: it is of order 10^{-9} watts m^{-3} for a mixture of O_2 and N_2. Since Hines estimates the power available from turbulence to be a few times larger than this, between 90 and 100 km, he concludes that turbulence can just maintain mixing of O_2 and N_2 up to 100 km, but not at greater heights. The precise level of the turbopause presumably also depends on the strength of mechanism causing the turbulence, which may be gravity waves. Hence, changes in atmospheric motions below the turbopause might result in changes in composition at higher levels. A more complete discussion of turbulence, and of the pertinence of parameters such as Reynolds and Richardson numbers, is given by Hines in the review cited above.

Unless some other mechanism for preventing separation is effective at greater heights, it seems that diffusive separation of atmospheric gases must be established near the turbopause, or at least within one or two scale heights above it. As previously mentioned, the most recent available experimental data do indeed indicate that diffusive separation begins at heights near 110 km.

5. Thermal Balance

The heat balance in the thermosphere depends on the following processes:

Production (Q): (a) photochemical processes, such as photoionization, dissociation, recombination, attachment. (b) corpuscular ionization. (c) atmospheric absorption of gravity waves, hydromagnetic waves. (d) joule heating by electric currents.

Loss (L): Radiation at wavelengths for which the thermosphere is optically thin. These include the visible airglow lines which are transmitted to the ground, and the infrared line of atomic oxygen at 63μ.

Conductive Transport: This is written as the divergence of a heat flux Φ and thus resembles diffusion.

These processes may be included in an equation of continuity. Following Nicolet (1961), we find it most convenient to write the equation in terms of temperature T, and make each item represent a change of energy per unit volume per unit time. Let c_p be the specific heat per unit mass at constant pressure. Then, if only vertical transport is considered,

$$\rho c_p \frac{dT}{dt} = Q - L - \frac{\partial \Phi}{\partial h} \qquad \text{(I-10)}$$

Before considering the form of the terms in this continuity equation, we note that, at the lower boundary of the thermosphere, the temperature minimum at the mesopause at 80 to 85 km, acts as a barrier to conduction. Thus, the thermosphere and the mesosphere can exchange heat only by radiation (or by forced convection driven by large-scale wind systems). The thermal regime in the mesosphere depends on the presence of ozone, which absorbs a wide band of solar ultraviolet radiation not significantly absorbed above the mesopause.

Solar ultraviolet heating is thought to make a major contribution to the production term Q. The equations are akin to those describing the rate of photoionization which we will investigate later. We write

$$Q(h) = \int I(\lambda,h)\left[\sum_i \epsilon_i \sigma_i(\lambda) n_i(h)\right] d\lambda \qquad \text{(I-11)}$$

in which the summation refers to different atmospheric gases and the formula is integrated with respect to ultraviolet wavelength λ. σ_i represents an absorption cross-section for the i^{th} gas, and ϵ_i the amount of heat liberated per unit of radiation absorbed. At any height the intensity of radiation $I(\lambda,h)$ is related to optical depth $\tau(\lambda,h)$ and the intensity $I(\lambda,\infty)$ incident at the top of the atmosphere by

$$\ln[I(\lambda,h)/I(\lambda,\infty)] = \tau = \sec \chi \, \Sigma_i \, n_i \, \sigma_i \, H_i \qquad \text{(I-12)}$$

where χ is the solar zenith angle, assumed not near 90 deg. At heights above about 250 km, $\tau \ll 1$ for all wavelengths. In this case, the total flux, $I_\infty = \int I(\lambda,\infty)d\lambda$, together with a total gas concentration $n(h)$ and mean values $\overline{\epsilon}$ and $\overline{\sigma}$, can be used to replace the integration in (I-11) which then reduces to

$$Q(h) = I_\infty \overline{\epsilon}\,\overline{\sigma}\, n(h)\, e^{-\tau} \qquad \text{(I-13)}$$

The rate of heat input $Q(h)$ is greatest at altitudes between 100 km and 200 km, where $\tau(\lambda) \approx 1$ for the wavelengths involved. Under these circumstances the full equation (I-11) must be used, as the approximation (I-13) is inaccurate. Even the more detailed equation neglects two further complications connected with photoionization heating. One is that ejected photoelectrons may travel considerable distances before giving up their kinetic energy, so that some of the energy may appear in remote locations. The other is that part of the energy is stored in the ionization, and does not appear as heat until the ionization recombines. This implies a time lag which may be of the order of hours at 300 km. Other sources of heat, previously mentioned, may be important, especially at times of magnetic disturbance.

The "radiative loss" term, which is given by Bates (1952), is generally regarded as having little effect above 150 km altitude and is omitted in many published solutions of the continuity equation.

If only vertical variations are considered in the conduction term, the heat flux Φ in the continuity equation (I-10) may be written

$$\Phi = -AT^{1/2} \frac{\partial T}{\partial h} \qquad \text{(I-14)}$$

The product $AT^{1/2}$ represents the thermal conductivity, A being a constant given by kinetic theory. According to Nicolet (1961), its value in (joules m^{-1} sec^{-1} $(°K)^{-3/2}$) is 0.21 for atomic hydrogen, 0.036 for atomic oxygen and 0.018 for N_2 or O_2.

The conditions at great heights in the thermosphere are largely governed by the conduction term, since the three other terms in the continuity equation all decrease upward as the atmospheric density decreases. If, as is generally supposed, the flux Φ tends to zero at great heights, then $\partial T/\partial h \to 0$ by (I-14) so that the upper thermosphere is isothermal. However, there exist complications (to be discussed later in Sec. II-5) concerning the thermal disequilibrium between ions, electrons and neutral particles.

To justify the assumption that $\Phi \to 0$ at great heights, we note that the outermost atmosphere is fully ionized and its thermal conductivity is large parallel to the magnetic field but extremely small across it. The flow of heat across the magnetopause (which effectively marks the termination of the atmosphere), is then very small except when hot plasma from the sun actually pentrates into the geomagnetic field. Hence, the suggestion that the earth's outermost atmosphere is at the temperature of the surrounding solar corona, perhaps 10^5 °K, is not generally accepted (Chapman, 1959). We shall use the term "limiting (thermospheric) temperature" for the temperature in the isothermal region, although other terms such as "thermopause temperature" and "exospheric temperature" have been used. By solving the equation for equilibrium conditions, (such as approximately hold in the afternoon), Hunt and Van Zandt (1961) obtain an estimate of ~1 erg cm^{-2} sec^{-1} for the heat produced by ionizing radiation in the ionospheric F region, which corresponds to the upper part of the thermosphere.

If time variations are considered, it must be noted that the properties of the atmosphere at any given height h will vary on account of thermal expansion or contraction. Hence, it is convenient to "follow the motion" of each "cell" of air, thereby applying the principles described in Sec. I-3 and formulate the equations in terms of reduced height z or pressure p, instead of real height h. Both Cummack (1962) and Harris and Priester (1962) use an approach of this type. The actual height and time variations of thermospheric temperature are not known in sufficient detail to determine all the parameters of the models, but observations of satellite drag, in particular, enable good estimates of the limiting thermosphere temperature to be made (Jacchia, 1960). The data indicate that the limiting temperature is greatest about 14 hours local time, whereas the computed models give a later maximum, at about 17 hours. This discrepancy led Harris and Priester to postulate that a substantial fraction of the heating is due to a "corpuscular" source, which peaks at about 09 hours local time. This question must still be regarded as open. After sunset, photoionization heating is absent and conduction appears to equalize the neutral ion and electron temperatures above 200 km within two hours or so.

Some graphs of scale height (or temperature) against height, obtained by combining data from several satellites, often show changes of slope around 200 km. These have been interpreted as "temperature inversion," or layers in which T decreases upward (Priester and Martin, 1960), and attributed to the fact that the rate of absorption of solar ultraviolet energy has a maximum in the lower F region, below 200 km. However, the rate of temperature increase due to heating depends on the heat production per particle which, by Eq. (I-13), is $Q/n = I_\infty \bar{\epsilon} \bar{\sigma} e^{-\tau}$ and is therefore greatest at the top of the atmosphere where $\tau = 0$. Even if some other heating process should operate so as to produce a greater rate of temperature rise below 200 km, the high thermal conductivity at 200 km and above would oppose the formation of an inversion, and doubts have been expressed as to its reality.

6. The Exosphere

The exosphere is, by definition, the region in which the mean free path exceeds the scale height. Using data contained in the U.S. Standard Atmosphere, we may estimate this level to be at about 590 km. A molecule moving upward at the base of the exosphere is unlikely to make any collision above this level, and thus moves in a ballistic orbit under the influence of gravity. This orbit will be elliptical if the upward velocity of the molecule is less than the velocity of escape v_E from the earth's gravitational field, which is about 11.4 km/s. Should a molecule acquire a velocity exceeding 11.4 km/s as the result of collisions, its orbit will be hyperbolic and it will escape from the atmosphere unless it suffers further collisions. Some molecules will possess elliptical "satellite" orbits which do not intersect the base of the exosphere, in which the probability of colliding with other molecules is small. The computation of the radial distribution of gas concentration $n(r)$ is extremely complicated, and has been the subject of some controversy (see Chamberlain, 1963, and references contained therein).

If we define an "escape temperature" T_E by the simple equation $1/2\ mv_E^2 = 3/2\ kT_E$, we find T_E to be 5200 °K, 21,000 °K, and 84,000 °K for H, He, and O atoms respectively. At sunspot maximum, the temperature of the exosphere may exceed 2000 °K and there will be a steady loss of hydrogen atoms at the upper end of the energy distribution. Helium will also be lost, but much more slowly. This gas is liberated at a steady rate by radioactive decay processes in the earth's crust, at a rate which can be estimated from geological data. Since the rate of escape depends on the temperature of the upper atmosphere, it was thought that this temperature could be estimated from the observed abundance. However, it seems that the problem is too complex to yield useful information on this subject (Chamberlain, 1963).

Hydrogen is generated by dissociation of water vapor and methane in the upper atmosphere, and then escapes from the top of the exosphere. In a detailed discussion of the hydrogen and helium content of the atmosphere, Kockarts and Nicolet (1962) estimate the upward flux of hydrogen atoms at 100 km to be 2.5×10^7 cm^{-2} sec^{-1}. It may then be deduced that

the average lifetime for hydrogen atoms in the atmosphere is a few days, as compared to a few years for helium atoms.

Great interest has been aroused by spectrometric observations which are connected with the hydrogen content of the atmosphere. Purcell and Tousey (1960) observed the solar Lyman α line from a rocket above 130 km. They found it to be broad (~1 Å) with a narrow absorption core, which could be attributed to a column of hydrogen atoms, 3×10^{16} (m^{-2}). The width of the absorption core corresponded to a temperature of order 1000 °K, more likely to be associated with the terrestrial atmosphere than the interplanetary medium. Moreover, the absence of a Doppler shift suggested that the hydrogen is stationary with respect to the earth. Diffuse Lyman α radiation has also been detected in the night sky by rockets and it is believed to be solar in origin, and scattered by hydrogen in the outer atmosphere. However, the amount of hydrogen required to account for the observed intensity is several times greater than the content quoted above, deduced from daytime observations. This difficulty has been well discussed by Donahue and Thomas (1963a,b) who suggest that it could be explained by the presence of a distant "cloud" of hydrogen ("geocoma") associated with the earth, or by a large day-night variation of the hydrogen concentration. However, Hanson and Patterson (1963) consider that a lateral flow of hydrogen would be efficient in preventing such a diurnal asymmetry.

7. Experimental Techniques

There are a number of experimental techniques available for the study of the neutral atmosphere. Below about 30 km it is possible to measure pressure, temperature and density with relatively inexpensive balloons. A "searchlight" probing technique has permitted ground-based measurements as high as 67 km (Elterman, 1951, 1954). In this method, a powerful searchlight beam which may be modulated to discriminate against the steady background radiation from the night sky, is directed upward. Another remote photo-sensitive detector then scans the searchlight beam to determine the intensity of the scattered light as a function of altitude. When only Rayleigh scattering is observed, as appears to be the case above

about 10 km, the received intensity is proportional to the concentration of air molecules. Furthermore, when the equation of hydrostatic equilibrium is introduced, the temperature and pressure profiles may be deduced from the measured concentration profile.

On one occasion, Elterman has obtained temperature profiles from rocket, sound propagation and balloon measurements nearly simultaneously with the searchlight experiment and all were in satisfactory agreement. His measurements have found that below 45 km there is little diurnal or seasonal temperature variation, but near the mesopeak at about 50 km and above, day-to-day fluctuations as well as diurnal and seasonal variations exist of 20 to 40 °K. The invention of the laser, since these experiments were performed with its attendant narrow bandwidth, offers the possibility of extending the measurements to even greater altitudes.

Another very fruitful method for study of the atmosphere below about 90 km has been the measurement of sound delay times from grenade explosions at high altitudes. As a rocket climbs to 100 km or more, the grenades are ejected and exploded every few kilometers. The delay times are recorded at a network of ground stations and from the records it is possible to deduce not only the temperature profile, accurate to within ±3 °K (Stroud et al, 1960), but also the horizontal winds in the mesosphere. A simplified presentation of the theory and number of other references are given in the paper of Stroud et al. Winds in the mesosphere show little or no diurnal variation but there is a strong seasonal variation in the arctic. Strong westerly winds (100 to 150 m/sec) in the winter--the so-called "polar jet streams"--change to more moderate easterly winds in the summer.

Most of the other methods require rockets to place the instruments within the environment it is intended to measure. For example, an experiment has been designed in which a collapsed sphere is launched to a high altitude and then ejected and inflated after the rocket power has been exhausted and the atmospheric drag has reached a tolerable magnitude (Bartman et al, 1956). The large area/mass ratio allows the drag force to exert measurable accelerations even in the very tenuous upper atmosphere. The drag force may be written as

$$D = \frac{1}{2} \rho V^2 A C_D \qquad \text{(I-15)}$$

where ρ is the air density, V is the sphere velocity, A is the cross-sectional area and C_D is a dimensionless drag coefficient. Although the value of C_D is a rather complicated function of how the air molecules are reflected from the surface of the sphere, Faucher et al (1963) believe that it can be calculated to within a few percent.

After the sphere has been erected and vibrations have damped out, a sensitive accelerometer is used to measure the drag force and then the density is calculated from Eq. (I-15). In a recent rocket flight reaching an altitude of about 250 km, Faucher et al detected measurable atmospheric drag below 135 km and have computed density values below this level. The results are not only useful in themselves, but may be compared with rocket data based on pressure gauge measurements which extend to even higher altitudes.

Lagow et al (1959) have compared the density and pressure profiles obtained in the arctic and in mid-latitudes from a number of rocket flights. A variety of pressure gauges were used in the measurements and from these, both the ambient pressure and the gas density were calculated up to an altitude of 210 km. Their results show rather large differences in scale height (and therefore temperature) between White Sands, New Mexico and Fort Churchill, Canada, on summer days. At high latitudes the density and scale height values appear too large to match satellite drag data. Sterne (1958) indicates reservations about the validity of the pressure measurements and also Johnson (1960) has pointed out the difficulty in maintaining large latitudinal pressure and temperature differences above 200 km.

Following a suggestion by Bates (1950), a number of experiments have been performed in which sodium and other contaminants have been released at high altitudes. When the gas is released all along the rocket trajectory, a trail develops which becomes highly distorted as time proceeds owing to wind shears and molecular diffusion in the upper atmosphere. The sodium trail observed at twilight is believed to be due to resonant scattering of the 5580 Å sunlight and it is rapidly extinguished following

sunset at the appropriate altitude (Bedinger et al, 1958). However, even at night a brief trail is observed with the energy for the photo-emission apparently derived from chemical reactions with atmospheric constituents.

At altitudes above 200 km, different methods must be employed for the measurement of atmospheric density. A "ribbon microphone" in which the incident flux of neutral molecules is modulated by a rotating shutter has been described by Sharp, Hanson and McKibbin (1962). The resulting ribbon displacements of only a few Angstroms produce an alternating voltage which is amplified with sufficient accuracy to obtain density measurements (proportional to the pressure oscillations) at an altitude of 550 km. Their results are consistent with values deduced from satellite drag observations and have the outstanding advantage of being nearly instantaneous measurements.

Since 1957, it has been possible to measure atmospheric density from a careful measurement of the rate of decrease of the orbital period of a satellite. Very important advances have been made in our knowledge of the upper atmosphere from these observations. Although the gas density at 500 km is about 10^{-10} of that at the ground, appreciable drag is experienced by most satellites at this altitude and useful results have been obtained between 200 and 1100 km (Jacchia, 1960). The method of analysis is particularly simple for circular orbits, as will be shown below, but such an orbit is very difficult to achieve in practice, and the gas density is not spherically symmetric in any case. The accurate equations applicable to elliptical orbits have been derived by Sterne (1958) and others, and King-Hele (1963) has given a relatively simple and useful derivation of the most important terms.

By equating the centrifugal and centripetal forces acting on a satellite in a circular orbit about the earth, we may obtain the relation $GM_E = rv^2$, where G = gravitational constant, 6.67×10^{-11} (newton m^2/kg^2), M_E = mass of earth, $5.97 \times 10^{+24}$ (kg), r = geocentric radius of the orbit and v = velocity of the satellite. Then, we find that the kinetic energy is given by

$$KE = \frac{1}{2} m_s v^2 = GM_E m_s / 2r \qquad \text{(I-16)}$$

where m_s is the satellite mass. From first principles we know that the potential energy is

$$PE = - GM_E m_s / r \qquad \text{(I-17)}$$

We should note that the magnitude of the PE is just twice that of the KE at any radius and that their derivatives with respect to r are also in the ratio of 2:1.

When atmospheric drag is included, the rate at which satellite energy is lost is Dv, where D is the drag force given in (I-15). This may be equated to the rate change of total energy:

$$-Dv = \frac{d}{dt} (KE + PE) = \frac{d}{dr} (KE + PE) \frac{dr}{dt} \qquad \text{(I-18)}$$

Solving for the rate of change of altitude,

$$\frac{dr}{dt} = - \frac{\frac{1}{2} \rho v^3 AC_D}{\frac{1}{2} m_s GM_E / r^2} = \frac{\rho v \, AC_D r}{m_s} \qquad \text{(I-19)}$$

For small values of ρ, the satellite will gradually spiral deeper into the atmosphere, gaining kinetic energy while losing potential energy twice as fast, in what may be termed a "quasi-circular" orbit.

We observe the paradoxical situation in which the drag force acts in the direction opposite to the velocity vector, yet the velocity of the satellite continually increases. This may be understood as follows: the impact of a molecule at one point in the orbit does reduce the KE and thus the satellite velocity by a very small increment. This puts the satellite in a slightly elliptical orbit with the point of impact at apogee. When the satellite reaches perigee half an orbit later, the

velocity will have increased to a value greater than prior to impact at the expense of a reduction in PE. For the quasi-circular orbit, the variations of KE, PE and r are all continuous, of course.

The measurements of atmospheric density rely upon the observation of the average rate change of satellite period, usually obtained from radio tracking stations. From Kepler's third law,

$$T^2 = \left(\frac{4\pi^2}{GM}\right) r^3 \qquad \text{(I-20)}$$

we obtain

$$2T \frac{dT}{dt} = \left(\frac{4\pi^2}{GM}\right) 3r^2 \frac{dr}{dt} \qquad \text{(I-21)}$$

Again using $GM = rv^2$ and Eq. (I-19),

$$\frac{dT}{dt} = -\left(\frac{3\pi AC_D r}{m_s}\right) \rho \qquad \text{(I-22)}$$

The value of C_D is usually considered to be about 2.2 for satellite applications. Equation (I-22) can then be used to calculate the density at the satellite altitude. The analogous equations for elliptical orbits will not be derived, but it develops that the quantity $\rho H^{1/2}$ is the parameter now determined by drag analysis. The values of ρ deduced when H is assumed are most accurate about one-half scale height above the satellite perigee.

II. MEASUREMENT OF IONOSPHERIC PARAMETERS

1. Introduction

In the preceding section, the vertical distribution of the nonionized molecules and atoms in the earth's atmosphere has been discussed. This is a very important preliminary to the discussion of the ionized portion of the atmosphere because the neutral molecules are obviously the parents of the charged particles to be discussed here. Our knowledge of the charge distribution has tended to precede that of the neutral composition principally because more simple measurement techniques are available. These measurements, in turn, have contributed to the study of the neutral composition.

Without discussing the theory of the formation of the ionosphere for the moment, in this section we will want to consider the various means available for the measurement of the pertinent ionospheric parameters. Principally, these are the electron "density" (or more precisely, concentration), the ion concentration and composition, the ion and electron temperatures and the movement of these charges.

The presence of the ionosphere was detected long before modern radio methods were developed. Over eighty years ago Balfour Stewart suggested the existence of a conducting layer in the upper atmosphere within which large currents were generated by the tidal oscillations of the atmosphere. These currents explained the observed magnetic deflections at ground level which were found to vary with solar activity and geographic latitude. Then, after Marconi had demonstrated the feasibility of trans-Atlantic radio communication in 1901, Kennelly and Heaviside suggested independently that a reflecting or refracting layer must exist such that the radio waves were "bent" around the curve of the earth. Direct radio investigations of the ionosphere may be dated from the pioneering work of Tuve and Breit (1925) and that of Appleton and his colleagues (1925).

2. Determination of Electron Density by Sounding

After forty years, the pulse sounding technique of Breit and Tuve is still a basic tool of ionospheric research. A sounder is a type of radar

which is capable of obtaining echoes from the ionosphere over a wide range of operating frequencies. The model C-4 ionosonde developed by the National Bureau of Standards has been in use at several stations for a number of years and is representative of the many designs now in use. In a typical mode of operation, the sounder is swept from 1 - 25 Mc/s in 13.5 sec, using a pulse repetition frequency of about 100 per second and a peak power of up to 30 kilowatts. Newer types of ionosonde have been developed, which provide better resolution and greater versatility in operation.

In a conventional recording system, the echo received from the ionosphere is used to modulate the intensity of a spot of light on an electronic time base. Distance along the time base represents the "time of flight" of the radio pulse which, if divided by the free space velocity, gives the equivalent path length, and this is twice the "virtual height" h' of the reflection point in the ionosphere. In the recorder, a photographic film is moved at right angles to the time base as the frequency is varied, so that the spot of light traces a graph of virtual height h' against radio frequency. Range and frequency calibration markers are usually inserted automatically. These recordings are commonly known as ionograms or $h'(f)$ curves.

The pioneer ionospheric observatory is situated at Slough in England, where an ionosonde has been operated regularly since 1932. Other stations were opened before the war at Washington, D.C., Watheroo in Western Australia, and at Huancayo on the magnetic equator in Peru. Since World War II many other stations have been operating and during the International Geophysical Year, in 1957-58, the total number was about 150. Normally, each station makes a sounding once an hour (sometimes once every 15 min or less) and the total number of ionograms now in existence amounts to some tens of millions.

To understand the form of the $h'(f)$ curves, it is necessary to consider briefly the equations for the propagation of waves in the ionosphere. Let N be the electron concentration (electron density), m and $-e$ the mass and electronic charge, and ϵ_o the permittivity of free space. In the absence of a magnetic field, the phase refractive index μ and group

refractive index μ', for waves of frequency f are related by the equation $\mu\mu' = 1$, and

$$\mu^2 = 1 - \frac{Ne^2}{4\pi^2 m\epsilon_o f^2} \qquad \text{(II-1)}$$

Note that $\mu \leqq 1 \leqq \mu'$ (which is usually true even in the presence of a magnetic field). The wave is reflected from a level where $\mu = 0$, or in other words, where the frequency f is equal to the local value of the plasma frequency f_N given (in c/s for N in electrons/m^3) by

$$f_N = \sqrt{80.6N} \approx 9\sqrt{N} \qquad \text{(II-2)}$$

In the presence of the magnetic field, the ionosphere is a doubly refracting medium, and two modes of propagation exist, for which the names "ordinary" and "extraordinary" are taken from crystal optics. The complete Appleton-Hartree equation replaces the simplified equation (II-1) and it is no longer true that $\mu\mu' = 1$ (Ratcliffe, 1959). The equation contains the frequency of gyration of electrons in the geomagnetic field B, given by $f_H = eB/2\pi m$, and the magnetic dip angle. It thus depends on the location of the observing station. For a more accurate treatment, the effect of collisions between electrons and heavy particles should also be included. An idealized $h'(f)$ curve is sketched in Fig. 5; its most obvious features are the "cusps" which mark the "critical frequencies" of the E and F layers.

Both "ordinary" and "extraordinary" traces are sketched in the figure. By day, the F layer is often divided and shows an "F1 cusp" at a frequency lower than the ordinary mode penetration frequency which is normally known as the "F2 critical frequency" and denoted by f_oF2. Waves of frequencies exceeding f_xF2 cannot be reflected at vertical incidence, but penetrate the ionosphere completely. The symbols f_oF1 and f_xF1 are used for the F1 cusp frequencies, if present, and f_oE and f_xE for the E layer cusp frequencies. At times additional stratifications

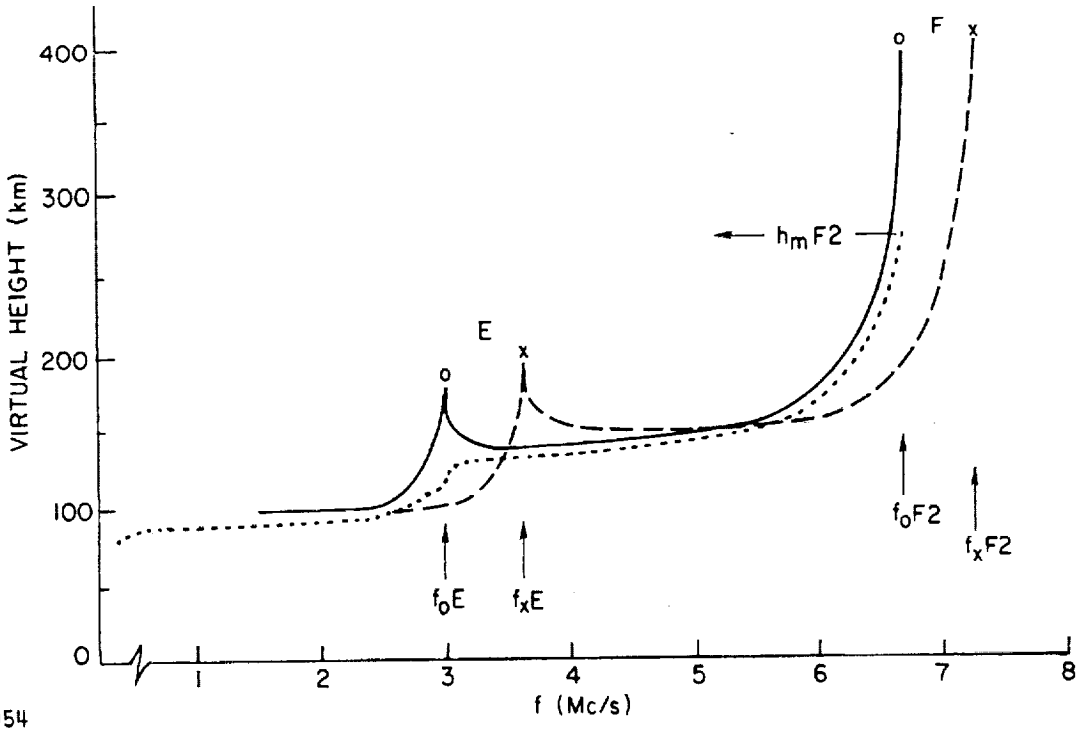

FIG. 5. AN IDEALIZED IONOGRAM, SHOWING VIRTUAL HEIGHT VS FREQUENCY. The solid and broken curves apply to the ordinary and extraordinary modes, respectively. The dotted curve represents the plasma frequency-real height profile necessary to produce the virtual height curves.

are observed; in fact, ionograms reveal a wide variety of phenomena, some of which are touched upon in subsequent sections. Also shown as the dotted curve in Fig. 5 is the plasma frequency profile which could have produced the virtual height curves.

The critical frequency $f_o F2$ (some authors omit the subscript "o") is the most widely studied property of the ionosphere. It is related to the greatest electron density N_m within each layer by the standard equation (II-2). But we note that (except for $N_m F2$) these values may not represent actual peaks (maxima) of the $N(h)$ distribution, but may just be points of inflection. The virtual heights at these points are large, and are actually infinite if $dN/dh = 0$. This, of course, is always the case at the F2 peak, but the E and F1 cusps may correspond to quite small "ledges" in the $N(h)$ profile, such as is sketched in Fig. 5.

We note that the separation of the ordinary and extraordinary cusps can be computed from the Appleton-Hartree equation. It is given by the equations

$$f_o = \left[f_x^2 - f_x f_H\right]^{1/2} \approx f_x - \frac{1}{2} f_H \qquad \text{(II-3)}$$

The approximation is good if the critical frequencies are much greater than f_H, as is generally the case for the F layer. (A typical mid-latitude value of f_H is 1.4 Mc/s). Under certain circumstances, a third trace is seen on ionograms, notably at high latitudes. The critical frequency f_z of this so-called z-trace is approximately $\left(f_o - \frac{1}{2} f_H\right)$. A discussion of this phenomenon is given by Ratcliffe (1959).

The virtual heights observed at and near the critical frequencies have little physical meaning, but the real heights h_mE, h_mF1 and h_mF2 are important quantities. The virtual height (or "group height") h' and the real height h at which a given frequency f is reflected are connected by an equation that depends on the distribution of electron density below the reflection point; it is

$$h' = \int_0^h \mu'(f,N)dh$$

Since $\mu' \geq 1$, the group height $h' \geq h$. Much effort has been devoted to solving this equation to obtain $N(h)$. This is accomplished by writing it as an integral with respect to plasma frequency instead of height (which assumes that N and f_N vary monotonically with height)

$$h'(f) = \int_0^f \mu'(f,N) \frac{dh}{df_N} df_N + h(0) \qquad \text{(II-4)}$$

where $h(0)$ is the height of the base of the ionosphere, below which $f_N = 0$.

A good review of the ways of inverting this equation has been given by Thomas (1959). The availability of electronic computers has made

obsolete the earlier methods in which a special form, such as a parabola was assumed for the $N(h)$ profile, though these are of academic interest.

The present-day methods of solving the integral equation (II-4) fall into two main classes, "lamination" and "polynomial." The former class, represented by the "matrix method" of Budden (1955) replaces the integration in (II-4) by a summation over a number of thin slabs, each corresponding to a discrete interval of plasma frequency. For this purpose, some simplifying assumption is made, the commonest being that the gradient dh/df_N is constant within each slab so that the function $h(f_N)$ is represented by a series of linear segments.

Suppose there are n slabs, and that $h'(f_i)$ is the virtual height for the frequency f_i reflected at the top of the i^{th} slab, at a real height h_i. We can then form a set of $n + 1$ equations

$$h'(0) = h(0)$$

$$h'(f_1) = h(0) + \frac{h(f_1) - h(0)}{f_1 - 0} \int_0^{f_1} \mu'(f_1, f_N)\, df_N$$

$$h'(f_2) = h(0) + \frac{h(f_1) - h(0)}{f_1 - 0} \int_0^{f_1} \mu'(f_2, f_N)\, df_N + \frac{h(f_2) - h(f_1)}{f_2 - f_1} \int_{f_1}^{f_2} \mu'(f_2, f_N)\, df_N \quad \text{(II-5)}$$

$$\vdots$$

$$h'(f_j) = h(0) + \sum_{i=1}^{j} \frac{h(f_i) - h(f_{i-1})}{f_i - f_{i-1}} \int_{f_{i-1}}^{f_i} \mu'(f_j, f_N)\, df_N$$

Additional equations are written up to $j = n$ (note that we take $f_{i-1} = 0$ for $i = 1$). By using the abbreviation

$$M_{ji} = (f_i - f_{i-1})^{-1} \int_{f_{i-1}}^{f_i} \mu'(f_j, f_N)\, df_N \quad \text{(II-6)}$$

we can write the equations compactly in the form

$$h'(f_j) - h'(0) = \sum_{i=1}^{j} [h(f_i) - h(f_{i-1})] M_{ji} \qquad \text{(II-7a)}$$

or

$$\Delta h'_j = \sum_{i=1}^{j} (\Delta h_i) M_{ji} \qquad \text{(II-7b)}$$

Note that $\Delta h'_j$ is the virtual height at frequency f_j measured from the bottom of the layer, Δh_i is the real width of the i^{th} slab, while M_{ji} is the average value of μ' within the i^{th} slab for waves of frequency f_j. This equation can obviously be written in matrix form, $\underline{\Delta h'} = \underline{\underline{M}} \cdot \underline{\Delta h}$, whose solution is $\underline{\Delta h} = \underline{\underline{M}}^{-1} \cdot \underline{\Delta h'}$. From the width of these slabs, the real height profile is obtained as

$$h_j = h'(0) + \sum_{i=1}^{j} \Delta h_i$$

It is common practice to perform both of the last two steps at the same time with an additional matrix multiplication (Budden, 1955).

It may be advantageous to use an unequally spaced set of frequencies f_i. These can be so chosen that the summation reduces to a simple averaging of a number of values of h', which can be carried out manually (Kelso, 1952). Schmerling (1958) has shown that this method can be adapted to include the magnetic field. Some authors do not explicitly include the term $h(0)$ in their equations. For example, Thomas (1959) imposes an additional condition on the matrix elements which takes account of this term, but neglects the effect of ionization in the first lamination (i.e., below the height $h(f_1)$ at which the first frequency f_o is reflected).

The assumption that dh/df_N = constant within each slab may be varied. In a comparison of different methods, King (1957) advocates the assumption, $dh/d(\ln f_N)$ = constant, whereas others have used a parabolic variation within each slab.

In the "polynomial" method of Titheridge (1961), it is assumed that the function $h(f_N)$ can be represented by a polynomial in f_N, of the form

$$h - h(0) \equiv h^* = \sum_{j=1}^{n} \alpha_j f_N^{j+1} \qquad \text{(II-8)}$$

First a set of sampling frequencies $f_1, f_2, \ldots, f_n$ is chosen. Then the heights h_i^* at which the plasma frequency takes the values f_i can be included in a matrix equation, $\underline{h}^* = \underline{\underline{A}} \cdot \underline{\alpha}$, in which each element of the column matrix $\underline{\alpha}$ is the coefficient appearing in Eq. (II-8), and the element a_{ij} is equal to f_i^{j+1}. Now the set of virtual heights at frequencies f_i can be written as $h^{*\prime} = \underline{\underline{B}} \cdot \underline{\alpha}$, in which the elements of $\underline{\underline{B}}$ contain integrals with respect to frequency of the group refractive index μ'. Hence $\underline{h}^* = (\underline{\underline{AB}}^{-1}) \cdot h^{*\prime}$. The elements of the matrix $\underline{\underline{AB}}^{-1}$ depend on the frequencies f_i and the parameters of the geomagnetic field, and can be computed for a given location and a given set of sampling frequencies. Thus sets of values of h' and h are connected by a matrix equation, as in the lamination method.

Whereas the lamination method represents the function $h(f_N)$ by a series of linear segments, the polynomial method instead assumes that a smooth polynomial of degree $(n + 1)$ in f_N can be drawn to pass through the n sampling points (h_i, f_i), although the coefficients of this polynomial are not required to be known. For a given number of sampling points, the polynomial method gives greater accuracy than the lamination method. Titheridge (1961) also describes a "modified polynomial method" of greater complexity, which is suitable for reducing ionograms containing a number of cusps.

There are several difficulties to be faced in the reduction of $h'(f)$ curves to $N(h)$ profiles. One of these is the so-called "valley ambiguity." All the methods of analysis that we have described give unambiguous results only if electron density N increases monotonically with height. If the $N(h)$ profile is re-entrant so that the same value of N occurs at more than one height, then the reduction procedures do not give a unique result. For instance, it is possible that N decreases with height immediately above the E layer to give a "valley" between the E and F layers. Indeed, this was generally thought to be the case until rocket observations proved otherwise. It is also possible, though less likely, that there could be a valley between the F1 and F2 layers.

Another difficulty arises from the fact that conventional ionosondes have a lower frequency limit, usually about 0.5 - 1 Mc/s, and record no echoes below this limit. Consequently, they obtain no information about the electron distribution below the E layer in the daytime or below the F layer at night. Special sounders have been built which operate down to 50 kilocycles (Watts, 1957), but this equipment is not in general use. The lack of data about these low frequencies can lead to errors of 10 - 20 kilometers in the height corresponding to higher plasma frequencies.

Titheridge (1959) has shown that if data from the extraordinary ray virtual height are included in the analysis, it is possible to correct for the low level ionization not included in the ionograms, and also to make some estimate of the ionization contained in the valleys. Although the method does not give a detailed distribution of electrons in the valley, Titheridge was able to show that on some occasions, only a very small valley existed between the E layer and F layer at night. Paul and Wright (1963) have given some results obtained with a very refined method of ionogram reduction. It seems, however, that we shall have to wait for the improved records which should be obtained from the most advanced ionosondes before the full potentialities of this method can be realized. It should then be possible to calculate the real height at which a given electron density occurs to within about 1 kilometer, whereas with the older methods of reduction, in which the difficulties described

above have not been fully overcome, the errors might be of the order of ten or even twenty kilometers (Thomas, Haselgrove and Robbins, 1958).

The successful launching of the Canadian satellite, "Alouette," in September 1962, inaugurated the era of the "topside sounder." This satellite is in a nearly circular orbit at a height of just over one thousand kilometers, and carries a compact sweep-frequency ionosonde, operating on radio frequencies of 0.5 - 11.5 Mc/s. Whenever the satellite is activated, soundings are made at intervals of 20 sec, during which time the satellite travels about 100 km. The interpretation of the ionograms obtained from the satellite and the reduction to $N(h)$ profiles presents some interesting problems. The analysis is complicated by the fact that neither the electron density N nor the gradient dN/dh is zero at the sounder, as is the case with a conventional ionosonde on the ground. On the other hand, there is generally less structure in the topside than in the bottomside of the ionosphere, so that there is less difficulty with valleys. Nelms (1963) has developed a reduction program which is based on the original Budden matrix method, whereas Fitzenreiter and Blumle (1964) use a lamination method which takes $dh/d(\ln f_N) = \text{constant}$ within each slab. Thomas, Long and Westover (1963) have used a polynomial method in which each real height is expressed as a polynomial in $f_N - f_V$, f_V being the plasma frequency at the vehicle. The topside records show a number of interesting magneto-ionic and plasma phenomena, but we shall not describe these in detail here (Calvert and Goe, 1963).

3. Propagation Methods

In contrast to the relative ease with which electron density measurements are made above 90 km where the concentrations are greater than 10^3 per cc, the region between 50 and 90 km presents formidable experimental difficulties. One useful method first described by Gardner and Pawsey (1953) relies on partial reflections from small discontinuities or gradients in the index of refraction in the lower ionosphere. The technique involves the transmission of short rf pulses (2 to 3 Mc/s) and the reception of the reflected energy as a function height (time). The received energy must be separated into its two characteristic modes, which

will be right hand and left hand circular except near the equator, as it is the ratio of the amplitudes of the modes that is important. For either mode, the received amplitude is given by

$$A \propto R \exp\left[-2 \int_0^h \mathcal{K}\, dh\right] \qquad \text{(II-9)}$$

where R is the power reflection coefficient and $\mathcal{K}$ is the attenuation per unit length. The upper limit of the integral is the reflection height. The power ratio of the extraordinary mode to the ordinary mode is therefore

$$\frac{A_x}{A_o} = \frac{R_x}{R_o} \exp\left[-2 \int_0^h (\mathcal{K}_x - \mathcal{K}_o)\, dh\right] \qquad \text{(II-10)}$$

From the appropriate expressions for the index of refraction, it may be found that the ratio (R_x/R_o) is a function of the electron collision frequency ν, but not the electron concentration, while the differential absorption $(\mathcal{K}_x - \mathcal{K}_o)$ depends on a different function of N and ν (Holt, 1963). If the collision frequency is determined independently, the appropriate functions can be calculated and Eq. (II-10) can be revised to give

$$\ln(A_x/A_o) - \ln(R_x/R_o) = -2 \int_0^h (\mathcal{K}_x - \mathcal{K}_o)\, dh$$

$$= \int_0^h f(\nu,h) \cdot N(h)\, dh \qquad \text{(II-11)}$$

In this equation (A_x/A_o) is measured while (R_x/R_o) and $f(\nu,h)$ are calculated from the assumed collision frequency profile. Then, the equation may be differentiated with respect to height and solved for $N(h)$.

An example of these calculations and observations is shown in Fig. 6 taken from Holt (1963). The ratio of the reflection coefficients rises with altitude owing to the increasing collision frequency. However, at the higher altitudes, the relative absorption of the extraordinary wave increases even faster, producing an amplitude variation which first increases, then drops off rapidly. Figure 6b shows the electron density profile calculated from these observations. At the lowest altitudes, the absorption is relatively small and the right hand side of (II-11) is approximately zero. Here, $(A_x/A_o) \approx (R_x/R_o)$ and the collision frequency may be calculated.

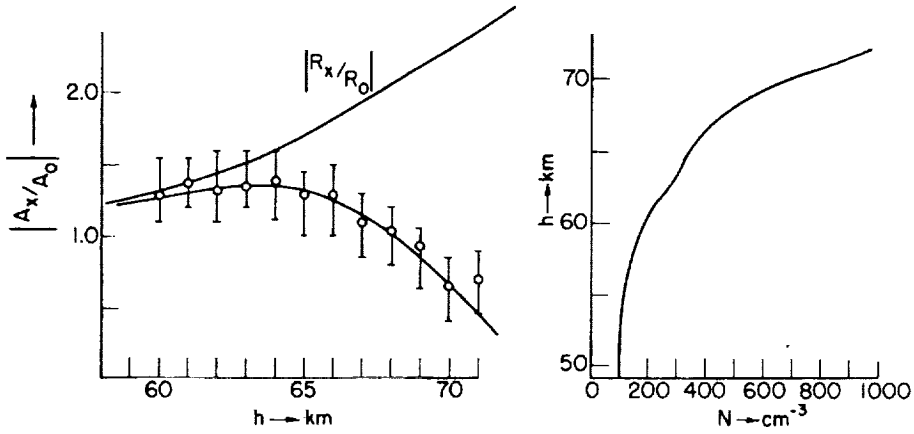

FIG. 6. (a.) OBSERVED AMPLITUDE RATIOS OF PARTIALLY REFLECTED EXTRAORDINARY AND ORDINARY WAVES (OPEN CIRCLES); THE BARS SHOW UPPER AND LOWER QUARTILES. The reflection coefficient ratio is calculated from an assumed collision frequency profile. (b.) THE DEDUCED ELECTRON DENSITY PROFILE. The measurements were made in August 1962, in Norway (after Holt, 1963).

An alternative technique first described by Fejer (1955) is based on radio wave interaction and permits the calculation of both the collision frequency and the electron density as a function of altitude. This method requires one transmitter (usually at a frequency of two to three Mc/s) to emit short pulses which are reflected from the ionosphere and

received at the ground. The received amplitude of this "wanted" signal is carefully measured. When a short interval (t_o) exists prior to the reception of every alternate wanted pulse, a second "disturbing" transmitter emits another short pulse at a different frequency and with as much power as possible. This situation is sketched in Fig. 7. In reality T_1, T_2 and R may all be at one location, but they are shown separated here for clarity.

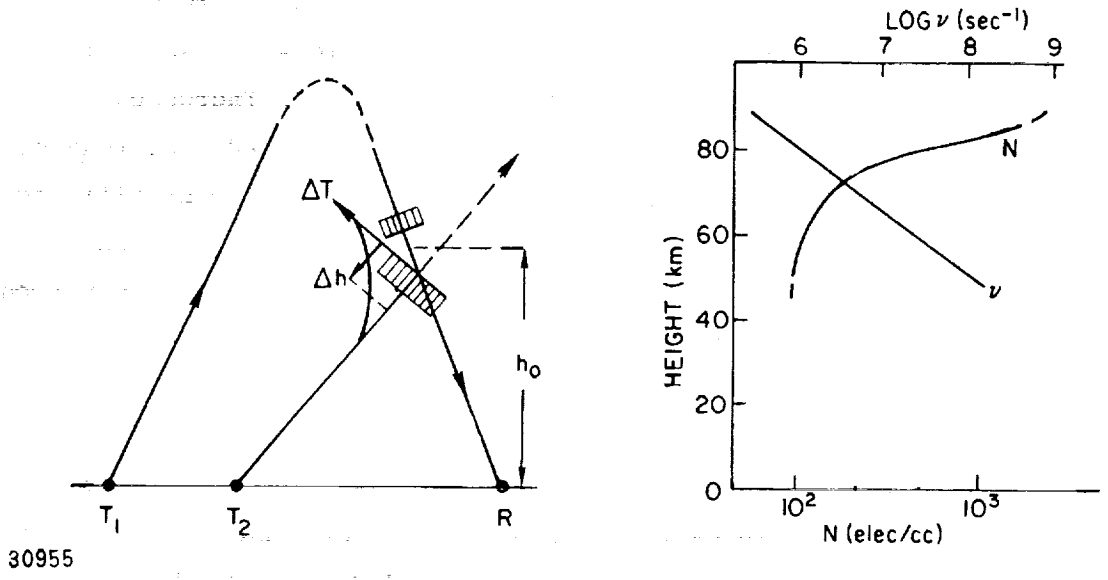

30955

FIG. 7. ILLUSTRATING THE MEASUREMENT OF N AND ν BY THE RADIO-WAVE INTERACTION TECHNIQUE. A pulse from the "disturbing" transmitter T_2 interacts with alternate pulses from the "wanted" transmitter T_1 at the altitude h_o. A region of slightly enhanced collision frequency follows in the "wake" of the disturbing pulse. The N(h) and ν(h) profile obtained by Barrington and Thrane (1962) is shown at the right.

At the instant shown, the downcoming "wanted" wave is just meeting the upgoing "disturbing" wave at the height $h_o \approx ct_o$. The electromagnetic wave comprising the pulse from T_2 forces the electrons in the ionosphere to oscillate at its wave frequency, and this energy is converted to heat (e.g., random velocity) by collisions with the neutral particles. If a fraction G of the excess electron energy is lost at each collision, the electron will come back to its original temperature

in a time $\tau \approx (G\nu)^{-1}$. Thus, the small excess electron temperature (ΔT) will diminish behind the pulse in a distance $\Delta h \approx c\tau$ as shown, where c is the velocity of light. We may expect ν to depend on temperature, and in this way, the disturbing pulse generates a region of slightly higher collision frequency as it passes through the ionosphere.

Now we wish to see what effect the increased ν produces in the amplitude of the wanted wave. When the wave frequency exceeds ν, an increase in ν will increase the absorption and reduce the received amplitude. However, at the lowest altitudes, below about 70 km, a collision is likely to occur before the electromagnetic wave has fully accelerated the electron ($\nu > \omega$), and in this case the increased ν reduces the energy loss and the absorption. The received amplitude of the wanted pulse which interacts with the disturbing pulse at altitudes below h_o is then compared with the next wanted pulse, for which no disturbing pulse was sent. The difference in these amplitudes may then be related to ν at h_o. As the time difference t_o is altered, the collision frequency at other altitudes is measured.

After the $\nu(h)$ profile has been determined, it is possible in principle to determine $N(h)$ from the height attenuation of the wanted wave. The calculation tends to be rather inaccurate and "best-fitting" profiles are sometimes employed (Barrington and Thrane, 1962).

In the last few years, the absorption of cosmic radio noise has led to another method of studying the lower ionosphere. An instrument called a riometer (for relative ionospheric opacity meter) scans across a small portion of the radio frequency spectrum, perhaps a hundred kilocycles, and determines the minimum noise level observed (Little and Leinbach, 1958, 1959). The scanning procedure is necessary to avoid strong interference at various (usually numerous) points across the band. Variations in the minimum noise level with local time are first corrected for the variation of incident radio flux with sidereal time and then the remaining changes are usually attributed to ionospheric absorption (Lusignan, 1960). Under normal circumstances at mid-latitudes, the D and F regions may each contribute about 1 db to the total absorption at wave frequencies between 20 and 30 Mc/s.

When the D region absorption can be separated or when it predominates during "disturbed ionospheric conditions," the absorption on several frequencies can be used to estimate the D region electron density profile (Parthasarathy et al, 1963). Since the absorption is proportional to the integral of $(N\nu)$ with respect to height, it is first necessary to assume the collision frequency profile. (Most recent work assumes that $\nu \propto T$, from which an "effective collision frequency" may be defined.) Then various electron density profiles may be tried and adjusted to best fit the absorption data.

One of the most widely used methods for obtaining electron density profiles is the cw propagation technique pioneered by Seddon (1953). The experiment is performed by firing a rocket equipped with two coherent transmitters in a trajectory as nearly vertical as possible. By Eq. (II-1) the index of refraction for radio waves is $\mu \approx 1 - \left(K_1 N/f^2\right)$, in which the magnetic field has been neglected and a sufficiently high wave frequency is assumed. The constant $K_1 = 40.3$ in mks units. The two radio transmissions are received on the ground and their precise frequencies (or phases) compared in the following manner. The phase velocity of either frequency is $v_p = c/\mu$ and the wavelength is $\lambda_m = v_p/f = \lambda_o/\mu$. These quantities will both change with height as the electron concentration varies. The "electrical length" of the paths is given by

$$L = \int \frac{ds}{\lambda_m} = \int \frac{\mu\, ds}{\lambda_o} \qquad \text{(II-12)}$$

The quantity L is simply the number of electrical wavelengths between the rocket and the receivers, and the time rate of change, $dL/dt = \dot{L}$, is the Doppler shift. For simplicity let us imagine that two frequencies in the ratio $f_2 = 2f_1$, were used. If the electrical length at the higher frequency is divided by two and then compared with the lower frequency, we obtain

$$\Delta L = \frac{1}{2} L_2 - L_1 = \frac{1}{2\lambda_{o2}} \int \left(1 - \frac{K_1 N}{f_2^2}\right) dh - \frac{1}{\lambda_{o1}} \int \left(1 - \frac{K_1 N}{f_1^2}\right) dh \qquad \text{(II-13)}$$

in which the integral extends along the ray path, assumed vertical, between the ground receiver and transmitter located at height h_v. Since $\lambda_{o2} = \frac{1}{2}\lambda_{o1}$, this becomes

$$\Delta L = \frac{1}{\lambda_{o1}} \int_0^{h_v} K_1 N \left(\frac{1}{f_1^2} - \frac{1}{f_2^2} \right) dh = \frac{3}{4} \frac{K_1}{cf_1} \int_0^{h_v} N \, dh \qquad \text{(II-14)}$$

The time derivative of (II-14) may be called the "differential Doppler frequency":

$$\delta \equiv \frac{1}{2}\dot{L}_2 - \dot{L}_1 = \frac{3}{4} \frac{K_1 N}{cf_1} \frac{dh_v}{dt} \qquad \text{(II-15)}$$

From this equation, the electron density profile $N(h)$ may be deduced from the measured differential Doppler frequency. In practice, there are additional complexities introduced by the magnetic field and the horizontal component of the rocket velocity. However, the effect of these correction factors may be reduced by making the vertical velocity as large as possible.

An analogous calculation can be made for the case of coherent transmitters in a satellite in a circular orbit above a spherically symmetric ionosphere; however, in this case only height-integrated electron density, or the electron content is obtained (Garriott and Bracewell, 1961). As before

$$\Delta L = \frac{3}{4} \frac{K_1}{cf_1} \int_0^{h_s} N \sec \chi \, dh \qquad \text{(II-16)}$$

The obliquity of the ray path has been included by letting $ds = \sec \chi \, dh$, where χ is the vertical angle of the ray. Now, the geometric range of the satellite in wavelengths is $R/\lambda_{o1} = 1/\lambda_{o1} \int \sec \chi \, dh$, thus

$$\frac{\Delta L}{\dot{R}/\lambda_{ol}} \approx \frac{\frac{3}{4}\frac{K_1}{cf_1}\sec\chi_F \int N\,dh}{\lambda_{ol}\sec\chi\, h_s} \qquad \text{(II-17)}$$

In the numerator, sec χ should be evaluated at the height of the centroid of the electron density profile in the F region, while in the denominator it should be evaluated at about $(h_s/2)$. But since sec χ is nearly constant with altitude, except at very large zenith angles, the values of sec χ may be cancelled, revealing that both sides of (II-17) should be constant with time during a satellite passage. Furthermore, their time derivatives

$$\frac{\delta}{\dot{R}/\lambda_o} \approx \frac{3K_1}{4f_1^2 h_s}\int_0^{h_s} N\,dh \qquad \text{(II-18)}$$

are in a constant ratio. Since δ is the most frequently measured parameter and $\dot{R}$ and h_s are known from the satellite orbit, the electron content, $\int N\,dh$, may be calculated. Again, more complicated procedures are available to account for the lack of a symmetrical electron distribution (Garriott and de Mendonça, 1963), but this simple derivation contains the essential elements.

Electron content measurements have also been made based on an entirely different principle which requires the presence of the earth's magnetic field in the ionosphere. When an electromagnetic wave passes through an ionized medium in the presence of a magnetic field (as it does in the ionosphere) the polarization of the wave is observed to rotate as long as propagation is not too close to perpendicular to the magnetic field. This phenomenon is called Faraday rotation. The angle through which the polarization is rotated is

$$\Omega = \left(K_2/f^2\right)\int NH\cos\theta\sec\chi\,dh \qquad \text{(II-19)}$$

where K_2 is a constant equal to 0.0298 in mks units, H = magnetic field intensity, θ = angle between magnetic field and ray direction and the rotation angle Ω is expressed in radians. Usually, the terms $(H \cos \theta \sec \chi)$ are taken outside the integral sign as an approximation, since they vary little over the portion of the path in the ionosphere where N is significantly large. A measurement of Ω in addition to knowledge of the pertinent geometric and magnetic field terms will therefore permit the electron content to be calculated.

This method was applied to the polarization of moon echoes by Evans (1957) at Jodrell Bank and the diurnal variation of electron content calculated. The most satisfactory approach involved the transmission of two closely spaced frequencies from which the "differential rotation angle" could be observed.

Even more extensive studies based upon the Faraday effect have been accomplished with satellite transmissions (Lawrence et al, 1963). There is a variety of analysis methods available usually based on either the change in rotation angle in a certain time interval or the rate of rotation during the passage. It is possible to improve the accuracy of the calculations by combining both Faraday and Doppler observations in a "hybrid" method (de Mendonça and Garriott, 1963). From these investigations; the variation of electron content with latitude, local time, season and solar activity has been investigated.

One of the principal purposes for continuing the study of electron content is as an indicator of ionospheric temperature. When the shape of the layer is assumed, the product of N_m and scale height (or temperature) is proportional to the electron content. Since N_m can be determined readily, measured values of electron content may be related to the plasma temperature.

4. Direct Measurements

One of the more useful direct measurement instruments is the dumbbell-shaped electrostatic probe devised by Spencer and his associates (Spencer et al, 1962). The instrument is launched to a high altitude and then ejected from the rocket to avoid any local perturbations. One end of

the device is forced to a negative potential by a sawtooth wave form and the resulting plasma currents are measured as in a Langmuir probe. The measurements are telemetered back to the ground where they may be interpreted in terms of the local ion concentration and the electron temperature. The results of five flights are compared by Brace et al (1963) and permit the comparison of high and middle latitudes, quiet and disturbed conditions and diurnal effects.

The ion concentration profiles follow quite closely the results of ionogram analysis and the profiles deduced from simultaneous two-frequency radio propagation experiments which were discussed in the previous section. However, the daytime electron temperatures are considerably larger than the temperatures deduced for the neutral atmosphere from satellite drag. This is not unexpected, since the electrons released by photoionization will have an excess energy of some 10 ev and a portion of this energy is eventually shared with the rest of the ambient electrons. The results of their electron temperature measurements are summarized in Fig. 8. The theoretical results of Hanson (1962) are very close to the quiet day profile shown here. At night the electrons have time to drop back to the ion and neutral temperature but under disturbed conditions or at high latitudes the electron temperatures remain above 2000 °K.

This temperature nonequilibrium has been further explored by Nagy et al (1963) by measurements made with a spherical ion trap and a thin cylindrical probe. A rocket was launched near noon from a site in Florida, U.S.A., and both ion and electron temperatures were calculated. Between 200 km and 300 km the ion temperature was about 1400 °K while the electron temperature was about 2600 °K. An extensive survey of electron temperature, as a function of position and local time, has been obtained from a probe experiment on the UK-1 satellite "Ariel" (Willmore, Henderson, Boyd and Bowen, in press, 1964). The data refer to altitudes between 400 and 1200 km.

Other direct measurement devices include the Gerdien condenser (useful in the lower ionosphere), rf impedance measurements at frequencies above the local plasma frequency, resonance probes operating near the plasma frequency, intermediate frequency measurements at VLF, and quasi-

D.C. instruments similar to Langmuir probes and ion traps. Most of these instruments have been operated on a number of occasions in the ionosphere and their results intercompared. The paper by Crawford and Mlodnosky (1964) reviews their operation and indicates the required assumptions in regard to electron and ion mobility in each frequency range.

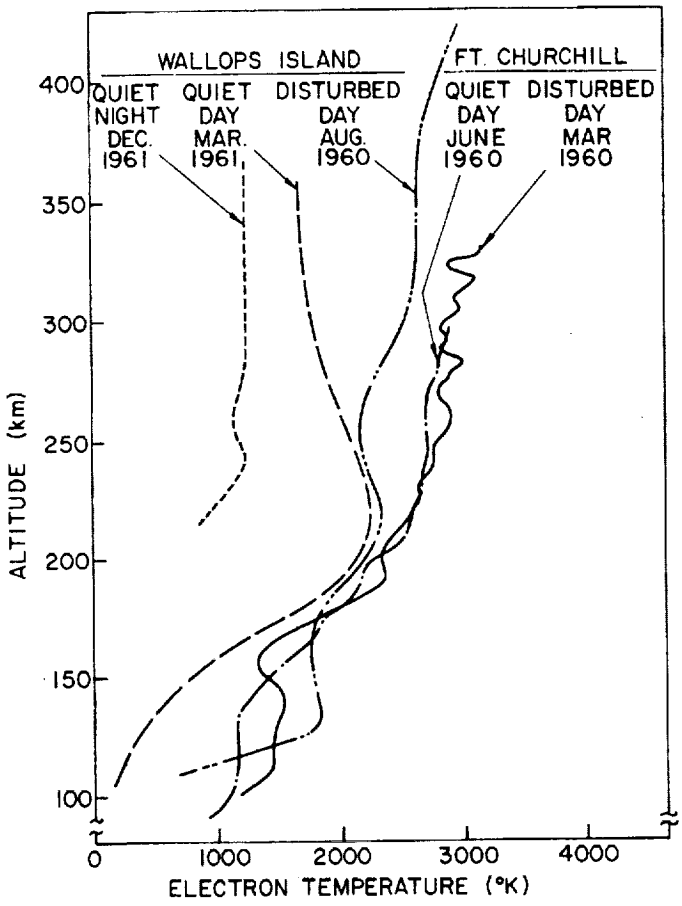

FIG. 8. ELECTRON TEMPERATURE PROFILES OBTAINED ON FIVE ROCKET FLIGHTS FROM WALLOPS ISLAND, VA. (Lat. 38 °N) AND FORT CHURCHILL, CANADA (55 °N). Variations with latitude, local time and magnetic activity all appear to be evident (after Brace et al, 1963).

5. Incoherent Scatter

Conventional ionospheric sounding depends on the reflection of radio waves by an ionized gas, as described before. This reflection process

depends on the collective behavior of electrons, which can be described (at least approximately) in terms of the refractive indices of the Appleton-Hartree equation. A second kind of echo, much weaker than the first, arises from scattering from irregularities or sharp gradients of ionization when the frequency of the radio waves exceeds the local plasma frequency. A third kind of echo, even weaker than the others, is due to the classical Thomson scattering of waves from individual electrons. This has become known as "incoherent scatter"; the power returned is directly proportional to the electron density.

In his initial paper on this subject, Gordon (1958) discussed the conditions under which ionospheric electrons scatter incoherently, so that the return is of the third kind. He found that incoherent scattering occurs if the electronic mean free path exceeds the radio wavelength and exceeds the scale size of irregularities and concluded that these conditions hold at meter wavelengths at heights above 100 km. Given a sufficiently powerful radar, the method could be used to measure electron densities throughout the F region and beyond, to a distance of one earth radius or more.

Experiments first carried out by Bowles (1961), with a 41 Mc/s radar, at 4 - 6 Mw peak power and a 100 μsec pulse length, yielded "scatter profiles" of electron density, from about 100 to 700 km altitude. A high powered scatter radar has now been built at Jicamarca, on the magnetic equator in Peru. It operates at 50 Mc/s and has a maximum peak power of 5 Mw feeding a large array of dipoles over 20 acres in size. Such powerful equipment can be used for purposes other than incoherent scatter, such as investigation of ionospheric irregularities by coherent scatter, and even planetary radar. Examples of electron density profiles to 7000 km altitude have been given by Bowles (1963). Another very large installation is operated by Cornell University in Arecibo, Puerto Rico.

Following the first observation, a number of theoretical papers on incoherent scatter were published (Fejer, 1960; Salpeter, 1960; Dougherty and Farley, 1960). These were largely concerned with the broadening of the spectrum of the returned signal due to thermal motions of the scattering particles. It is found that the breadth of the spectrum depends

on the ionic (rather than the electronic) thermal velocity, and that the spectrum does not have a simple Gaussian form. Applications of this theory give values of temperature broadly consistent with other estimates. In fact, the scattering is not fully incoherent, but depends on weak statistical fluctuations of electron density; in this case, the scattering cross-section corresponds to half of the classical value, the latter being $e^4/4\pi\epsilon_o^2 m^2 c^4 = 1 \times 10^{-28}$ m^2.

More recently, efforts have been made to extend the theory to include complications existing in the actual ionosphere. These are the inequality of electron and ion temperatures in the F region, the existence of light ions (He^+ and H^+) in the upper F region, and the geomagnetic field. The situation appears to be complicated because it may be difficult to distinguish between the effects of the first two factors, though magnetic field effects do not seem likely to be of importance in practice. Some of these matters are dealt with by Fejer (1961), Hagfors (1961), Farley, Dougherty and Barron (1961), Salpeter (1963) and Moorcroft (1964).

There are three ways of obtaining data about ionospheric temperatures from incoherent scatter data. First, the slope of a topside N(h) profile gives the sum of electron and ion temperatures, provided the mean molecular mass M_+ of the ions is known, because as we shall see in Sec. III-5

$$d(\ln N)/dh = M_+ g/R(T_e + T_i) \qquad \text{(II-20)}$$

This equation is not, however, applicable near the magnetic equator. Secondly, the ratio (T_e/T_i) can be deduced from the echo spectrum, again provided the ion species is known. Thirdly, the scattering cross-section, which depends on T_e/T_i, can be deduced from the intensity of the echo if the electron density is known independently from ionosonde data. Obviously, this method requires accurate absolute calibration of the radar system.

It is scarcely surprising that the results so far published involve certain assumptions, mostly about the ionic composition or height dependence of T_e and T_i. Evans (1962) and Pineo and Hynek (1962) find that $T_e/T_i = 1$ at night but is greater by day; Evans reports a maximum ratio of about 1.6 just before noon. Both of these investigations were

carried out with about 2 Mw peak power at 440 Mc/s and cover a range of altitudes between 200 and 700 km. Greenhow, Sutcliffe and Watkins (1963), using 0.1 Mw peak power at 301 Mc/s, measured the diurnal variation of scattering cross-section (and hence of T_e/T_i) near the F2 peak. They found that $T_e/T_i \cong 3$ during the day, but gradually decreases at night to a value of unity after midnight. They also find that by day, $T_e/T_i \cong 4$ near 200 km, but decreases upward. Bowles, Ochs and Green (1962), observing at low latitudes, also find increases of T_e/T_i near sunrise.

Another proposed application of high-power radar equipment may be mentioned here. This is the artificial heating of electrons in the F region. Farley (1963) shows that small but probably detectable changes in the electron profile might be produced by the 50 Mc/s radar at Jicamarca. If a lower frequency, near f_oF2, were employed, it should be possible to produce increases of T_e of several hundred degrees and appreciable reductions of N_mF2 with average powers as low as 100 kw.

III. PROCESSES IN THE IONOSPHERE

1. The Balance of Ionization

We now turn to consider the physical processes which control the ionosphere. In this section, we present only the simplified theory against which the behavior of the actual ionospheric layers can be compared in Sec. IV. We deal here only with the large-scale structure of the ionospheric layers, and completely neglect small-scale irregularities which are considered in Sec. IV-6.

The processes can be divided into two broad categories: those that result in production or destruction of ionization, and those that result in movement of ionization. The terms "photochemical" and "transport" serve as convenient, though not ideal, labels for these two categories. Later, we shall see that the relative importance of these categories varies with height; photochemical processes dominate the lower ionosphere (D and E regions), and we shall in fact suggest that the F2 layer represents a transition from a "photochemical" to a "transport" regime.

It is usual to form an equation of "continuity" or "balance," whose terms represent the effects of the various processes which alter the electron density N. Within a cell of unit volume, we have

[Rate of change of electron density N] = [Gain by production]

- [Loss by destruction] - [Loss by transport]

Continuity equations can also be written for the positive and negative ions, or indeed for any constituent whose concentration is subject to change.

If the transport processes result in a net drift velocity $\underline{v}$, then the loss due to transport is the divergence of the flux $N\underline{v}$. Using symbols q and L to represent production and loss, we have

$$\partial N/\partial t = q - L(N) - \mathrm{div}(N\underline{v}) \qquad \text{(III-1)}$$

This is not unlike the heat conduction equation (I-10) of Sec. I-5. Before we attempt to solve this equation, or even evaluate the terms, it is worth discussing its nature. As it stands, the equation contains derivatives with respect to space and time. But, except in a few special circumstances (as perhaps near sunrise) horizontal gradients of N and $\underline{v}$ are likely to be much smaller than vertical gradients. Horizontal variations generally involve scale distances of hundreds or thousands of kilometers, but vertical scales are a few tens of kilometers. So we can often retain just the vertical contribution to the transport term, $\partial(Nw)/\partial h$, where w is the vertical velocity.

The principal production process for the creation of ion-electron pairs is generally accepted to be the absorption of solar UV and X ray radiation, at least in low and middle latitudes. Photons with energies greater than about 12 ev can ionize one or more of the major atmospheric constituents. This process not only produces the ionization but it also provides the heat input which is necessary to maintain the high temperatures which are found above the E region. The excess energy of the photon is transformed into the kinetic energy of the ion-electron pair and then the remainder of the ionization energy is transformed eventually to heat upon recombination.

At high latitudes and during magnetic storms (and perhaps at other times), there also appears to be a significant production of ions and electrons from collisions between high-energy charged particles precipitated in the atmosphere and the neutral molecules. This "corpuscular ionization" might be produced by the leakage of charge particles stored in the Van Allen belts or perhaps by charged particles in the solar wind. The importance of corpuscular ionization is not yet well established and is a topic of considerable current interest. Finally, if negative ions should be formed in the lower ionosphere by an attachment process, the electrons can be released by photodetachment, which provides another mechanism for electron production.

The important loss processes may be summarized as atomic ion and electron (radiative) recombination; molecular ion and electron (dissociative) recombination; and, in the lower ionosphere, the attachment of an

electron to a neutral molecule. The production and loss processes which are believed to be appropriate to the ionosphere are discussed in some detail in Secs. III-3 and III-4.

The transport term includes the effects of several processes. For many purposes, we may think of the plasma as a gas which represents a minor constituent of the atmosphere. Like the other constituents, it is acted on by gravity and by a force arising from any gradient in its own partial pressure. Unlike the other constituents, the charged particles are also acted upon by electric and magnetic forces. The plasma will diffuse through the neutral air if the forces acting on it are not in equilibrium. Electrons and ions diffuse together because, if they did not, their separation would lead to a large electric field which would quickly bring them together. This so-called "ambipolar" or "plasma" diffusion is opposed by collisions between the charged particles (principally the ions) and the neutral gas. It proceeds rapidly in the F region, but slowly in the lower ionosphere, where collisions are frequent. We develop the equations relating to plasma diffusion in Secs. III-5 and III-6.

The plasma tends also to be set in motion by movements of the neutral air, which may be due to large-scale wind systems or to temperature changes. But, particularly in the F region, the plasma tends to move parallel to the geomagnetic field lines. It can also be moved across the field lines by large-scale electric fields. Under certain circumstances, especially in the E region, the ions and electrons may move with different velocities so that an electric current flows. We find it convenient to postpone discussion of this topic until Sec. VI, which deals with the relationship between geomagnetism and the ionosphere.

A particular form of plasma diffusion is the interchange of ionization between the ionosphere and the magnetosphere, where the positive ions are mainly protons. This requires a charge exchange process which has been discussed by Hanson and Ortenburger (1961). Possibly a downwards diffusion of plasma from the exosphere could help to maintain the F2 layer at night, though it is not clear that this process would be sufficient.

In the lower ionosphere, two simplifications can often be made. Transport processes are not very important, and if they are neglected entirely, a "photochemical" equation results, containing only the one derivative $\partial N/\partial t$. Furthermore, the "time constant" associated with the loss term $L(N)$ may be so short that $\partial N/\partial t$ is much smaller than the other terms, so the "photochemical equilibrium" equation $q = L(N)$ is adequate. This is generally the case in the D, E and F1 layers by day, except for rapidly-varying phenomena such as eclipse effects. Transport can be then included as a small perturbation if required.

2. Chapman's Theory

A surprisingly good description of many of the features of the earth's ionosphere can be obtained from a theoretical study of the simplest model of the atmosphere and the incident flux. The theory was developed by Chapman (1931a, b) and has proven such a useful description that it is identified with his name. We will therefore consider an atmosphere composed of a single constituent with a monoenergetic UV flux incident upon it. A "flat earth" will be assumed at first but this can be generalized to a spherically stratified atmosphere with little difficulty. The temperature profile will remain arbitrary, but we will later specialize our discussion to the case of a linear temperature variation with altitude. Chapman's original work considered the isothermal case, which is readily obtained from the equations below.

The intensity of the incident solar radiation beyond the atmosphere will be denoted by I_∞ (photons/cm^2/sec). There is a certain probability that each molecule will be ionized in unit time when subjected to unit flux density, and this probability is usually expressed as a "cross-section" which will vary with wavelength and the molecular species. For our simple model, a single cross-section σ is assigned. As the radiation passes through the atmosphere, the incremental reduction in intensity is

$$dI = -I \sigma n \, ds \qquad \text{(III-2)}$$

in which ds is an element of path length in the direction of power flow. (Many derivations replace (σn) with $(A\rho)$, in which A is the "mass absorption coefficient" and ρ is the gas density.) Since $-ds = \sec \chi \, dh$, where χ is the zenith angle above a flat earth

$$(dI/I) = \sigma n \sec \chi \, dh \qquad \text{(III-3)}$$

When this equation is integrated, we obtain

$$I(h)/I_\infty = \exp \left\{ -\sigma \sec \chi \int_h^\infty n \, dh \right\} \qquad \text{(III-4)}$$

Using the result of Eq. (I-6), namely

$$\int_h^\infty n \, dh = n(h) \, H(h) \qquad \text{(I-6)}$$

we obtain

$$I(h)/I_\infty = \exp \{-\sigma n H \sec \chi\} \equiv e^{-\tau} \qquad \text{(III-5)}$$

which serves to define the "optical depth," τ. The height at which $\tau = 1$, corresponding to a reduction of $(1/e)$ in the incident radiation, provides a convenient measure of the depth of penetration of the radiation.

We will assume that the absorption of one photon produces one ion-electron pair, which is true for most of the UV spectrum. Then, the production rate q (pairs/cm^3/sec) is obtained from

$$q(h) = dI/ds = \cos \chi \, (dI/dh) \qquad \text{(III-6)}$$

$$q(h) = -I_\infty \cos \chi \, e^{-\tau} \, (d\tau/dh) = -I_\infty \sigma \, e^{-\tau} \, \frac{d}{dh} (n H) \qquad \text{(III-7)}$$

From Eq. (I-6) we see that $d(n\,H)/dh = -n$, so that

$$q(h) = I_\infty \sigma\, n(h)\, e^{-\tau} \qquad \text{(III-8)}$$

To locate the production peak, we set $d(\ln q)/dh = 0$, giving

$$\frac{1}{n}\frac{dn}{dh} = \frac{d\tau}{dh} = \sigma \sec \chi \frac{d}{dh}(n\,H) \qquad \text{(III-9)}$$

We see that q is greatest at the level where the downward increase of gas concentration just compensates for the rate of attenuation of the radiation. From the perfect gas law $p = nkT$ we deduce, as in Eq. (I-7),

$$\frac{1}{n}\frac{dn}{dh} = -\frac{1}{H}\left(1 + \frac{dH}{dh}\right) \qquad \text{(III-10)}$$

When Eqs. (III-9) and (III-10) are combined, we observe that

$$n \sigma \sec \chi\, H = 1 + \frac{dH}{dh} = \tau \qquad \text{(III-11)}$$

at the peak. For positive scale height gradients, the peak of production lies just <u>below</u> the level of unit optical depth.

This equation suggests two convenient levels at which our reference altitude, $h = h_o$, might be established. We could set (a) $n_o \sigma H_o = 1 + (dH/dh)_o$, that is at the altidue of maximum production for an overhead sun, or (b) $n_o \sigma H_o = 1$, the altitude of unit optical depth for overhead sun. Although the choice is quite arbitrary, we will select the former definition. In the simple case in which H is independent of height, these levels naturally coincide; otherwise level (a) lies Γ_o scale heights below level (b), where $\Gamma_o = (dH/dh)_o$.

We can now obtain the maximum production rate for overhead sun from Eq. (III-8):

$$q(h_o) = I_\infty \sigma\, n_o e^{-(1+\Gamma_o)} = \frac{I_\infty (1 + \Gamma_o)}{H_o \exp(1 + \Gamma_o)} \equiv q_o \qquad \text{(III-12)}$$

We would like to put these equations in terms of the reduced height parameter, z. It is therefore convenient to specialize our equations to the case of a linear temperature and scale height variation. We may write $H = H_o + \Gamma(h - h_o)$ and then proceed as follows:

$$z = \int_{h_o}^{h} \frac{dh}{H_o + \Gamma(h - h_o)} = \frac{1}{\Gamma} \ln\left(\frac{H}{H_o}\right) \qquad \text{(III-13)}$$

obtaining

$$H = H_o \, e^{+\Gamma z} \qquad \text{(III-14)}$$

and there is a similar equation for $T = T_o e^{+\Gamma z}$. The expression for the neutral concentration is

$$n = \frac{p}{kT} = \frac{p_o \, e^{-z}}{k \, T_o e^{+\Gamma z}} = n_o \, e^{-z(1+\Gamma)} \qquad \text{(III-15)}$$

When Eqs. (III-14) and (III-15) are inserted in (III-8), we find

$$q(z) = q_o \exp\left[(1 + \Gamma)(1 - z - e^{-z} \sec \chi)\right] \qquad \text{(III-16)}$$

(A rather different expression is obtained when h_o is identified with the height of unit optical depth.)

To find the reduced height of the production maximum, we solve Eq. (III-11) for z_m;

$$\sigma \sec \chi \, n_o \, e^{-z_m(1+\Gamma)} \, H_o \, e^{+\Gamma z_m} = 1 + \Gamma \qquad \text{(III-17)}$$

Therefore,

$$z_m = \ln (\sec \chi) \qquad \text{(III-18)}$$

which, of course, is zero for overhead sun. When Eq. (III-18) is inserted in Eq. (III-16) we find the maximum production rate to be

$$q_m = q_o(\cos \chi)^{1+\Gamma} \qquad \text{(III-19)}$$

For the case of an isothermal layer ($\Gamma = 0$), Eq. (III-16) reduces to the simple Chapman formula

$$q = q_o \exp [1 - z - e^{-z} \sec \chi] \qquad \text{(III-20)}$$

This function has the interesting property that as χ varies, its shape is unchanged, its peak is shifted to the level $z_m = \ln (\sec \chi)$ and its amplitude is scaled by the factor $\cos \chi$. This can be shown be writing the above equation in the form

$$q = (q_o \cos \chi) \exp \left[1 - (z - z_m) - e^{z_m - z}\right] \qquad \text{(III-21)}$$

In Fig. 9, the ratio (q/q_o) is plotted for several values of χ. We see that above the peak, q depends very little on χ. This is also illustrated in Fig. 10, which shows $q(\chi)$ curves for several fixed values of z. At large positive values of z, $q(\chi)$ is almost independent of χ until χ approaches 90 deg and $\sec \chi > e^{-z}$. As z decreases, the function $q(\chi)$ becomes increasingly sensitive to χ. In the ionosphere, this means that the maximum of q, which occurs at noon when χ is least, becomes increasingly sharp with decreasing z. Some of the properties of this function have been discussed by Cummack (1961).

In the actual ionosphere, the production formula is considerably more complicated. First, there may be several atmospheric gases, differently distributed, in which case the product (σn) in Eq. (III-2) must be replaced by a summation, $\sum_i \sigma_i n_i$. Some equations for a two-gas mixture were given by Rishbeth and Setty (1961). Also, the ionizing radiation is not monochromatic, but consists of a range of wavelengths, and the

An approximation to the Chapman function can be obtained in the following manner. In Fig. 11, we are shown a point a distance h_o above the earth at which the sun's zenith angle is χ_o and for which we will evaluate the Chapman function. The minimum altitude of the ray is $h_g = (R_o + h_o) \sin \chi_o - R_o$, which we may call the "grazing height."

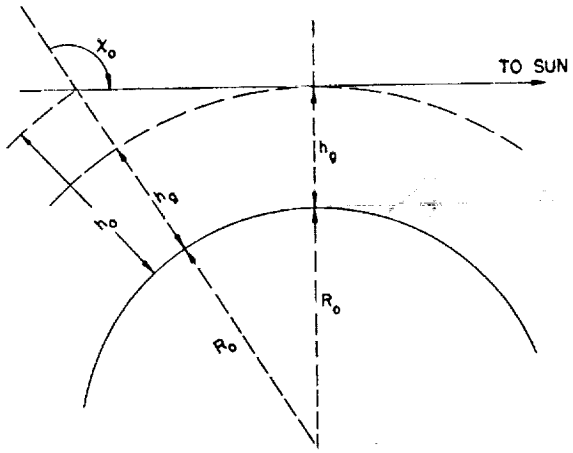

FIG. 11. GEOMETRY USED IN THE CALCULATION OF Ch (χ_o).

From the two preceding equations, we obtain

$$Ch\ (\chi_o) = \frac{\int n \sec \chi \, dh}{H\, n(h_o)} \qquad \text{(III-24)}$$

although this is not in the same form as originally expressed (Chapman, 1953). Expanding these terms,

$$Ch\ (\chi_o) = \frac{\int_{h_g}^{\infty} n(h_g) \sec \chi \exp\left\{\frac{h - h_g}{H}\right\} dh \pm \int_{h_g}^{h_o} n(h_g) \sec \chi \exp\left\{\frac{h - h_g}{H}\right\} dh}{H\, n(h_g) \exp\left\{\frac{h_g - h_o}{H}\right\}} \qquad \text{(III-25)}$$

In this equation, the upper sign is used for $\chi_o > 90$ deg, while the lower sign is applied when $\chi_o < 90$ deg.

If we now measure the reduced height from the grazing level, so that $\tau \equiv (h - h_g)/H$, the last equation becomes

$$Ch\ (\chi) = e^{\tau_o} \left\{ \int_o^\infty e^{-\tau} \sec \chi\ d\tau \pm \int_o^{\tau_o} e^{-\tau} \sec \chi\ d\tau \right\} \qquad \text{(III-26)}$$

Some additional work will show that these integrals may be approximated by

$$\int e^{-\tau} \sec \chi\ d\tau \approx \sqrt{\frac{R_o}{2H}} \int \frac{e^{-\tau}\ d\tau}{\sqrt{\tau}} \qquad \text{(III-27)}$$

which is sufficiently accurate as long as $H \ll R_o$, so that $\exp(-\tau) \to 0$ well before the height variable approaches the value R_o. Also, it should not be applied for small χ, where the optical depth is proportional to $\sec \chi$ anyway. However, it is quite a good approximation near $\chi = 90$ deg where the Chapman function is required, and is quite useful in almost all cases of ionospheric interest. The integrals may then be evaluated in terms of the error function, giving

$$Ch\ (\chi_o) \approx \sqrt{\frac{\pi R_o}{2H}} \exp(\tau_o) \left\{1 \pm \text{erf} \sqrt{\tau_o}\right\} \qquad \text{(III-28)}$$

Since the error function is tabulated in many places, Eq. (III-28) may be more conveniently applied than $Ch\ (\chi_o)$, and it may also be more readily evaluated in a computer. $Ch\ (\chi_o)$ has been tabulated by Wilkes (1954) as a function of χ_o and the ratio of the ionosphere radius to scale height. $Ch\ (\chi_o)$ departs markedly from $\sec \chi$ for $\chi \gtrsim 80$ deg and for large H, as shown in Fig. 12. The approximation in Eq. (III-28) does not depart significantly from the true values of $Ch\ (\chi_o)$ shown below.

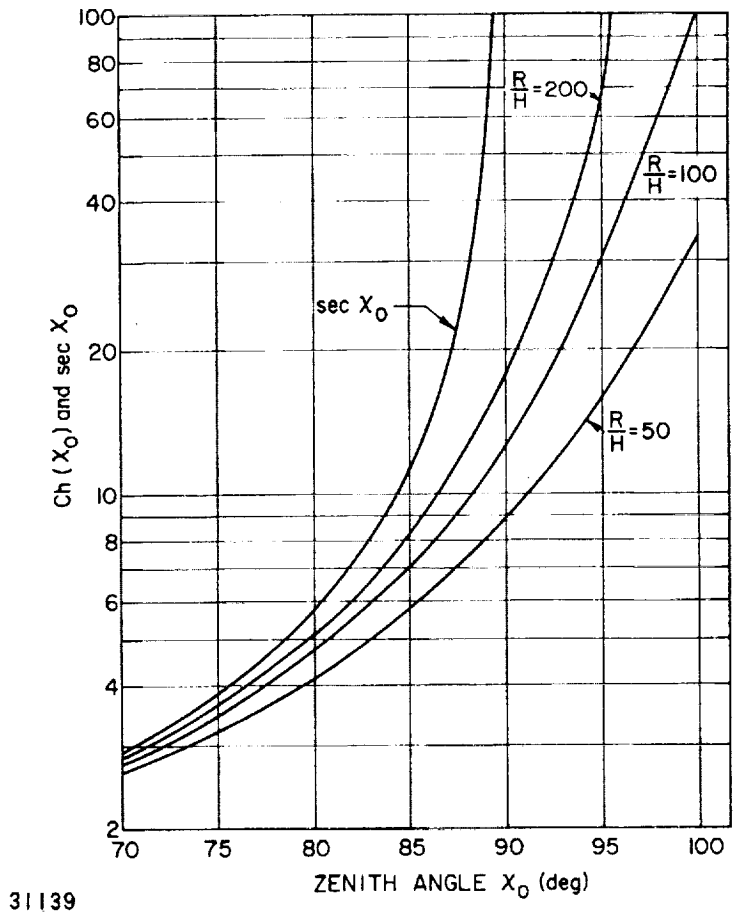

FIG. 12. SEC χ_o AND Ch (χ_o) VS χ_o, PARAMETRIC IN (R/H). R and H are the geocentric radius and scale height of the atmospheric layer.

When considering problems at large zenith angles, it is necessary to replace sec χ with Ch (χ_o) wherever it occurs in the preceding equations. From Fig. 12, it is clear that the optical depth does not become infinite at χ_o = 90 deg and that significant production may occur for zenith angles as large as 95 deg or 100 deg. This is particularly true at the greater altitudes, because the ray paths from the sun do not penetrate deeply into the atmosphere even for $\chi \approx 100$ deg.

Having found the production function $q(z)$, it is a simple matter to find the photochemical equilibrium electron density profile when the transport term in Eq. (III-1) is neglected. When electron loss is proportional to N^2, the continuity equation becomes $\partial N/\partial t = 0 = q - \alpha N^2$, from which

$$N = \sqrt{q/\alpha} \qquad \text{(III-29)}$$

and therefore the peak electron density N_m and the critical frequency f_o of a Chapman layer are connected by

$$f_o \approx 9\sqrt{N_m} \propto (\cos \chi)^{1/4} \qquad \text{(III-30)}$$

If there is a vertical temperature gradient, we may expect the exponent of $\cos \chi$ to be different. We can see from Eq. (III-19) that if $\Gamma = dH/dh$ is independent of height,

$$f_o \propto (\cos \chi)^{0.25(1+\Gamma)} \qquad \text{(III-31)}$$

3. Production and Loss

The production of ionization is principally complicated by the wide spectrum of the radiation generated in the chromosphere and the corona of the sun. Wavelengths from a few Angstroms to almost 2000 Å are all important in the ionosphere. The spectral lines characteristic of hydrogen, helium, carbon, silicon and many other elements are all found in the radiation spectrum.

We should also distinguish between an absorption cross-section which expresses the probability that a given molecule will absorb a photon and an ionization cross-section which is the probability that an ion-electron pair will be produced. In the previous section on Chapman layers, they were assumed identical. More precisely, σ should be interpreted as the absorption cross-section and then each equation for production multiplied by the ratio of the ionization to the absorption cross-section. Since these cross-sections are dependent upon wavelength and molecular species, we may expect the incident radiation to be absorbed over a wide range of altitudes as implied by Eq. (III-11).

The best current values for flux intensity vs wavelength come from the rocket measurements of Hinteregger and Watanabe (1962) and the measurements made in the Orbiting Solar Observatory (Lindsay, 1963). Fig. 13

shows the EUV flux vs wavelength and is derived principally from the references just mentioned, but it includes some results of other experimenters. From Eq. (III-12) we can calculate the maximum production rate at any wavelength, but the absorption cross-section is needed to compute

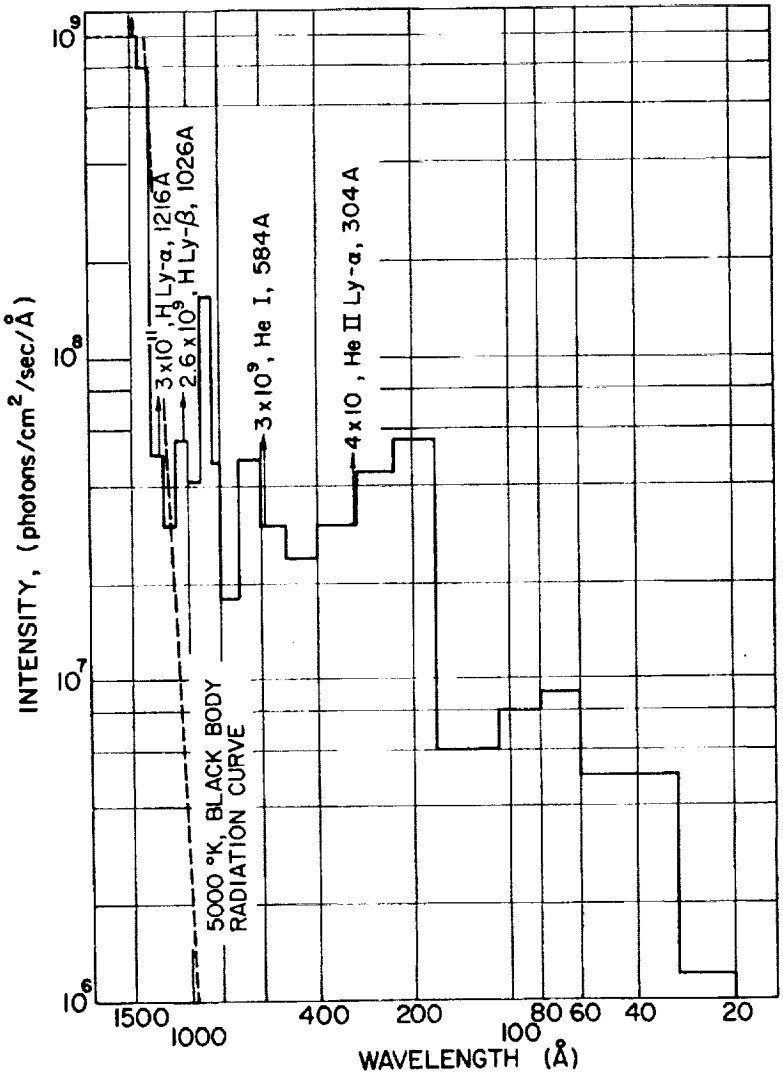

31140

FIG. 13. EXTREME-ULTRAVIOLET (EUV) FLUX VS WAVELENGTH, BASED ON THE DATA OF WATANABE AND HINTEREGGER (1962). Several of the more prominent line emissions are shown, along with the distributed radiation. The 5000 °K black body emission is shown as a broken line, and it may be seen that the solar radiation exceeds this value below about 1100 Å.

the altitude at which it occurs. Based on Hinteregger's cross-sections and the model atmosphere used in Sec. I, Fig. 14 shows, as a function of wavelength, the height of unit optical depth, at which vertically incident radiation is attenuated to a fraction $1/e$ of its intensity above the atmosphere. We can now compute the production profiles as well, and these are shown in Fig. 15 for the case of overhead sun. They refer to a fairly low level of solar activity, current at the time of their rocket experiment in 1961. We see in Fig. 15a that $q[O^+]$ is greatest at about 170 km.

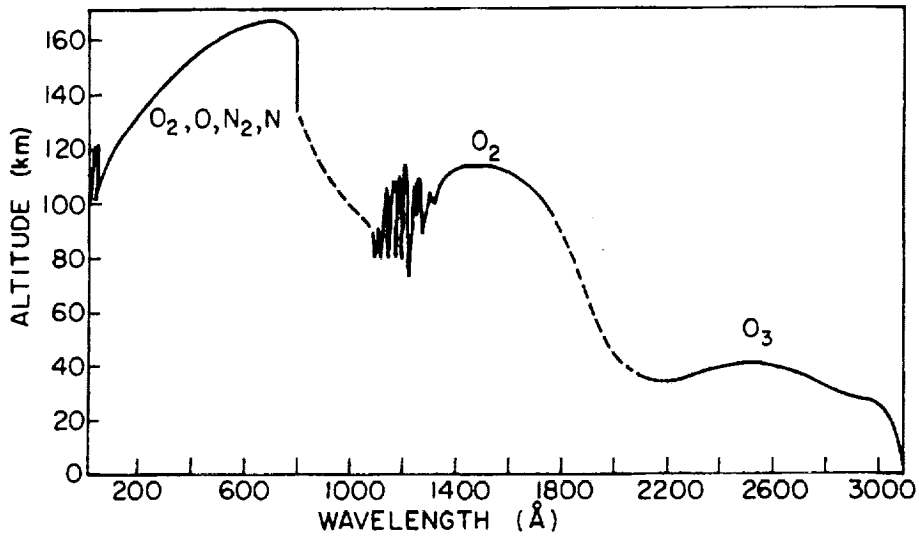

31138

FIG. 14. THE ALTITUDE OF UNIT OPTICAL DEPTH VS WAVELENGTH (after Friedman, 1960).

Figure 15b shows that $q[N_2^+]$ also peaks at this level, though as mentioned later it is uncertain how much the ionization of N_2 contributes to the observed electron density. According to Fig. 15c, a major part of the E region ionization arises from the wavelength band 911 - 1027 Å, which cannot ionize O or N_2, and which includes the very strong solar Lyman β line at 1026 Å. This greatly exceeds the contribution made by X rays in the range 10 - 170 Å, although Norton, Van Zandt and Denison (1963) consider the latter to be more important in the E region.

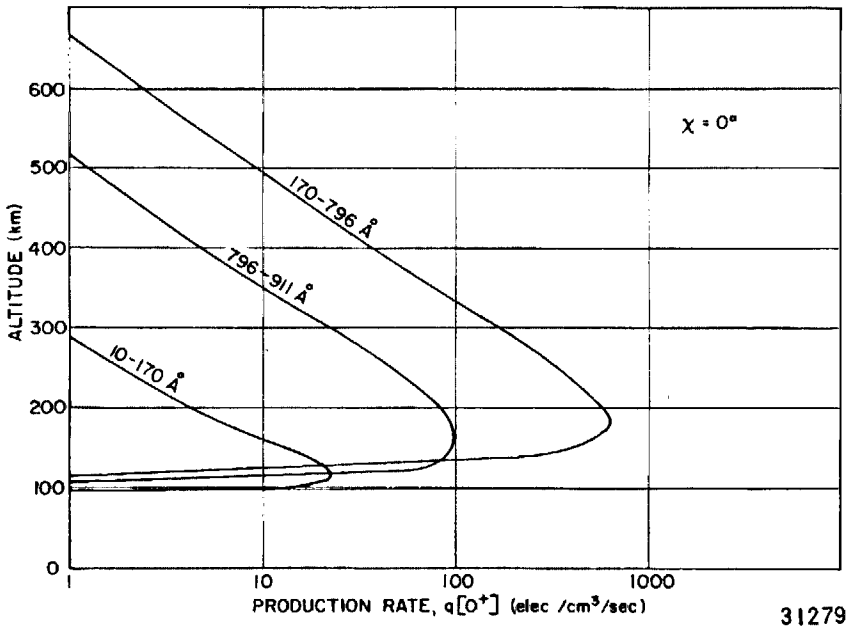

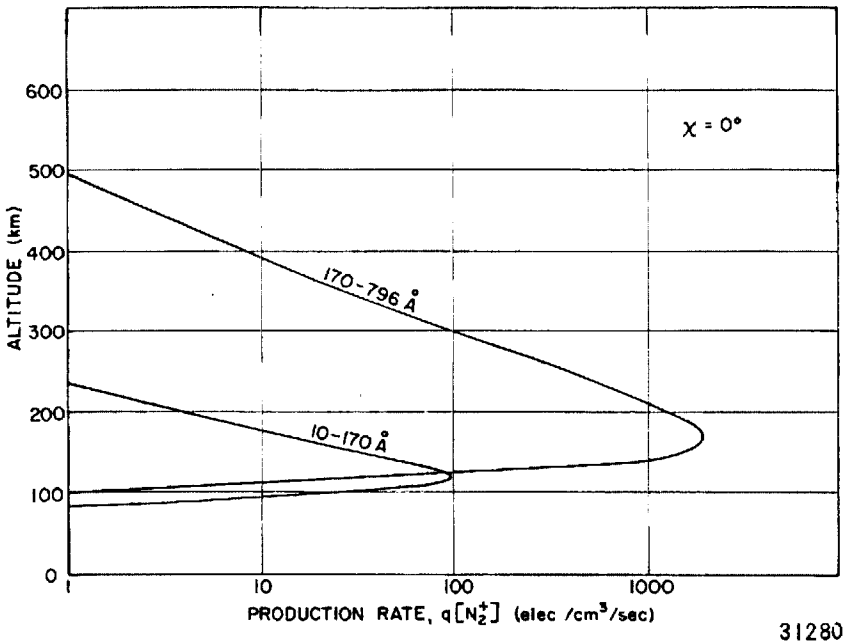

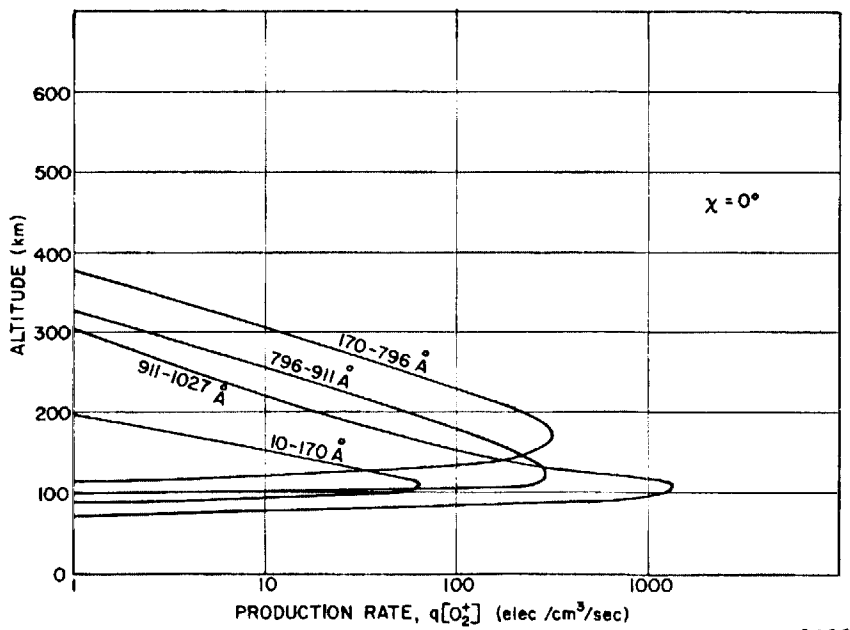

FIG. 15a,b,c. ILLUSTRATING THE WAVELENGTH DEPENDENCE OF THE PRODUCTION PROFILES FOR O^+, N_2^+ AND O_2^+. The neutral atmosphere is that of Harris and Priester, applicable near 0400LT, while the solar flux (see Fig. 13) and ionization cross-sections were obtained from Watanabe and Hinteregger. The zenith angle is zero.

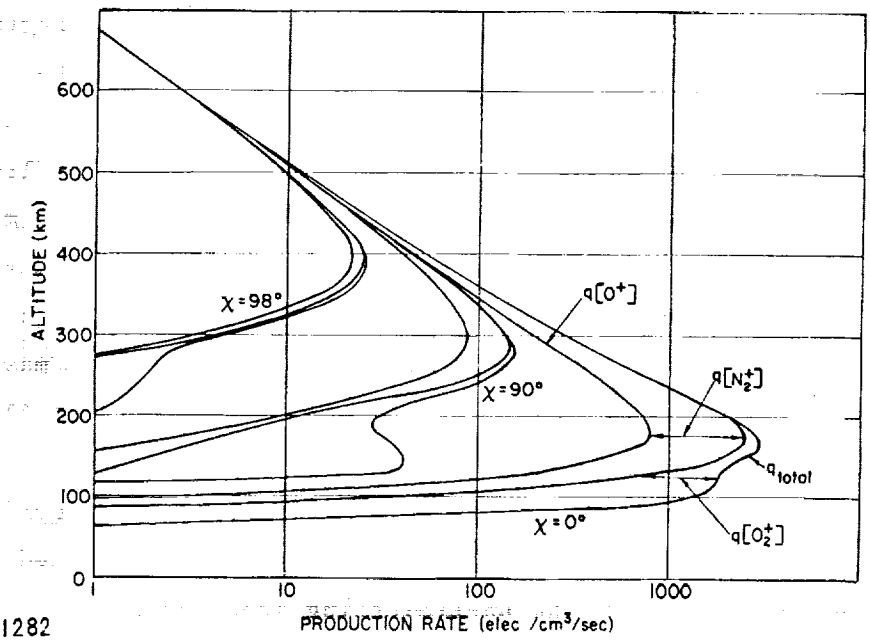

FIG. 15d. ILLUSTRATING THE ZENITH ANGLE DEPENDENCE OF THE PRODUCTION PROFILES FOR O^+, N_2^+ and O_2^+. The same models were used as in Figs. 15a,b,c. Three curves are drawn for each zenith angle χ = 0, 90, and 98 deg. The curve with the smallest production rate in each set is $q[O^+]$. The difference between this curve and the middle curve in each set is $q[N_2^+]$. The difference between the middle curve and the total production rate is $q[O_2^+]$, as is shown for χ = 0 deg.

Ionization can be produced not only by solar photon radiation, but also by energetic particles which can enter the atmosphere most easily at high magnetic latitudes. The enhancements of ionization observed at high latitudes during magnetic disturbance are certainly due to fast electrons or protons. The mechanisms by which these particles acquire their energy are part of the general problem of high-latitude and magnetic storm phenomena. We note, however, that the depth to which particles penetrate depends on their energy. Some calculations of penetration depths have been given by Bailey (1959) and Rees (1963). It has been suggested that corpuscular ionization is responsible for much of the ionization and heating in the F2 layer (Antonova and Ivanov-Kholodnyy, 1961; Harris and Priester, 1962a). The only radiation likely to be absorbed at these heights would be soft electrons of not more than a few hundred ev.

The ionization process would lead to emission of the 6300 Å airglow line of atomic oxygen, and this can be used to set an upper limit to its rate.

The luminosity vs height profile for a monoenergetic source has the same shape as the ionization profile; it is only necessary to alter its magnitude. For the 3914 Å radiation from excited N_2^+, it is estimated that about 1 photon is emitted for every 50 ion-electron pairs produced, and each pair requires about 35 ev for ionization. If the luminosity profile is measured with a photometer, the production profile may be calculated from which the energy and intensity of the incident flux may be estimated (Rees, 1963).

The kinds of photochemical reaction which are thought to control the ionospheric electron density are considered next. The idealized chemical equations are given although the participating ions and neutral particles will not be identified in most cases until the experimental data are discussed in the next section. The mechanisms for loss of ionization have been discussed in two important articles by Bates and Massey (1947); the pertinent reactions are listed below.

(a) Ion-ion recombination (coefficient α_i)

$$X^+ + Y^- \rightarrow X + Y$$

(b) Electron-ion recombination (coefficient α_e)

Three-body: $X^+ + e + M \rightarrow X + M$

Radiative: $X^+ + e \rightarrow X^* \rightarrow X + h\nu$

Dissociative: $XY^+ + e \rightarrow X^* + Y^*$

The asterisks indicate that the atoms may be left in excited states, and subsequently lose this energy by radiation or during collisions with other particles. The symbol M denotes a neutral particle which exchanges energy and momentum but does not take part in the chemical reaction. Three-body processes can occur in the lower D region, but are so rare at greater heights as to be quite unimportant. Apart from this means, recombination of electrons and atomic ions can take place only by the very slow radiative process (coefficient $\sim 10^{-12}$ cm^3/s) or possible by other equally slow reactions. Only in the uppermost F region is

radiative recombination likely to be the fastest loss process, and we shall see that at such heights transport processes (especially diffusion) are so completely dominant that loss coefficients are irrelevant. Elsewhere in the F and E regions, the dissociative recombination process, with coefficients of order 10^{-7} or 10^{-8} (cm^3/s), are more important.

Since a large proportion of the ions are originally atomic, dissociative recombination must be preceded by reactions involving formation of molecular ions, namely:

(c) Ion-atom interchange (rate coefficient γ)

$$X^+ + YZ \rightarrow XY^+ + Z$$

While it is generally accepted that ion-atom interchange followed by dissociative recombination is the principal loss process in the E and F regions, there is considerable controversy as to precisely which reactions are important. Although charge-exchange reactions can also lead to formation of molecular ions, the ion-atom interchange process is thought to be more rapid (Bates, 1955).

(d) Attachment (coefficient a) and collisional detachment (coefficient d_c)

$$X + e + M \leftrightarrows X^- + M$$

(e) Associative detachment

$$X^- + Y \rightarrow XY + e$$

(f) Photodetachment (coefficient d_p)

$$X^- + h\nu \rightarrow X + e$$

A summary of the conclusions of this section is provided in Table I with additional comments regarding the importance of the various processes.

4. The D, E and F1 Photochemical Regime

In the lower ionosphere, transport may be neglected and only photochemical terms appear in the continuity equations for the ion concentrations N_+, N_- and the electron concentration N_e. For the present, we add the subscript "e" for the sake of clarity. These equations are therefore written as

processes. Hence, by day, λ decreases upward, and is probably small above 90 km. At night, however, $d_p \approx 0$ and λ depend on the ratio a/d_c. Above 100 km, ionic recombination would limit the equilibrium nighttime value of N_-, and at greater heights where $1/a$ exceeds a few hours, equilibrium conditions are scarcely applicable.

When, as in the daytime D region, attachment and detachment are so rapid that λ is constant, we can substitute Eq. (III-35) into Eq. (III-32) and obtain

$$(1 + \lambda)\, dN_e/dt = q - (1 + \lambda)(\alpha_e + \lambda\alpha_i)N_e^2$$

$$= q - \alpha_E N_e^2 \qquad \text{(III-37)}$$

The so-called "effective" coefficient α_E, as defined in these equations, rapidly approaches α_e with increasing altitude because of the decrease of λ.

So far, we have described the chemical processes in rather general terms. In reality, discussion of the D region is hampered by the fact that the ions present have not been identified. Since nitrogen does not form stable negative ions, it has generally been assumed that O^- or O_2^- is the most important. There is, however, some controversy about the electron affinity of atomic oxygen, which is important because it determines whether visible light or UV is required for photodetachment, and thus influences our interpretation of D region phenomena, especially at sunrise. Other suggestions, such as O_3^- and NO_2^-, as to the dominant negative ion have been advanced (e.g., Reid, 1961). Neither have the positive ions been identified, but NO^+ (which, as we shall see, is the dominant ion in the E layer) may be the principal ion. It can be formed either by photoionization of NO or by various chemical reactions. Presumably O_2^+ and N_2^+ are also present. Further consideration of D and E region photochemical processes may be found in Nicolet and Aikin (1960), Crain (1961), Poppoff and Whitten (1962, 1964), Pierce (1963), and Webber (1962).

Let us now examine the situation at greater heights, in the E and F1 regions, where the reactions involving negative ions are unimportant. Under these circumstances, the only important recombination process is dissociative recombination of electrons and molecular positive ions. Since a large proportion of the neutral atmosphere is atomic, especially in the F region, atomic ions are produced by photoionization, but these do not recombine with electrons directly, except by the very slow radiative process. Instead, they undergo an ion-atom interchange reaction and the molecular ions thus formed combine with electrons. We shall consider the electron distributions resulting from this situation in a general way, before discussing the actual reactions which occur.

In writing the continuity equations for the concentrations of electrons N, atomic ions N_A and molecular ions N_M, we assume that the ion-atom interchange reaction involves molecules "m," but that we can neglect the direct production of molecular ions by photoionization. This could be a realistic situation, since it is possible that the dissociative recombination rate of N_2^+ is quite large (perhaps 10^{-7} or more) in which case the ion would recombine so rapidly that it would not contribute to the "observable ionization." Proceeding on this assumption for the moment, we write

$$dN/dt = q - \alpha N N_M$$

$$dN_A/dt = q - \gamma n(m) N_A \qquad \text{(III-38)}$$

$$dN_M/dt = \gamma n(m) N_A - \alpha N N_M$$

Charge neutrality again requires $N = N_A + N_M$. If we write $\beta = \gamma n(m)$, and assume equilibrium, we can eliminate the ionic concentrations N_A and N_M, and obtain a quadratic equation in N (Hirsh, 1959):

$$\alpha\beta N^2 - \alpha q N - \beta q = 0 \qquad \text{(III-39)}$$

of which the positive root is

$$N = (q/2\beta)\left[1 + (1 + 4\beta^2/\alpha q)^{1/2}\right] \qquad \text{(III-40)}$$

This reduces to

$$N = N_\alpha = \sqrt{q/\alpha} \qquad \text{if} \quad 4\beta^2 \gg \alpha q$$

$$N = N_\beta = q/\beta \qquad \text{if} \quad 4\beta^2 \ll \alpha q \qquad \text{(III-41)}$$

$$\text{or} \qquad N^2 = N_\alpha^2 + NN_\beta \qquad \text{in general}$$

Alternatively, the quadratic can be written as

$$\frac{1}{q} = \frac{1}{\beta N} + \frac{1}{\alpha N^2} \qquad \text{(III-42)}$$

which reduces to

$$q = \alpha N^2 \qquad \text{if} \quad \beta \gg \alpha N$$

$$q = \beta N \qquad \text{if} \quad \beta \ll \alpha N \qquad \text{(III-43)}$$

The conditions ">>" and "<<" occurring in Eq. (III-43) are, of course, roughly equivalent to those in Eq. (III-41).

These equations demonstrate how the two-stage loss process proposed by Bates and Massey (1947) gives rise to a transition between a "quadratic" loss law (αN^2) and a "linear" loss law (βN). Returning to the balance equations (III-38), we see that $N_A/N_M = \alpha N/\beta$ at equilibrium, so that when the rate of electron loss is determined by the dissociative recombination reaction, the ions are mainly molecular and the "αN^2 law" applies. The coefficient α may depend on temperature, but is otherwise not height dependent, unlike β which varies as the molecular concentration

$n(m)$ and therefore decreases rapidly upward. So at greater heights, we expect the condition $\beta \ll \alpha N$ to apply, in which case the ion-atom interchange reaction controls the rate of loss and the ions are mostly atomic.

As we shall see in a moment, rocket data on the ionic composition confirm that this transition between "αN^2" and "βN" loss laws occurs in the lower F region, at about 160 - 200 km. This happens to coincide with the level at which the F region production rate q is greatest, and Ratcliffe (1956) showed that this might account for the splitting of the F2 layer into F1 and F2 components. To demonstrate this, we investigate the shape of the equilibrium electron distribution by evaluating the formula (III-40) using the Chapman production function $q(z,\chi)$ for an isothermal layer, Eq. (III-21), and a height-independent recombination coefficient α. If we introduce a new quantity $k = H_i/H_\beta$, the ratio of the scale heights of the ionizable gas and the linear loss coefficient, we can write $\beta \propto e^{-kz}$.

Since $\beta = \gamma n(m)$, k depends on the molecular mass of the gas participating in the ion-atom interchange reaction, which may be O_2 or N_2. Since the principal ionizable gas is O, we have $k = 32/16 = 2$ for O_2 and $k = 28/16 = 1.75$ for N_2 provided these gases are diffusively separated, which is found to be the case above the E region. If the coefficients γ were very temperature dependent, the value of k might be modified, but probably is not very different from the above-mentioned values in the F region.

We found in the previous section that the shape of the Chapman production function does not change as the solar zenith angle χ varies, but that the level of the peak varies according to the relation $z = \ln \sec \chi$. The form of Eq. (III-40) suggests that a single parameter, $\beta^2/\alpha q$, determines the shape of the electron density distribution $N(z)$. Let r denote the value of $\beta/\sqrt{\alpha q}$ at the level of peak production. Provided r (and k) are kept constant, changes of q and β can alter the magnitude of the function $N(z)$ and displace it with respect to the z-axis, but do not affect its shape. We note that from Eq. (III-41),

$$r = \beta/\sqrt{\alpha q} = N_\alpha/N_\beta \qquad \text{(III-44)}$$

and in Fig. 16 plot $N(z)$ for $r = 1$, $r = 2$, $r = 3$. The graph is drawn in such a way that the dotted curve, which represents $N_\alpha = \sqrt{q/\alpha}$ for $z = 0$, is the same in each case, but different values of β_o are chosen so as to give three dashed curves N_β, and three solid curves for N. We see that if $r = 1$, the $N(z)$ profile is almost smooth, but that a "ledge" appears for $r = 2$ and is more prominent for $r = 3$. On an $h'(f)$ curve, such a ledge would produce a prominent cusp, as shown by Hirsh (1959), and we may identify this with the splitting of the F layer into F1 and F2 components.

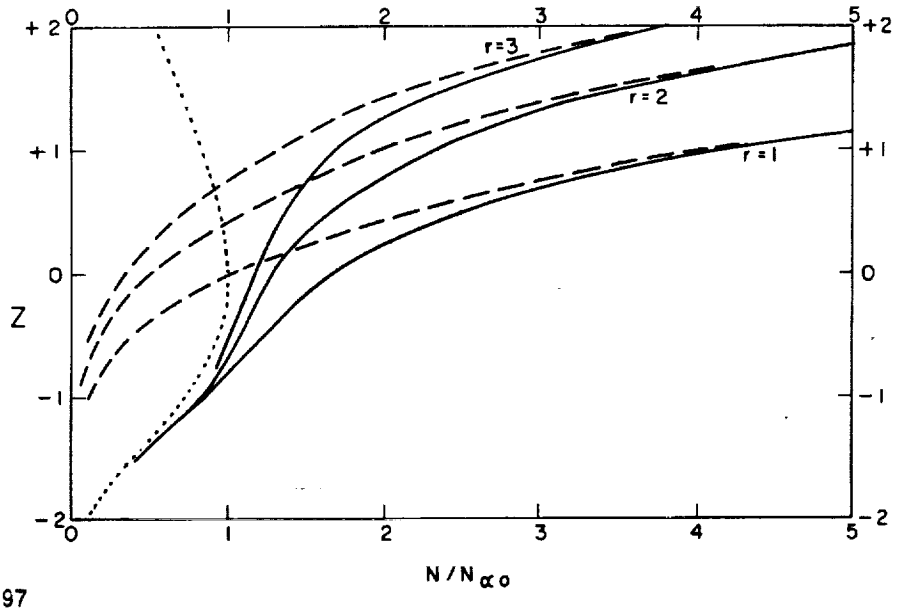

31097

FIG. 16. ELECTRON DENSITY PROFILES FOR THE "TRANSITION REGION," ASSUMING A CHAPMAN PRODUCTION FUNCTION $q(z)$ WITH PEAK AT $z = 0$ AND A RECOMBINATION COEFFICIENT α, INDEPENDENT OF HEIGHT. The linear loss coefficient is $\beta_o \exp(-1.75z)$, and three values of β_o are used, such that $r = \beta_o/\sqrt{\alpha q_o}$ takes the values 1, 2, 3. The $N(z)$ profiles correspond to:

..... $N_\alpha = \sqrt{q/\alpha}$

- - - - $N_\beta = q/\beta$, for three values of β_o

——— N computed from full equation (III-43)

The relevance of this analysis of the F region lies in the fact that, since r is evaluated at the level of peak q, it varies with solar zenith angle χ. Remembering that the level of peak production is given by $z_m = \ln(\sec \chi)$, that the peak value of q is $(q_o \cos \chi)$ and that $\beta(z) = \beta_o e^{-kz}$, we have

$$r(\chi) = \beta(z)/\sqrt{\alpha q} = \beta_o (\cos \chi)^k / \sqrt{\alpha q_o \cos \chi}$$

$$= r(0) \, (\cos \chi)^{k-1/2} \qquad \text{(III-45)}$$

Thus, if $r(0)$ is constant, as would be expected on a first-order theory of the atmosphere, we see that as χ increases, $r(\chi)$ decreases and the "splitting" of the layer becomes less pronounced, or even disappears. This is consistent with the observations that, at mid-latitude stations, the F1 layer is most prominent around noon, and is more commonly observed on summer days than in winter. Since $r(0) \propto 1/\sqrt{q_o}$, and q_o varies with the solar cycle, we can also account for the observation that the F1 layer is more prominent at sunspot minimum than at sunspot maximum. Moreover, the F1 layer sometimes appears during a solar eclipse at times when it would not normally be seen, and this may arise from the reduction of q_o and consequent increase of r.

The above discussion does not depend critically on the identity of the reactions, but we should now be more specific about the ionic constituents. Examples of the experimental results obtained from rocket-borne ion mass spectrometers are shown in Fig. 17 (Johnson, Meadows, and Holmes, 1958). Below 150 km molecular ions (NO^+ and O_2^+) are predominant, but atomic ions (O^+) dominate above 200 km. This is broadly consistent with the "transition" theory outlined above. Other ions, such as N_2^+ and N^+ are present as very minor constituents. We have previously shown evidence that the major neutral constituents in the thermosphere are O and N_2, with some O_2. Thus the ions produced by photoionization are O^+, N_2^+ and O_2^+; since O_2 is a minor constituent in most of the thermosphere, we expect most of the O_2^+ ions to be produced by "transfer" reactions (i.e., ion-atom interchange or charge exchange), and this is certainly true of the NO^+ ions.

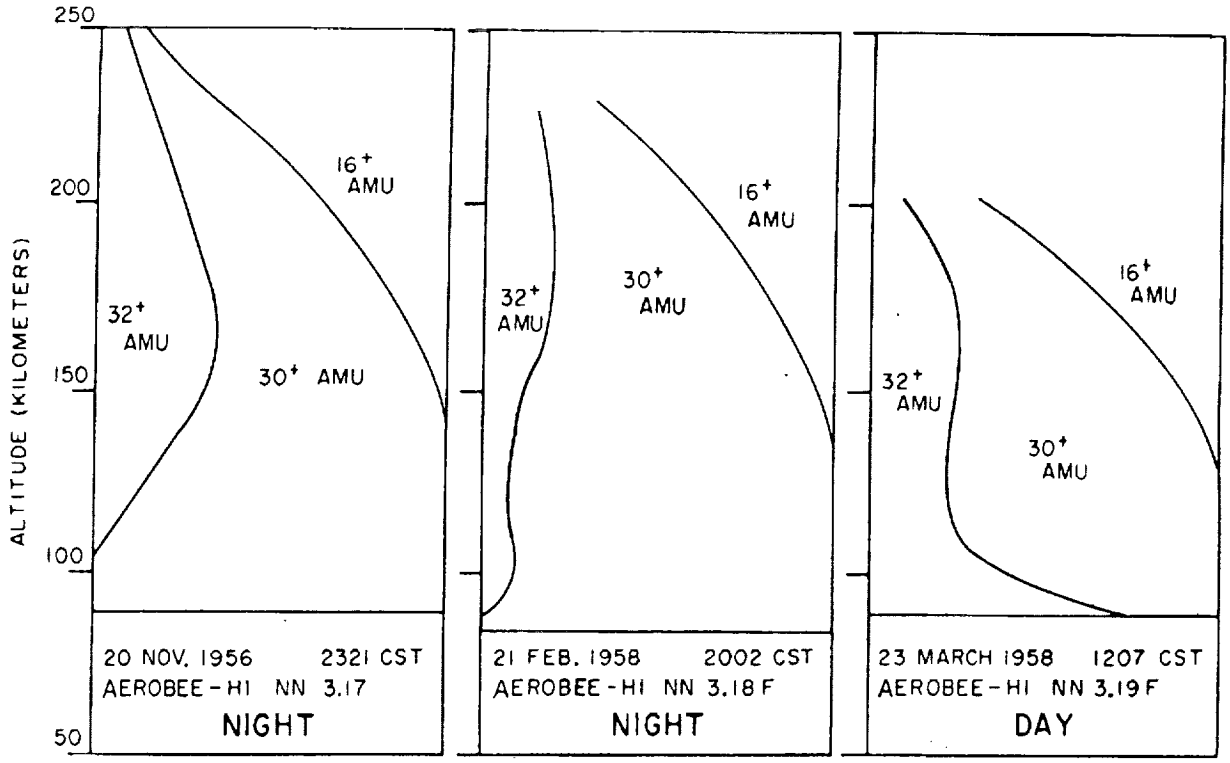

FIG. 17. RELATIVE ION CONCENTRATION VS ALTITUDE FOR THREE ROCKET FLIGHTS (after Johnson et al, 1958).

In Table II we give a list of reactions which is not exhaustive, but includes those reactions which seem likely to be of greatest importance. Reactions which have been omitted include those which are endothermic and some which are probably unimportant because they involve only "trace" constituents (such as atomic nitrogen) or for other reasons. Orders of magnitude of the coefficients γ and α have been given in Table 1.

The formation and decay scheme sketched above is the simplest which could, in principle, account for the observed ion compositions. The equations relevant to this scheme have been given by Yonezawa and Takahashi (1960). It should be noted that the production of atomic nitrogen by these reactions does not necessarily lead to an appreciable concentration of this gas in the atmosphere; this will depend on the removal mechanisms which we do not discuss here.

Since N_2^+ ions are so scarce in the E and F regions, this scheme would imply that they are destroyed so rapidly by the recombination (R3)

TABLE II. PHOTOCHEMICAL REACTIONS

Photoionization (rate q)

$O + h\nu \rightarrow O^+ + e$ (Q1)

$N_2 + h\nu \rightarrow N_2^+ + e$ (Q2)

$O_2 + h\nu \rightarrow O_2^+ + e$ (Q3)

Transfer or Interchange (rate coefficient γ)

$O^+ + O_2 \rightarrow O_2^+ + O$ (T1)

$O^+ + N_2 \rightarrow NO^+ + N$ (T2)

$N_2^+ + O \rightarrow NO^+ + N$ (T3)

$N_2^+ + O \rightarrow O^+ + N_2$ (T4)

$N_2^+ + O_2 \rightarrow NO^+ + NO$ (T5)

Dissociative Recombination (rate coefficient α)

$O_2^+ + e \rightarrow O^* + O^{**}$ (R1)

$NO^+ + e \rightarrow N^* + O^*$ (R2)

$N_2^+ + e \rightarrow N^* + N^{**}$ (R3)

Simple Scheme for Positive-Ion Formation and Decay

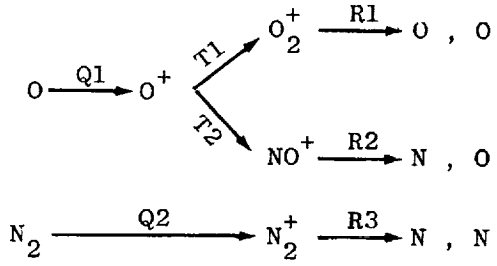

that they do not contribute to the observed ionization, though this does contribute to the input of heat. However, it now seems that this scheme is too simple, and that the coefficient of (R3) is not large enough to account for the scarcity of N_2^+ ions, so that additional reactions [such as (T3), (T4), (T5) or others] must be operative. There is considerable controversy even as to which of these is possible, let alone which is most important. Further discussion of possible reactions and data on the results of laboratory determinations of reaction rates are contained in the comprehensive reviews by Nawrocki and Papa (1961) and Whitten and Poppoff (1964) and in the paper by Nicolet and Swider (1963).

Although measurements have been made of the dissociative recombination coefficients for O_2^+, NO^+ and N_2^+, and of the rate coefficients for the transfer reactions (T1) and (T2), none of these parameters can be regarded as well known. In some cases, different results are at variance by an order of magnitude. Thus, although it is easy to write down the continuity equations for the various positive ion concentrations and the electron concentration, and to devise computer methods for their solution, it is not so easy to reach definite conclusions about which particular reactions are most important, even though the ionic composition is known as a function of height. However, it is possible to make some rather general statements, such as the necessity for some removal process for N_2^+ ions besides dissociative recombination; and to find ranges of values within which the various coefficients might lie.

There is also a long-standing difficulty concerning the rates of reactions (T1) and (T2), which almost certainly make the major contribution to the loss coefficient β in the F2 layer (e.g., Bates and Nicolet, 1960). We have

$$\beta(h) = \gamma_{T1}\, n[O_2] + \gamma_{T2}\, n[n_2] \qquad \text{(III-46)}$$

Most available data on all the quantities on the right-hand side of this equation give values of β which seem to be too large for the F2 layer, although some recent values quoted by Langstroth and Hasted (1962) for γ_{T1} and γ_{T2} may be small enough to remove the discrepancy.

The products of some reactions, notably the dissociative recombinations (R1) - (R3) in Table II, are formed in an excited state and may subsequently emit radiation. The energy-level diagrams for the atoms are described by Chamberlain (1959). Sufficient energy is liberated in reaction (R1) to raise at least one atom to a state from which it cascades to the ground level, with successive emission photons of 5577 Å green line and the 6300/6364 Å red lines. The intermediate state has such a long lifetime (~1 min), however, that at E region heights the atom is more likely to suffer collisional deactivation than to emit the red line. However, reaction (R2) liberates only enough energy to excite the red lines, 6300/6364 Å. Nighttime rocket experiments have shown that nearly all of the red emission originates above 150 km, and nearly all of the green line originates below this height (Heppner and Meredith, 1958; Tousey, 1958). The absence of green emission from the F2 layer can be used as evidence that reactions (T2) + (R2) are more important in the F2 layer than (T1) + (R1). Since the red line is emitted from the F region, one would expect its intensity to be related to the integrated rate of loss of ionization, $\int \beta N \, dh$. Correlations between its intensity at night and the critical frequency f_oF_2 have been found at low latitudes (Barbier, 1961) but not at middle latitudes (Duncan, 1960). Since it is now possible to observe the 6300 Å line even by day (Noxon and Goody, 1962), this technique should provide a valuable check on loss coefficients in the F region.

5. Plasma Diffusion

The foregoing description of F region photochemical processes fits the hypothesis of Bradbury (1938), concerning the formation of the F2 layer at about 300 km. No mechanism seemed to be capable of causing a peak of production at such a height, and so Bradbury supposed the production peak to lie at a lower height (now known to be near the F1 layer) and attributed the upward increase of electron density to a rapid upward decrease of loss coefficient.

This hypothesis does not of itself account for the location of the F2 peak. If the linear loss coefficient β varies as e^{-kz} (the ratio

$k = H_i/H_\beta$, as defined previously), then the electron density well above the production peak is approximately $q/\beta \propto \exp[(k-1)z]$. If $k > 1$, as seems nearly certain, then q/β increases indefinitely upward, and we must find some explanation for the existence of a peak of N. The possibilities include:

(i) Failure of the Chapman formula for q at heights where the ionized/neutral concentration ratio (N/n) is not small.

(ii) Existence of an additional loss process, such as radiative recombination, which might dominate at great heights.

(iii) Lack of equilibrium, such that N never approaches the limiting value q/β.

(iv) Action of some transport process (such as diffusion) to limit N at great heights.

Of these possibilities, (iv) and perhaps also (iii) are most likely to control the F2 layer; in particular, the process of plasma or ambipolar diffusion is thought to limit the upward increase of electron density and lead to the formation of the F2 peak. Diffusion arises from the tendency of the electron-ion gas or plasma to assume a hydrostatic distribution under gravity. We recall that the neutral atmospheric gases are in hydrostatic equilibrium above 100 km, but the great chemical activity of the ionization causes its distribution to be determined by photochemical processes right up to the F2 peak.

The importance of diffusion was suggested by Hulburt (1928) and the mathematical expressions were derived by Ferraro (1945). Early solutions of the continuity equation, with diffusion included (Mariani, 1956), treated it as a small perturbation only. But Yonezawa (1956) discussed in detail the problem of the formation of the F2 peak and showed that diffusion could provide an explanation.

To formulate the diffusion equation for the ionization, we balance the partial ion pressure gradient against the total force per unit volume acting on the ions. These are gravity, the electrostatic force due to the macroscopic electric field E which we assume to be present, and frictional forces due to collisions with ions and electrons. Considering only vertical forces and velocities, the equations for ions and electrons are:

$$\partial(N_i kT_i)/\partial h = -N_i m_i g + N_i eE - N_i m_i \nu_{in}(w_i - w_n) \qquad \text{(III-47)}$$

$$\partial(N_e kT_e)/\partial h = -N_e m_e g - N_e eE - N_e m_e \nu_{en}(w_e - w_n) \qquad \text{(III-48)}$$

in which we symbolize concentration N, Boltzmann's constant k, temperature T, gravitational acceleration g, mass m, electronic charge $-e$, collision frequency ν (with neutral particles) and vertical drift velocity w. Suffixes i, e, n refer to ions, electrons, and neutrals. The frictional terms can be derived from kinetic theory. We simplify the equation by the following assumptions: $m_i \gg m_e$, $N_i = N_e$, $w_i = w_e = w_D$, $w_n = 0$ (neutral air at rest), $m_i \nu_{in} \gg m_e \nu_{en}$ (collisions with neutral particles important for ions but not for electrons). On adding the equations, the terms in $\underline{E}$ vanish (and, because of Newton's Third Law, so do the ion-electron collision terms which we omitted from the equations). This means that the electrons interact with the ions only via the electric field. Rearranging to solve for the drift velocity of the plasma

$$-w_D = \frac{1}{m_i \nu_{in}} \left\{ \frac{1}{N} \frac{\partial}{\partial h} [Nk(T_i + T_e)] + m_i g \right\} \qquad \text{(III-49)}$$

In the F region, the electron, ion and neutral temperatures may all be different. Except at great heights, it is probable that $T_i = T$ (the suffix n has been dropped). Then we introduce the neutral scale height $H = kT/m_n g$ and set $\mu \equiv m_i/2m_n$ and $\tau \equiv T_e/T_i = T_e/T$. The ion-neutral diffusion coefficient is defined as $D_{in} = kT/m_i \nu_{in}$, so that the equation becomes

$$-w_D = D_{in}(1 + \tau) \left[\frac{1}{N} \frac{\partial N}{\partial h} + \frac{1}{T} \frac{\partial T}{\partial h} + \frac{2\mu}{(1 + \tau)H} + \frac{\partial \tau / \partial h}{1 + \tau} \right] \qquad \text{(III-50)}$$

and if $T_e = T_i = T$ at all heights (i.e., $\tau = 1$)

$$-w_D = 2D_{in} \left[\frac{1}{N} \frac{\partial N}{\partial h} + \frac{1}{T} \frac{\partial T}{\partial h} + \frac{\mu}{H} \right] \qquad \text{(III-51)}$$

Since $D = 2D_{in} = 2kT/m_i \nu_{in}$, and ν_{in} is proportional to both the gas concentration and $\sqrt{T}$, we may write, to a first approximation,

$$D = \frac{b\sqrt{T}}{n} \qquad \text{(III-52)}$$

Ferraro (1945) uses a more complicated temperature dependence, so that b is a slowly-varying function of T; this is further discussed in a later note (Ferraro, 1957). Values of b can be calculated from theory (Chapman and Cowling, 1952) but the factor of 2, discussed above, was omitted by Ferraro. This was pointed out by Johnson and Hulburt (1950), who treated the whole diffusion problem from a different standpoint. Ferraro assumed a mean molecular mass of 25 a.m.u. for the plasma, whereas it is now believed that in the F2 layer the neutral gas is mainly atomic oxygen and the ions mostly O^+. Thus, numerical values of b must be treated with caution, especially since Dalgarno (1958) finds that, for ions diffusing through their parent gas, b is reduced by charge-exchange between ions and neutrals, possibly by a factor of four. There are also many variations of notation in the literature; for instance, some authors write $D = b/n$ and so include the dependence on T within the quantity b.

The contribution of diffusion to the continuity equation can be written as

$$-\partial(Nw_D)/\partial h = D\,\mathbb{D}\,N \qquad \text{(III-53)}$$

where $\mathbb{D}$ is a differential operator. The evaluation of $\mathbb{D}$ involves fairly complicated algebra, but expressions have been given by Shimazaki (1957) for the case in which the scale height gradient dH/dh is independent of height. We shall restrict our derivation to the isothermal case, $dH/dh = 0$. We also take $\mu = 1/2$ (corresponding to $m_n = m_i$) in Eq. (III-51) and express $\mathbb{D}$ in terms of reduced height z by taking $H \cdot \partial/\partial h \equiv \partial/\partial z$. For this simple model, the neutral particle concentration $n \propto e^{-z}$ so that $D \propto e^{+z}$. Using these relations, Eq. (III-51) reduces to

$$-w_D = \frac{D}{H}\left\{\frac{1}{N}\frac{\partial N}{\partial z} + \frac{1}{2}\right\} \qquad \text{(III-54)}$$

and by Eq. (III-53) the diffusion term in the continuity equation takes the form derived by Ferraro (1945)

$$D\,\mathbb{D}\,N = \frac{D}{H^2}\left\{\frac{\partial^2 N}{\partial z^2} + \frac{3}{2}\frac{\partial N}{\partial z} + \frac{N}{2}\right\} \qquad \text{(III-55)}$$

The effect of gravity and the height dependence of D are responsible for the appearance of terms in $\partial N/\partial z$ and N, in addition to the second derivative $\partial^2 N/\partial z^2$ which is characteristic of diffusion formulas.

Since D increases exponentially upward, whereas the other coefficients q and β in the continuity equation decrease upward, at some level diffusion dominates so completely that the continuity equation reduces to $\mathbb{D}N = 0$. The solution of this equation is

$$N = A_1 e^{-1/2\, z} + A_2\, e^{-z} \qquad \text{(III-56)}$$

The first term corresponds to diffusive equilibrium, with $w_D = 0$, such that the ionization assumes a scale height twice that of the ionizable gas. For the second term, $w_D \neq 0$; and this represents a boundary condition of a finite flux of ionization at $z \to +\infty$, which is upward if the coefficient $A_2 > 0$. If ionization is gained or lost by diffusion at the top of the ionosphere (i.e., to or from the magnetosphere), the $N(z)$ distribution should contain a component of this type.

Finally, we note that in the F region the ionization can diffuse only along the lines of geomagnetic force. The usual way of treating this problem is to use the components of w_D and $(\partial/\partial h)$ parallel to the field. This introduces a factor of $\sin^2 I$ into the coefficient D, where I is the magnetic dip angle (Ferraro, 1945). However, this approach is incorrect if the neutral air is in motion, as may be the case (Dougherty, 1961). Near the magnetic equator the "$\sin^2 I$" factor

fails and a more complicated form of the operator $\mathbb{D}$ is required which includes horizontal as well as vertical diffusion. This has been derived by Kendall (1962) and Lyon (1963).

The equation for the diffusion of ions (III-50) serves as a convenient starting-point for discussing the equilibrium distribution of charged particles in the topside F region. At these heights, photochemical processes can be neglected, and the collision frequency ν_{in} is so small that the continuity equation reduces to the partial pressure, gravitational and electric field terms of Eq. (III-50). The situation is interesting because several species of positive ion may be present. We suppose all ions to be singly charged and to possess the same temperature T_i, though this need not be the same as the electron temperature T_e. For the j^{th} species of ion, and for the electrons, the equations are

$$d(N_j kT_i)/dh = -N_j m_j g + N_j eE \qquad \text{(III-57)}$$

$$d(N_e kT_e)/dh = -N_e m_e g - N_e eE \qquad \text{(III-58)}$$

Since $\Sigma N_j = N_e$, the equations can be added to eliminate E. We then denote the mean positive ion mass by m_+, so that $m_+ N_e = \Sigma N_j m_j$, and set $T_e/T_i = \tau$ obtaining

$$-\frac{1}{N_e}\frac{dN_e}{dh} = \frac{gm_+}{kT_i(1+\tau)} \qquad \text{(III-59)}$$

when the small gravitational term $(N_e m_e g)$ is neglected. The electric field E may now be found from Eq. (III-58) and inserted in the ion equation to give

$$-\frac{1}{N_j}\frac{dN_j}{dh} = \left[m_j - \frac{\tau m_+}{1+\tau}\right]\frac{g}{kT_i} \qquad \text{(III-60)}$$

We have neglected temperature gradients for simplicity, although they could be readily included. A further simplification is to assume thermal equilibrium, $\tau = 1$, which reduces the last two "scale height" equations to

$$H_e = 2kT/(m_+ g)$$

and (III-61)

$$H_j^+ = kT/\left(m_j g - \frac{1}{2} m_+ g\right)$$

We see that if only one ionic species is present, its "effective scale height" is twice that of the neutral species of atomic mass m_+ (as before). However, a light ion for which $m_j < \frac{1}{2} m_+$ actually has a negative scale height, so that N_j increases upward, as discussed by Mange (1960). The Eqs. (III-59) and (III-60) can be solved by a method due to Hanson (1962). It is convenient to use the "geopotential height" defined below Eq. (I-9) in Sec. I-3, in order to take account of the vertical variation of g. A specimen equilibrium distribution computed for a mixture of O^+, He^+ and H^+ ions, is shown in Fig. 18.

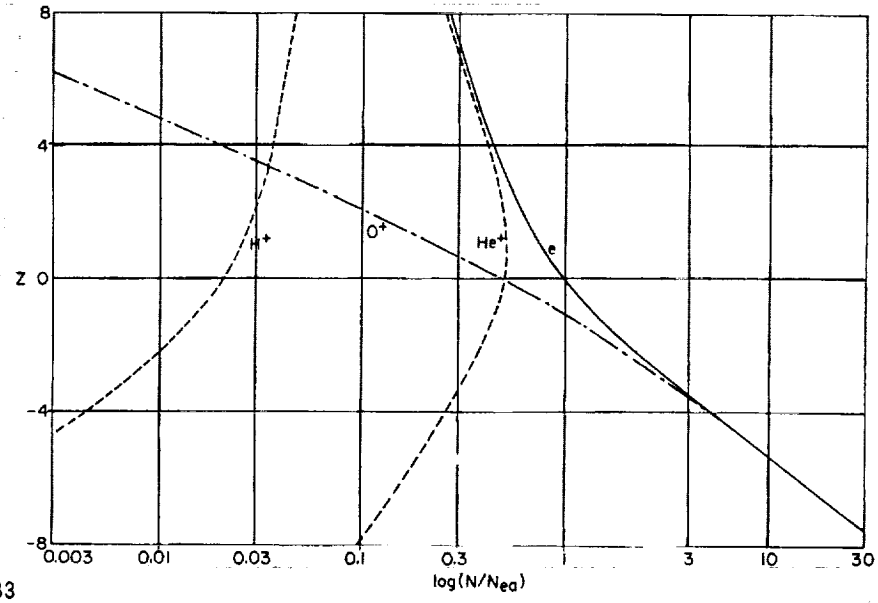

31283

FIG. 18. IDEALIZED DISTRIBUTIONS OF ELECTRONS (e) AND OF O^+, He^+ and H^+ IONS, COMPUTED BY SOLVING EQS. (III-59), (III-60). Electron and ion concentrations are given in terms of the electron density N_{ea} at the level $z = 0$, at which height the ionic composition is taken to be $[O^+] = [He^+] = 49\%$, $[H^+] = 2\%$. The level at which the He^+ and H^+ concentrations are equal is near $z = 17$. The unit of reduced height z is the scale height of neutral atomic oxygen.

6. Solving the Continuity Equation

Much of the progress in ionospheric theory has been achieved by obtaining solutions of the continuity equation and comparing them with observation. Of course, the full equation is so complicated, and its coefficients so poorly known, that drastic simplifications have to be made. In this section, we will start with the simplified equation

$$\partial N/\partial t = q - L(N) - \partial(Nw)/\partial h \qquad \text{(III-62)}$$

Only the vertical velocity component w is included in the movement term and all losses are included in $L(N)$. When discussing the variation of these quantities with reduced height, we should remember that the unit of z is the scale height H_i of the ionizable gas.

In earlier sections, we have already discussed the "Chapman," "Bradbury," and "transition" layers which apply to the situation of photochemical equilibrium, when the equation reduces to $q = L(N)$. If time variations are included, but movements neglected, a first-order total differential equation is obtained, which can be solved analytically in some cases, otherwise numerically (Millington, 1932).

If the movement term is reinstated, the equation becomes a partial differential equation in h and t. It may be simplified by following the motion of a "cell" of ionization, using the total derivative appropriate to vertical motion,

$$d/dt \equiv (\partial/\partial t) + w(\partial/\partial h) \qquad \text{(III-63)}$$

in which we have specified $(dh/dt) = w$. Insertion of this operator into the continuity equation yields

$$dN/dt = q - L(N) - N\partial w/\partial h \qquad \text{(III-64)}$$

The usefulness of these equations lies in the fact that if $\partial w/\partial h$ can be neglected, as may be the case for electromagnetic drifts, Eq. (III-64) reduces to a purely "photochemical" equation. However, as the altitude

of the "cell" changes, q and L will vary, so that the equation must in general be solved numerically. Use of this technique has been limited by the unsatisfactory state of the theory of electromagnetic drifts.

The principle of "following-the-cell" may also be applied to thermal motions. This is especially pertinent to the F region where large diurnal temperature changes occur. Suppose that the neutral atmosphere expands and contracts, so that the air moves vertically. The gas concentration, which largely determines q, β and the diffusion coefficient D, changes in a complicated way at any fixed height h, but within any particular cell, the concentration just varies inversely with temperature. This is obvious from the perfect gas equation, if we remember that the pressure within a given cell is constant, being the weight of the overlying air. Then q, β and D are best written as functions of pressure, or of reduced height z.

An approach of this type was used in a discussion of temperature effects on the equilibrium electron distribution by Garriott and Rishbeth (1963). It is found that, within certain assumptions, the shape of the electron density profile in terms of reduced height, e.g. N(z), is unchanged with temperature variations, but that the magnitude is altered in proportion to $T^{-1/2}$. These results have been extended in an approximate manner to the time varying case by Rishbeth (1964). It is found that the temperature variations can so distort the N(t) curves that the maximum of N occurs before noon, at heights below the peak. Shimazaki (1957) has also used this technique when both electromagnetic and thermal motions are considered. The implicit assumption, that the moving air carries the ionization with it, is probably valid except near the magnetic equator. There will be complications if the temperature changes affect the composition at the turbopause of if large horizontal flows of air occur, but even in these circumstances a "following-the-cell" approach may be useful.

When diffusion is introduced into the continuity equation, as must be done if the F2 peak is to be adequately treated, the continuity equation contains the diffusion operator $\mathcal{D}$ which involves $\partial/\partial h$ and $\partial^2/\partial h^2$. Equilibrium solutions of this equation are of some interest, even for the

F2 layer because it is true during much of the day that $\partial N/\partial t$ is smaller than other terms in the continuity equation. At least they provide an insight into the relative importance of different processes.

Equilibrium solutions of the diffusion equation, with electromagnetic drift, were obtained by Yonezawa (1956, 1958). Rishbeth and Barron (1960) solved the equation numerically in a number of cases, using Chapman-type production functions and exponential formulas, $D \propto e^{z}$ and $\beta \propto e^{-kz}$, for the diffusion and loss coefficients. Several values were used for the constant k. (We recall from Sec. III-4 that $k = 2$ and $k = 7/4$ if the loss reactions depend respectively on molecular oxygen and molecular nitrogen in a diffusively-separated atmosphere, and that $k = 1$ if all the atmospheric constituents are fully mixed.) From such calculations, the following generalizations about the behavior of a daytime equilibrium layer can be made:

(a) The F2 maximum electron density occurs at a level where diffusion and loss are of comparable importance, i.e., where $\beta_m \sim D_m/H_i^2$, in which the subscript "m" refers to the maximum.

(b) At the maximum, and below it, the electron density is approximately given by $N \sim q/\beta$, just as it would be in the absence of diffusion.

(c) Well above the maximum, the electron density distribution is exponential, and takes the form $N \sim e^{-z/2}$ [as we obtained in Eq. (III-60)].

(d) These conclusions are substantially unaltered if gradients of scale height are present.

(e) Vertical electromagnetic drift, magnitude w, alters the level of the maximum by an amount of order wH_i/D_m scale heights; N_m is still given, very roughly, by (b).

Points (a), (b), (c) are illustrated by the sketch in Fig. 19. More detailed discussions of "equilibrium layers" have been given by Bowhill (1962) and Nisbet (1963). The theory of the decay of the nocturnal F2 layer has been investigated by Martyn (1956) and Duncan (1956), who used the assumption $\beta \propto e^{-z}$, and by Dungey (1956) who used the form $\beta \propto e^{-2z}$. All these authors assume $D \propto e^{z}$. They investigate solutions which decay without change of shape, with an "effective" decay coefficient β'; i.e., of the form

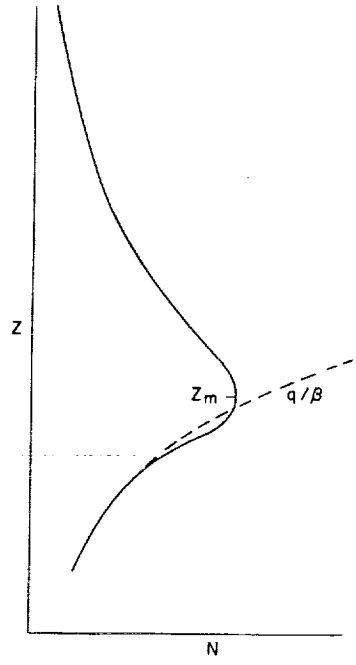

FIG. 19. EQUILIBRIUM ELECTRON DENSITY DISTRIBUTION $N(z)$ FOR THE F2 LAYER. Below the peak $N \approx q/\beta$ (photochemical equilibrium) and above the peak $N \propto \exp(-1/2\ z)$ (diffusive equilibrium). At the peak, the relations $\beta = D/H_i^2$ and $q = \beta N$ are approximately valid.

$$N(z,t) = N_s(z) \cdot e^{-\beta' t} \qquad \text{(III-65)}$$

The results of these investigations may be summarized as follows. There exist a number of "shape-preserving" or "stationary" distributions $N_s(z)$ which are such that their peaks lie at heights h_s. At these heights, the loss and diffusion coefficients are connected by equations of the type $\beta_s = u_1 D_s/H_i^2$, and the effective decay coefficient is given by equations $\beta' = u_2\beta_s$, where u_1 and u_2 are numbers of order unity. Usually we are only interested in the most slowly-decaying stationary layer which has the smallest value of β'. The special case investigated by Duncan and by Martyn, namely $\beta \propto e^{-z}$, is of interest because it happens that $u_1 = u_2 = 1$, and also that the "shape preserving" function is the "Chapman alpha layer" which arose previously in an entirely different context, namely, the equilibrium between photoionization and a square-law loss process (Eqs. III-29 and III-21). If an upward (or downward) electromagnetic drift is applied, then the peak of the layer is raised (or lowered), but the effective decay coefficient is still equal to the value of β at the maximum. In other cases, such as that studied by

Dungey (with $\beta \propto e^{-2z}$, which is probably closer to the situation in the actual F2 layer), the analysis is more complicated and the numbers u_1, u_2 take different values. For instance, in the absence of vertical drift, $\beta = 1.86\ \beta_s$ so that the decay of the layer corresponds to the value of β at some height below the peak of the layer.

Time-varying solutions of the full diffusion equation, giving the theoretical diurnal variation of electron density, are naturally more difficult to obtain. Gliddon and Kendall (1960) were able to obtain an analytic solution, in terms of Green's functions, but had to make the assumption $\beta \propto e^{-z}$. They used the upper boundary condition $N \propto e^{-z}$, which does not correspond to diffusive equilibrium. In a comprehensive paper (Gliddon and Kendall, 1962) they compared results obtained with this boundary condition and with the more usual assumption, $N \sim e^{-z/2}$, and also discussed eclipse phenomena and the effects of vertical electromagnetic drift, which they had to assume independent of height and time.

Briggs and Rishbeth (1961) constructed an electromechanical analogue computer to solve the diffusion equation. This method, though approximate, has the advantage that the functions $q(h,t)$, $\beta(h)$ and $D(h)$ are not restricted to special mathematical forms but may be derived from any empirical atmospheric model. The assumption of complete mixing (corresponding to $\beta \propto e^{-z}$ in a mathematical model) was used initially but in later work (Rishbeth, 1963) β was assumed proportioned to the N_2 concentration (corresponding to $\beta \propto e^{-1.75z}$).

These calculations provide a rather simple description of the diurnal behavior of a layer controlled by photoionization, linear loss and diffusion. At sunrise, the electron density near the peak increases at a rate which depends primarily on the production rate q, and diffusion and loss play a secondary role. The height of the peak, which corresponds to the F2 peak in the actual ionosphere, falls because of the rapid production of ionization in the lower F region, and reaches a minimum before noon. By this time, diffusion and loss become important and for a few hours the layer is not far from equilibrium, in the sense that $\partial N/\partial t$ is small compared to other terms in the continuity equation. Under these conditions, the peak remains near a level where $\beta \sim D/H_i^2$,

as in the case of the "equilibrium layer" discussed earlier. Also, at heights up to the peak, the "equilibrium approximation" $N \cong q/\beta$ is valid, and the maximum value of N lags after noon by a time $\sim 1/\beta(h)$. Above the maximum, however, diffusion is so rapid that the variation of N closely follows the variation of N_m. Later in the day, N_m decreases and h_m rises as solar control weakens.

After sunset, h_m approaches the "night stationary" level h_s and the layer develops into the "shape preserving" form which decays exponentially with time throughout the night, in the manner of Eq. (III-60). The pressure level (or z coordinate) of the maximum electron density is higher than in the daytime. Duncan (1956) showed that when $\beta \propto e^{-z}$, the maximum occurs for $\beta = 0.25\ D/H_i^2$, while Dungey (1956) showed that for $\beta \propto e^{-2z}$, the level was at $\beta \approx 0.11\ D/H_i^2$. However, this increase is more than offset by the thermal contraction of the atmosphere at night and the real height of the maximum would be expected to decrease (Rishbeth, 1964).

IV. MORPHOLOGY OF THE IONOSPHERE

1. D Region

Until the last few years, most of the information about the height variation of electron density and collision frequency in the lowest ionosphere was derived from the indirect evidence obtained from radio propagation experiments. These consisted of phase and amplitude measurements of low frequency waves (in the range 10 - 200 kc/s) which are reflected in the D region; and of measurements of absorption, polarization and cross-modulation of waves at higher frequencies (up to a few Mc/s) which are reflected in the E or F regions but traverse the D region. Some of these techniques were discussed earlier in Sec. II.

The long-wave experiments give information about reflection heights, which vary with the solar zenith angle. Frequencies around 16 kc/s are reflected at 70 - 75 km by day but from the E layer by night (Bracewell et al, 1951), the transition occurring rather suddenly at sunset and sunrise. The data have been interpreted in terms of one or more discrete layers of ionization below the E layer (Bracewell and Bain, 1952).

Absorption measurements, at a series of radio frequencies, have shown a frequency dependence consistent with simple magnetoionic theory except near the critical frequencies f_oE and f_oF1, when complications are to be expected. The absorption is found also to depend on the solar zenith angle χ and on the mean sunspot number R. Appleton and Piggott (1954) found that at 4 Mc/s

$$|\log \rho| \propto (\mathrm{Ch}\ \chi)^{-0.8}$$
$$|\log \rho| \propto (1 + 0.01\ R) \qquad \text{(IV-1)}$$

where ρ is the "reflection coefficient" of the ionosphere and is a measure of the total absorption along the path. These measurements suggest a strong solar control of the D region, at least at the mid-latitude station (Slough, 52°) where the most extensive studies have been made. In winter, however, the absorption is much greater on certain days and

the long-wave and reflection coefficient measurements suggest that additional ionization is present in the D region. The occurrence of this "winter anomaly" has been discussed by Thomas (1962a) and Dieminger (1952). Thomas finds that the excessive absorption occurs over geographical areas of about 1000 km in extent, but there seems to be no correlation with magnetic disturbance, except perhaps on a long-term basis. It may be that the ultimate cause of the anomaly lies at lower levels in the atmosphere.

The only method so far devised that makes extensive use of the long-wave phase and amplitude data depends on "full wave" solutions of the wave propagation equations (Barron and Budden, 1960) for a variety of models, combined with trial-and-error fitting of the parameters to the data.

According to Nicolet and Aikin (1960) the chief production process in the upper D region is the photoionization of NO by Lyman α radiation (λ = 1216 Å). This radiation penetrates into the D region because it cannot ionize any of the gases found at higher levels, and neither is it strongly absorbed by them. Below 100 km it is absorbed by molecular oxygen (which it dissociates) but a fraction is expended in the photoionization of NO, which has a rather low ionization potential. Although neutral NO has not been detected spectroscopically in the D region, Nicolet (1961) considers that various chemical reactions can supply the trace (only 10^{-10} of the total concentration) that is required.

The model of Nicolet and Aikin, Fig. 20, shows the component of ionization due to Lyman α is greatest between 70 and 80 km (for $\chi = 0$). It is possible that a peak of electron density exists in this region, but in any case a positive gradient of electron density exists between 70 and 75 km and this could account for the long-wave reflections observed at this level. However, it may be that the main contribution to D region ionization is made, not by Lyman α, but by hard X rays in the range 1 - 8 Å. Above 85 km, the bottom of the E region production curve (due to softer X rays of 10 - 100 Å) gives rise to another large electron density gradient, but this should really be considered as part of the E layer.

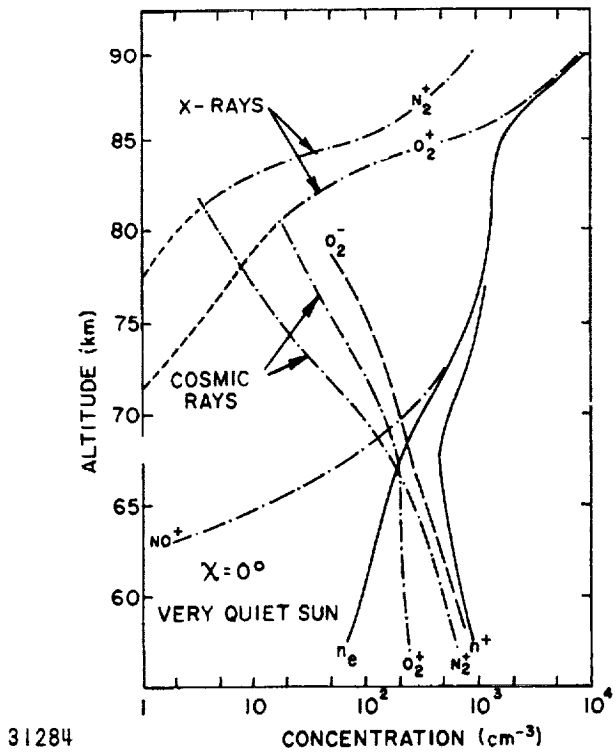

FIG. 20. CONCENTRATIONS OF POSITIVE IONS, NEGATIVE IONS AND ELECTRONS VS ALTITUDE FOR A VERY QUIET SUN (after Nicolet and Aikin, 1960).

During solar flares, the D region ionization is greatly enhanced, severe absorption is produced, and the reflection height of long waves drops by several kilometers. These events are called "sudden ionospheric disturbances," or SID's and will be mentioned again in Sec. VII. Since such an event starts at the same time as the visual flare and is observed at all latitudes, it is presumably due to electromagnetic radiation which must be more penetrating (i.e., possess a smaller cross-section) than that responsible for the normal D layer, since the height of peak photoionization is independent of its intensity but depends on the absorption cross-section σ.

Another type of disturbance is the "polar cap absorption" (PCA) which we mention here because of its interest in connection with D region photochemistry. It begins a few hours after solar flares and is thought to be initiated by the arrival of solar protons with energies on the

order of 10 Mev. It persists for several days with a pronounced diurnal variation, which is attributed to attachment and photodetachment processes. However, an alternative suggestion is that the disturbance creates extra neutral NO which can then be photoionized (Herzberg, 1960).

Other D region disturbances are probably associated with ionization by charged particles. This is especially true of the "blackouts" and "auroral absorption" observed at high latitudes. Ionization by electrons has been discussed by Rees (1963), and by solar protons by Webber (1962).

Even in the normal D region, most of the production below 70 km is due to cosmic rays. This source differs from the solar radiation in that it acts by night as well as by day, but it is very latitude-dependent because of the effects of the geomagnetic field on the motions of the incoming charged particles. According to the curves given by Webber (1962), the rate of electron production by galactic cosmic rays increases downward throughout the D region, and indeed throughout the whole mesosphere. But the $N(h)$ profile is quite different from the production rate $q(h)$, because of the altitude dependence of the various loss coefficients, and in most published models N increases monotonically with height up to (at least) 70 km. However, Pierce (1963) has suggested that rates of collisional detachment are such as to produce a nighttime "C region" peak of electron density, perhaps 10^2 cm^{-3}, at about 50 km. The existence of this peak had also been suggested on the basis of long-wave radio propagation (Moler, 1960).

In the lower D region, ionization has little effect on radio propagation, partly because the free electron density is small ($N_e \ll N_- \approx N_+$) and partly because the collision frequency greatly exceeds the plasma frequency. Therefore, the ionization below about 50 km is generally considered to belong to the field of atmospheric electricity rather than ionospheric physics.

Many of the papers already cited show values of the negative-ion ratio $\lambda = N_-/N_e$ derived from theoretical calculations. Most authors find that the level where $\lambda = 1$ occurs at about 70 to 81 km by day, and about 90 to 100 km by night. Some comparisons have been made by Hultqvist (1963) but there is still considerable disagreement on this

topic. The behavior of the D region at sunrise and sunset is very relevant to the question of ion composition. Long-wave reflection and absorption experiments show that the electron density starts to increase about an hour before ground sunrise (Bracewell et al, 1951). Although the height at which this ionization appears may not be well known (especially in the case of absorption experiments), the fact that it is produced when $\chi > 90$ deg implies that the effective radiation has traversed lower levels in the atmosphere. Aikin (1961) showed that Ly α and X rays do not penetrate the D region until near ground sunrise, so that the initial increases are attributed to photodetachment from negative ions. If the "screening height"--the lowest height traversed by the radiation--was well known, it would be possible to deduce whether visible or ultraviolet light is involved. One expects visible light to be cut off only by the solid earth (or by clouds in the lower atmosphere), whereas UV light is screened by the ozonosphere.

This problem is acute in connection with the "polar-cap absorption" previously mentioned, because the values of χ and the related screening heights are inconsistent with the simple theory that electrons are produced by photodetachment from O_2^- or O^- ions, which can be accomplished by visible light. Because of this difficulty, it has been suggested that the ionization responsible for polar-cap absorption lies below 55 km, in which case the observations would be consistent with screening by the solid earth (Hultqvist and Ortner, 1959). An alternative suggestion is that the negative ions are not O^- or O_2^-, as originally supposed, but some other ion (perhaps O_3^- or NO_2^-) which has a high electron affinity, such that ultraviolet light is required for photodetachment. The screening height for this radiation would then be consistent with the data (Reid, 1961) but this subject is still controversial. A recent review of D region processes is that of Reid (1964).

2. E and F1 Regions

The E and F1 layers of the ionosphere are generally regarded as being fair approximations to the idealized Chapman layer. Although the Chapman theory does provide a first-order description of the behavior of

the critical frequencies, more detailed study indicates that the layers are more complex. There is little doubt that the layers are within the "photochemical regime" described in Sec. III-4, although transport processes can produce appreciable perturbations.

In applying the theory of photochemical processes to the E and F1 layers, it is generally satisfactory to assume $\partial N/\partial t = 0$. For a simple Chapman layer in an isothermal atmosphere, we found in Sec. III-2 that the critical frequency is related to solar zenith angle χ by the equation

$$f_o = 9000\ [(q_o/\alpha)\ \cos\chi]^{0.25} \quad (c/s) \qquad (IV\text{-}2)$$

where q_o is the peak production rate for overhead sun $(\chi = 0)$ and α the recombination coefficient, expressed in cgs units. Many investigators assume a relation of the type $f_o \propto (\cos\chi)^n$ and find the value of n as χ varies with time of day or with season, at any one station; or as χ varies with latitude, for a number of stations. A study of diurnal variations (Tremellen and Cox, 1947) gave $n = 0.3$ (or somewhat more) for diurnal variations, but seasonal variations give a result closer to the theoretical value 0.25. A possible reason why $n > 0.25$ in the E layer was mentioned earlier; that is, the existence of a positive scale height gradient, $\Gamma = dH/dh$. In Eq. (III-31), we deduced that $n = 0.25(1 + \Gamma)$, so that the diurnal variation of f_oE implies that $\Gamma \approx 0.2$, reasonably consistent with models of the thermosphere. However, there seem to be seasonal and geographical variations which cannot yet be explained in detail.

The dependence of f_oE on the mean sunspot number R is studied by assuming Eq. (IV-2) to hold; it is then found that the square of the "noon" maximum electron density is given by

$$q_o(E)/\alpha(E) \approx 180\ (1 + 0.010\ R) \times 10^8\ cm^{-6} \qquad (IV\text{-}3)$$

(Allen, 1948). The height of maximum production for $\chi = 0$ for the E layer has been found by Robinson (1959) to be about 108 km.

The recombination coefficient α has been determined to be greater than 10^{-8} cm^3/sec from eclipse observations (Ratcliffe, 1956b); and by measuring the "sluggishness," i.e., the interval by which the time of greatest N_mE lags behind local noon, which should correspond to $1/2\ \alpha N$ and is of order 10 min (Appleton, 1937, 1953). From the decay of the E layer at night, Titheridge (1959) finds $\alpha = 2 \times 10^{-8}$ cm^3/sec. However, in all these analyses, the E region was assumed to contain only a single ionic constituent. It may be necessary to consider the presence of two ions with different recombination coefficients to satisfactorily explain the observations (Bowhill, 1961).

As regards the latitudinal variations of f_oE, there are departures from the normal Chapman layer behavior which may be caused by electromagnetic movements associated with the quiet-day (S_q) currents flowing in the E region. This explanation is favored by Beynon and Brown (1959); moreover, Appleton, Lyon and Pritchard (1955) find a systematic latitude variation of the post-noon lag of N_mE which seems to be due to movements rather than to changes in the "sluggishness" time $1/2\ \alpha N$.

We must point out that the vertical structure of the E layer is less simple than the previous discussion might imply. On ionograms, two or more cusps often appear, and so it may be difficult to assign a definite E layer critical frequency. If a sequence of ionograms is studied, however, it is usually found that one particular cusp displays a more consistent diurnal variation than the others, and this is usually tabulated as the "actual" critical frequency. Occasionally a second cusp, at a higher frequency, is found to vary in a consistent way, and it is then denoted as f_oE2. Additional stratifications of a more or less temporary nature are often observed (Becker and Dieminger, 1950; Dieminger, 1959; Robinson, 1959).

The term "sporadic E," or Es, is applied to E region ionization which does not behave in any regular manner. It is generally considered that this phenomenon is not closely related to the ordinary E layer produced by ultraviolet radiation, and we shall deal with it in a later section (IV-7).

Since the E layer is produced, not by monochromatic radiation but by a variety of wavelengths (including X rays and ultraviolet lines

such as Lyman β), it is not surprising that a complex structure exists. So far, however, the data are insufficient for any correspondence between individual spectral lines and ionogram features to be established. Although conventional ionograms do not give very detailed information about ionization between the E and F1 layers, rocket N(h) profiles have shown that there is little (if any) decrease of N above the E layer, that is, there is no pronounced "valley."

For the F1 layer, the solar cycle variation is quite well described by the formula

$$q_o/\alpha = 500\ (1 + 0.016\ R) \times 10^8\ cm^{-6} \qquad (IV\text{-}4)$$

(Ratcliffe and Weekes, 1960). Eclipse and other observations, summarized by Ratcliffe (1956b), give value of α in the range (1/2 to 1) $10^{-8}\ cm^3 sec^{-1}$. The height of maximum production h_o for the F1 layer is very difficult to determine from ionogram data. For summer noon at Slough, Thomas, Haselgrove and Robbins (1958) found $h_m F1$ to lie at about 185 km at sunspot minimum (1953) and 190 km at moderate solar activity (1950). These heights would be expected to lie near h_o, or a fraction of a scale height above it.

Although the F1 ledge is not always observed on ionograms, its behavior approximates that of a Chapman layer when it does appear. According to Allen (1948), the critical frequency $f_o F1$ varies diurnally as $(\cos \chi)^{0.2}$. This is different from the behavior of $f_o E$, mentioned earlier, but is consistent with the theory that the F1 ledge lies at the transition between regions of "quadratic" and "linear" loss laws. The index n would be expected to be less than the value 0.25, because the "transitional" recombination coefficient $\alpha\beta/(\alpha N + \beta)$ decreases upward. There is evidence of some geomagnetic control of the F1 layer (Cummack, 1961), which might possibly result from electromagnetic movements such as we discussed in connection with the E layer.

3. F2 Region Problems

Early investigations of the F2 layer critical frequency revealed that it does not behave at all in the manner of a simple Chapman layer.

Although we now have available perhaps 10^8 values of f_oF2, together with many computed electron density distributions for selected stations, the physics and chemistry of the F region are only partially understood, and the rates of the photochemical processes are known to within only a factor of two, at best. Some of the outstanding problems of F2 layer morphology are:

(a) behavior of the F2 peak (N_mF2, h_mF2) and the diurnal behavior of electron densities at fixed heights

(b) the topside of the F layer

(c) the seasonal and annual anomalies

(d) the equatorial anomaly

(e) high latitude behavior

Each of these problems will be discussed in turn and some of the proposed explanations advanced, even though they may be only tentative suggestions. Little mention of electromagnetic drifts will be made, although these may be responsible for some of the anomalies. Mainly, this omission is made because of the great difficulty in obtaining quantitative measurements of electromagnetic drifts. The theory of drifts is described in more detail in Sec. VI.

We should state also that all our remarks apply to the average behavior of the undisturbed F2 layer. More than the other layers, the F2 layer is subject to day-to-day variations of perhaps 20 percent, and may even change appreciably from one hour to the next. Some discussion of this variability is given in a review of F2 layer morphology by Wright (1962).

(a) The F2 peak and N(h,t) curves. In Figs. 21a and 21b, we reproduce the variations of N_mF2 and h_mF2 for quiet days at Slough for a number of months of low solar activity (1953) and moderately high activity (1950), given by Thomas, Haselgrove and Robbins (1958). These display some of the anomalies we shall discuss. Figure 21a shows the seasonal anomaly (for Jan 1950) and also reveals that N_mF2 is fairly sharply peaked about noon in winter but is rather irregular in other seasons.

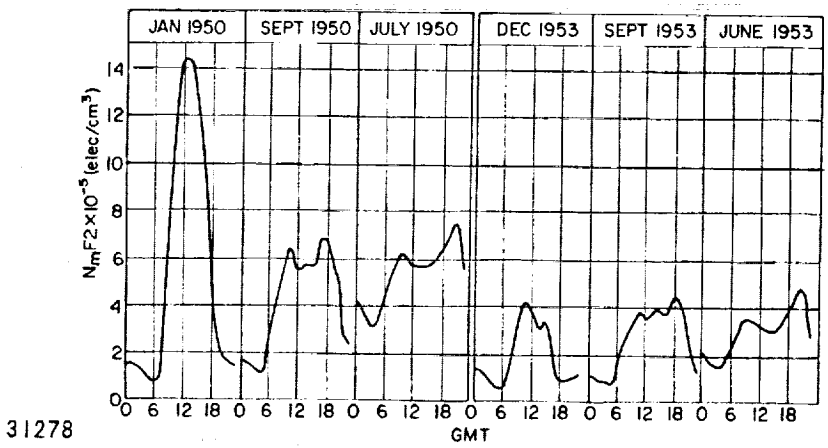

a. N_mF2. The six curves show the seasonal and solar cycle variations.

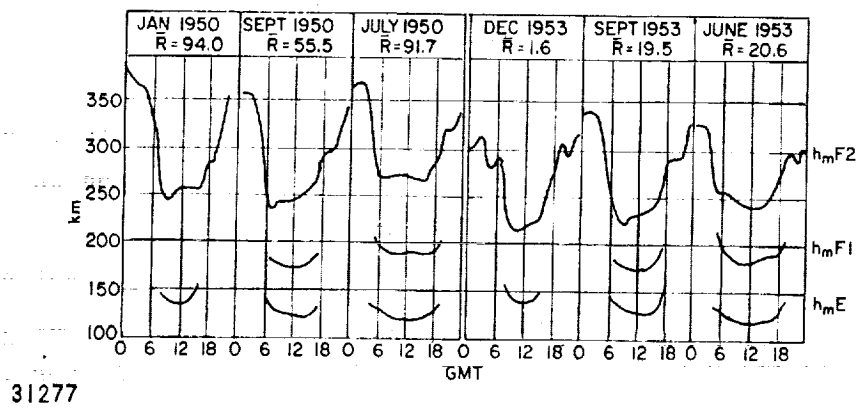

b. h_mF2 (after Thomas et al)

FIG. 21. AVERAGE DIURNAL VARIATION FOR THE 10 INTERNATIONAL QUIET DAYS IN EACH MONTH AT SLOUGH.

The $N(h,t)$ curves of Fig. 22 show many features typical of the mid-latitude F2 layer. Up to 200 km, the curves are fairly regular, consistent with control by photochemical processes at these heights. Higher up, where transport processes are important, the curves are less regular and not symmetrical about noon. Although we should expect the maximum of N to occur at a time about $1/\beta$ later than noon, it seems that movements so affect the layer that the maximum N may be attained before noon. This may well result from thermal expansion of the F

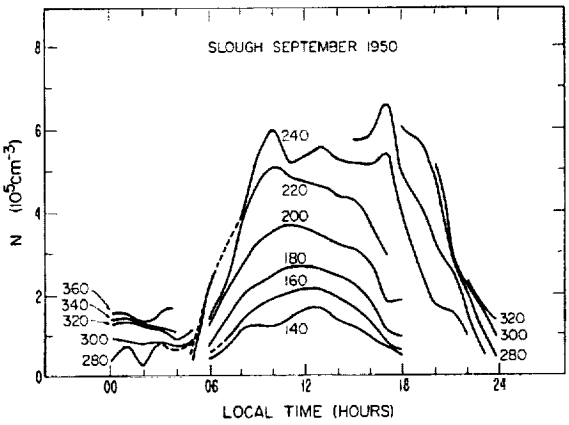

FIG. 22. N(t) CURVES, SHOWING THE AVERAGE DIURNAL VARIATION OF ELECTRON DENSITY AT FIXED ALTITUDES (in kilometers) FOR MAGNETICALLY QUIET DAYS DURING ONE MONTH AT SLOUGH. (After Croom, Robbins and Thomas, 1959a.)

region. As the F region cools and contracts in the evening, there is a tendency for N to increase and on occasions both morning and afternoon maxima of N at fixed heights, or of N_m, are observed.

The heating and cooling of the atmosphere alters the height at which $D/H_i^2 \approx \beta$, near which h_mF2 should occur. Although the drop of h_mF2 at sunrise, and its subsequent rise (Fig. 21b), are broadly consistent with the theoretical behavior outlined in Sec. III-6, the difference between noon and midnight h_mF2 (generally 100 km) is much greater than would be expected from theory, especially when the day-night temperature changes are allowed for (Rishbeth, 1964). At lower latitudes, the difference is smaller, and changes sign near the equator where h_mF2 is higher by day than by night. These facts are unexplained, though some kinds of movements might be responsible.

At night, N_mF2 decreases rather irregularly. This decrease may not be sustained throughout the night, especially on long winter nights when N_mF2 appears to reach a "base level." The N(t) curves of Fig. 22 illustrate this. N_m may then fluctuate irregularly but does not show a steady decrease. In fact, there is sometimes a slight increase well before F layer sunrise.

The base level is also evident in the behavior of the total electron content of the whole ionosphere, as determined by lunar-echo Faraday rotation observations (Evans and Taylor, 1961). Again, the explanation may be an upward drift of the ionosphere due to electromagnetic forces, or it might be due to corpuscular ionization, such as the flux of soft electrons postulated by Antonova and Ivanov-Kholodnyy (1961). An alternative source might be provided by slow downward diffusion of ionization from the exosphere, as investigated by Hanson and Ortenburger (1961), but theoretically this appears to be inadequate to maintain the F layer (Hanson and Patterson, 1963). Also, it seems unlikely that photoionization by EUV could provide enought ionization at night, since an attempt to detect He II 304 Å radiation at night yielded negative results (Byram et al, 1961).

(b) The topside of the F layer has been investigated in many rocket experiments. Most of these yield an exponential N(h) profile roughly consistent with diffusive theory, and give useful information about the variations of temperature in the F region, though the results are sometimes anomalous (Bowhill, 1963).

One of the interesting discoveries from the UK-1 satellite "Ariel" is that field-aligned "ledges" exist in the topside F region (Sayers, Rothwell and Wager, 1963). One of these seems to be associated with the "troughs" of the F region equatorial anomaly, while the others are found at higher latitudes. Further discussion of these ledges, based on "Alouette" data, has been given by Lockwood and Nelms (1964).

The "Alouette" topside sounder has provided a powerful tool for investigating the upper F region. So far, only preliminary results have been published, including a number of topside N(h) profiles and some latitudinal distributions (Warren, 1963; King, 1963; Knecht and Van Zandt, 1963). Plots of log N(h) sometimes show a change of slope between 600 and 800 km, which is thought to represent the transition between O^+ ions and He^+ ions (Calvert, Rishbeth and Van Zandt, 1964). Not all the profiles, however, can be fitted by a simple model of this type (Bauer, 1964).

c. Seasonal and annual anomalies. These anomalies have been known for a long time. The most detailed analysis of seasonal and annual variations of N_mF2 has been made by Yonezawa and Arima (1959) and Yonezawa (1959). Over the world as a whole, there exists an annual variation of N_mF2, which is about 20 percent greater in December than in June. This may be compared with the annual 3 percent variation of the earth-sun distance, which is a minimum in January. In addition, there is a "seasonal" anomaly in that daytime N_mF2 tends to be greater in winter than in summer. In the northern hemisphere these two effects act in phase to give a resultant anomaly, which is very large at high solar activity (see data for 1950 in Fig. 21a) but scarcely evident at sunspot minimum (as for 1953). Croom, Robbins and Thomas (1960) have shown that this effect is most pronounced within a certain range of latitudes (probably magnetic latitude) and the solar-cycle dependence has been further studied by Thomas (1963).

Rishbeth and Setty (1961) found that, just after layer sunrise, dN/dt in the F2 layer is much greater in winter than in summer; and that the increase of N begins at a larger value of χ (about 97 deg) in winter than in summer (about 93 deg). This seasonal sunrise anomaly can be seen in the slopes of the $N_m(t)$ curves of Fig. 21a and is particularly interesting because at sunrise the continuity equation is dominated by the photochemical terms, especially q. These authors suggested that seasonal changes of atomspheric composition--in particular, the ratio $n[O]/n[N_2]$--could affect q and β.

Such changes could occur in the F region if there occurred a change in the O/N_2 ratio at the turbopause near 100 km, where diffusive separation of neutral gases begins (Sec. I-4); or if the altitude of the turbopause itself varied. These ideas have been developed by G. A. M. King (1961), who suggested that travelling disturbances might affect the height of the turbopause; and by Wright (1963, 1964). Recently, it has been suggested that large-scale meridional circulations of air in the mesosphere and lower thermosphere give rise to changes of the O/N_2 ratio at the turbopause, and hence also in the F region (King, 1964). This can be related to seasonal changes in mesospheric temperature (Young and

Epstein, 1962); here we may have an important connection between the ionosphere and lower atmosphere. We note that no satisfactory explanation of the F region seasonal anomalies in terms of ionospheric movements, or in terms of temperature changes, has ever been devised.

(d) The equatorial F2 layer. The F2 layer at low latitudes is very peculiar. Sometimes, electron densities are greater at midnight than at noon. Norton and Van Zandt (1964) succeeded in explaining daytime $N(h,t)$ curves in terms of photochemical processes only, taking into account the diurnal temperature changes in the atmosphere. Vertical diffusion is neglected because ionization cannot diffuse across the geomagnetic field lines. It can, however, diffuse along the field (i.e., horizontally) and this may affect the latitude distribution of ionization.

A plot of noon values of N_mF2 as a function of latitude, shows a pronounced "trough" centered on the magnetic dip equator, with "crests" about 15 deg or 20 deg to the north and south (Appleton, 1946). This trough is also found in plots of N at fixed heights below (Croom, Robbins and Thomas, 1959b) and above (King, 1963) the F2 peak. Studies by many authors, most recently Lyon and Thomas (1963) show that the anomaly exists during most of the day, being most pronounced around sunset, but disappears after midnight. The anomaly shows rather different features in different longitudes.

It was suggested by Mitra (1946) that the anomaly might be due to the diffusion of ionization away from the equator, causing an accumulation of electrons to the north and south. To test this suggestion theoretically, it is necessary to use a form of the diffusion equation which takes account of the geometry of the geomagnetic field. Solutions of this equation, for equilibrium conditions, lead to the conclusion that diffusion is not sufficient to produce a trough as large as is actually observed and that other processes are responsible (Rishbeth, Lyon and Peart, 1963), though this subject is very controversial (Goldberg, Kendall and Schmerling, 1964). It is also quite possible that electromagnetic drifts contribute to the equatorial anomaly (Duncan, 1960).

(e) High latitudes. The morphology of the F2 layer at high latitudes is very complicated. Probably transport processes play a larger

part than at lower latitudes, especially during the polar night when the F layer persists despite the absence of solar photoionization. Observations of f_oF2 at the South Pole (Knecht, 1959) and Halley Bay (Bellchambers and Piggott, 1960) show unusual variations of F2 layer parameters, for which no complete explanations have been given.

4. F Region Rates

In principle, it should be possible to determine the rates of production and loss in the F region from the large amount of available $N(h,t)$ data. But in practice it has proved difficult to assign reliable numerical values to these rates. The reason for this seems to be that the F2 layer is so complex that it is difficult to isolate the effects of any one process. In the lower F region, photochemical processes dominate and the situation should be simpler, but it turns out that the best data give only the ratios of quantities such as q, α, β and D, not their absolute values. This situation is now being resolved by rocket observations of the solar spectrum, which give absolute values of q. Even these, however, are influenced (to some extent) by uncertainties about atmospheric composition. Another approach, of course, is the laboratory determination of rate coefficients. It cannot be yet said that these are sufficiently accurate to provide definitive values. In some cases, there is conflict with the ionospheric evidence and it may be that laboratory and ionospheric conditions are not really comparable. Ionospheric data relating to various process rates are considered below.

Noon electron density. We saw previously that observations of the F1 layer lead to the relation $(N_mF1)^2 \sec \chi = (q_o/\alpha) = 500\ (1 + 0.16\ R) \times 10^8\ cm^{-6}$ (Eq. IV-4). For the F2 layer, at heights up to the peak, we have suggested that $N \cong q/\beta$, but owing to the variability of the F2 layer, no general formula for N_mF2 can be given. Allen (1948) finds that at several stations $N_mF2 \propto (1 + 0.02\ R)$, and this linear dependence incidentally supports the theory that the rate of loss in the F2 layer is given by βN and not by αN^2.

Night decay. Values of β for the F2 layer have been deduced from nighttime $N(t)$ variations. After sunset, the decay of N at

any height h should at first depend on the local loss coefficient $\beta(h)$. Once the nighttime "stationary" layer is established, the decay would depend on the value of β at the peak (Sec. III-6), but electromagnetic and thermal motions apparently complicate the analysis. Ratcliffe et al (1956) suggested the empirical formula (with h in km)

$$\beta(h) = 10^{-4} \exp [(300 - h)/50] \text{ sec}^{-1} \qquad \text{(IV-5)}$$

from a study of $N(h,t)$ data from several stations. Owing to the difficulty of obtaining acceptable nighttime $N(t)$ curves for the lower F region, values of α have not been deduced for the F1 layer by this method. As we have discussed, it now appears that the loss coefficient is quite sensitive to temperature variations, since the neutral concentrations at any fixed height vary with temperature. This effect has been studied by Nisbet and Quinn (1963) and others even more recently.

Eclipses. Since this topic is discussed in Sec. IV-5, we only mention here that the observations do not lead to unambiguous values of α for the F1 layer. Similar remarks apply to methods based on the classical Chapman layer theory (Appleton, 1937). In the F2 layer, the situation is usually hopeless because of movements, although in some cases this difficulty appeared not to be serious (Van Zandt et al, 1960).

Sunrise. Just after F layer sunrise, the peak of q lies in the F2 layer and we expect to have $\partial N/\partial t \approx q(\chi) \approx q_o/\text{Ch } \chi$. Rishbeth and Setty (1961) found values of $q(\chi)$ but, owing to uncertainties in Ch χ and in other terms, this method does not lead to accurate values of q_o.

From these methods, we can obtain values for production and loss rates, but these are probably only accurate to within a factor of two. Values of the ambipolar diffusion coefficient D have to be deduced indirectly, since direct measurements have not been made and the theory is not entirely satisfactory. Shimazaki (1964) has obtained values of D and β from detailed analysis of night $N(h,t)$ data. His values of D are considerably smaller than those needed to explain the behavior of the daytime F2 layer.

We must emphasize that the coefficients q, β and D depend very much on neutral air densities, which in turn depend on scale heights. Hence, they must vary considerably with solar activity, and there is no such thing as the value of β at any given height. Some illustrative calculations have been made by Rishbeth (1964), whose suggested values of β at 300 km, as a function of solar activity and F region temperature, are compared with other determinations in Figs. 23a, b. The noon value of q at 300 km increases very rapidly with increasing solar activity, because the incident flux of radiation and the concentration of ionizable gas, atomic oxygen, are both increased. Values of q, β and D are tabulated in Table III. Theoretical $N(h,t)$ curves calculated with these coefficients agree with many daytime F2 data, but in order to make them consistent with the survival of the F2 layer throughout the night, it has to be assumed that some nocturnal source of ionization exists.

5. Eclipse Effects

On those infrequent occasions when the sun is partially or totally occulted by the moon, first order perturbations are observed in the electron density distribution in the ionosphere. This is particularly true in the D, E and F1 regions, but sometimes they also extend up to the F region peak. These events provide useful methods for the calculation of the production and loss terms in the continuity equation and provided early evidence that the E and F1 layers are produced by electromagnetic--not corpuscular--radiation. Although absorption and therefore electron density varations in the D region have been observed during eclipses, most studies relate to the higher layers.

When considering the E and F1 regions, we may start with the appropriate continuity relation $\partial N/\partial t = q - \alpha N^2$, which we found in an earlier section. The variation of q_m with time on a non-eclipse or "control" day is sketched in Fig. 24 as a solid line. From Chapman's theory, $q_m = q_o(\cos \chi)$ for an isothermal atmosphere, but on the eclipse day we must multiply this by a factor $\phi(t)$ equal to the uneclipsed fraction of the sun's disk, assuming the ionizing radiation is emitted

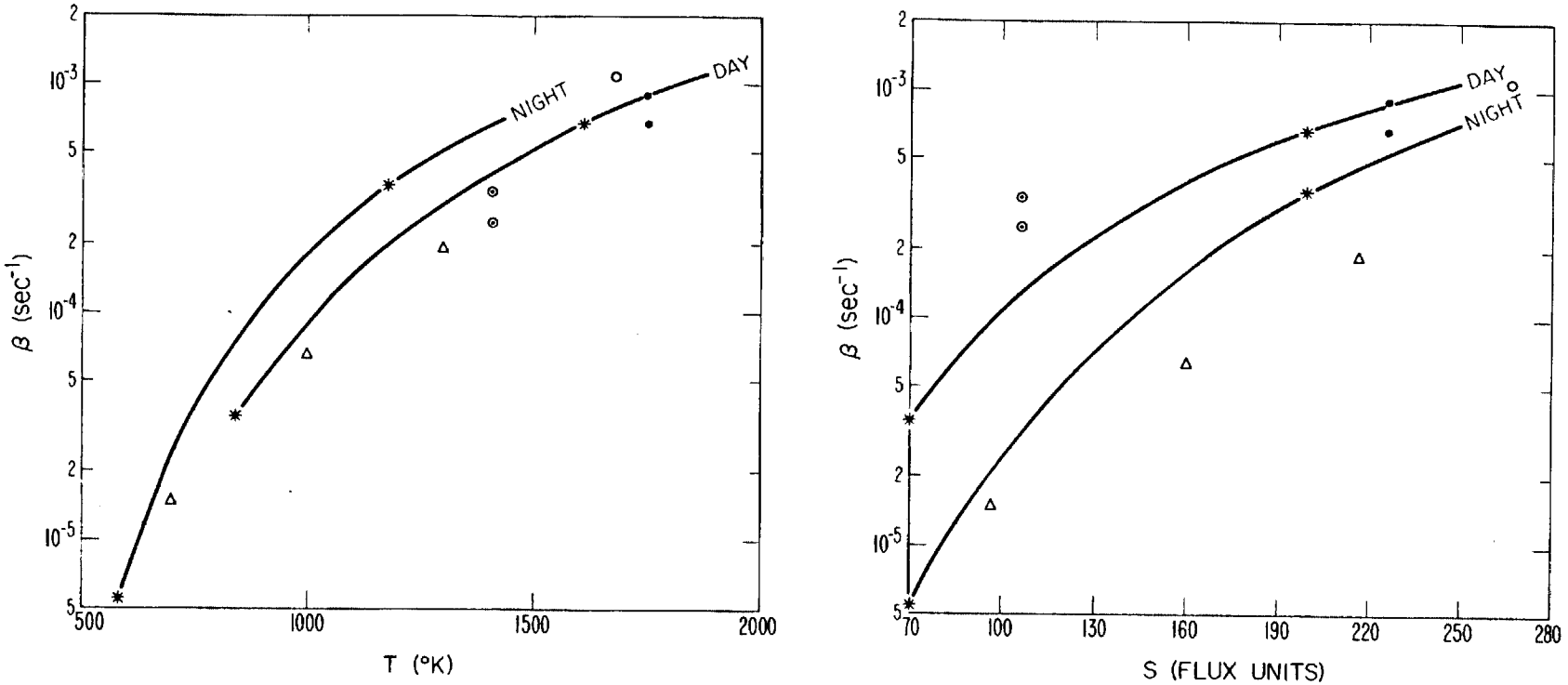

a. Temperature T

b. 10.7 cm solar flux density S

FIG. 23. LOSS COEFFICIENT AT 300 KM, β(300), AS A FUNCTION OF TEMPERATURE AND 10.7 CM SOLAR FLUX DENSITY FOR NOON AND MIDNIGHT. Points identified by * are taken from Table III and joined by continuous lines computed with the aid of Harris and Priester models for other values of S. Their models are used for interconversion of S and T.

△: Nisbet and Quinn (1963), observations of night F layer
○: Norton and Van Zandt (1964), equatorial F2 layer model, t = 12 hr
⊙: Norton et al (1963), model of E and F layers, t = 10 hr (below) and 12 hr (above)
●: Van Zandt et al (1960), eclipse observation, t = 09 hr (below) and 12 hr (above)
(In the last two cases, the values for 12 hr are rough estimates, obtained by connecting the values given for the earlier hours for changes in atmospheric density between those hours and noon.)

TABLE III. ROUNDED VALUES OF F2 LAYER PARAMETERS
(from Rishbeth, 1964)

Parameters	Sunspot Minimum	Sunspot Maximum	Unit
Zurich sunspot no. R*	0	200	
Solar 10.7 cm flux S*	70	200	10^{-22} w $m^{-2}(c/s)^{-1}$
Values at 300 km:			
Temperature T			
(noon)	840	1610	°K
(Harris and Priester, midnight)	580	1180	°K
Photoionization q			
(noon)	50	750	cm^{-3} sec^{-1}
Loss coefficient β			
(noon)	0.4	7	10^{-4} sec^{-1}
(midnight)	0.06	4	10^{-4} sec^{-1}
Diffusion coefficient D			
(noon)	7	2	10^{10} cm^2 sec^{-1}
(midnight)	14	2	10^{10} cm^2 sec^{-1}

*Both these parameters are used to describe solar activity. For present purposes, a linear relation between them is assumed, and is defined by the values quoted.

uniformly across the disk. Thus $q = \phi q_o(\cos \chi)$, and this function, as well as the maximum electron density N_m, are shown in Fig. 24 for a hypothetical total eclipse.

At second contact t_2, the production function is zero and we may calculate the recombination rate as

$$\alpha = - \frac{\partial N_m / \partial t}{N_m^2} \qquad \text{(IV-6)}$$

in which the implicit assumption has been made that the height of N_m does not change during the eclipse. At the E region peak, Minnis (1955) has found $\alpha \approx 1.5 \times 10^{-8}$ cm^3 sec^{-1} using this method.

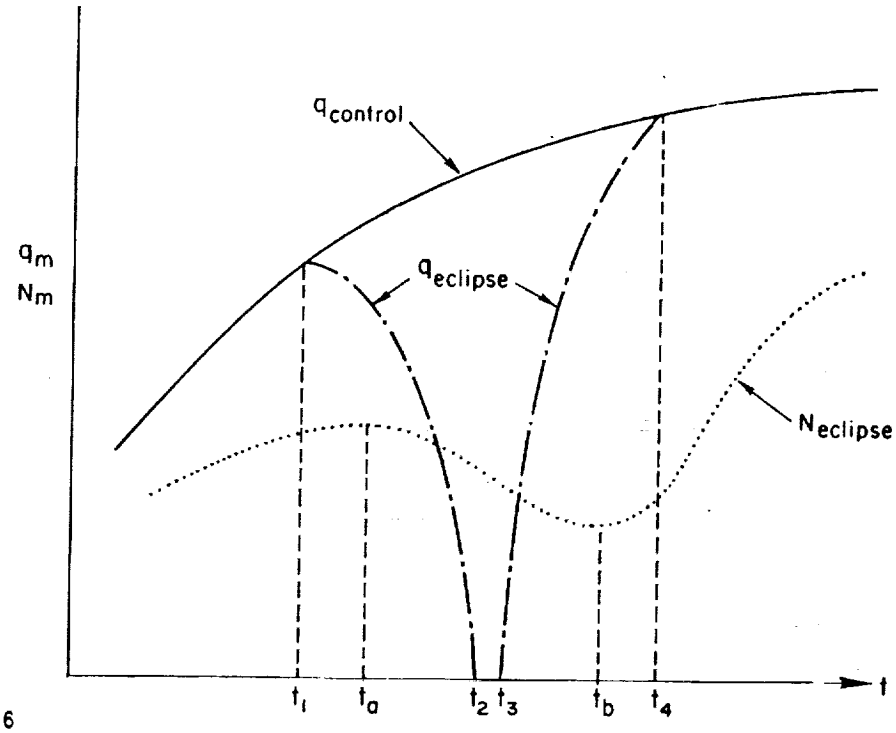

FIG. 24. ILLUSTRATING THE VARIATION OF PRODUCTION RATE ON A CONTROL DAY AND THE PRODUCTION RATE AND MAXIMUM E REGION ELECTRON DENSITY ON THE DAY OF A HYPOTHETICAL TOTAL ECLIPSE. From curves similar to these, it is possible to calculate the recombination coefficient.

It is also possible to assume a value for α and predict the shape of N_m vs time for the eclipse, looking especially for the time separation between third contact t_3 and t_b, the electron density minimum. The time difference is expected to be a few minutes, but the observations do not show any very consistent pattern (Ratcliffe, 1956).

It now appears likely that α has been somewhat underestimated in the eclipse analyses because some of the X ray radiation may originate in the solar corona and thus fail to be occulted by the moon. Elwert (1958) has calculated that 10 to 20 percent of the X ray radiation may come from above the photosphere. Since q is usually a much larger

term than $\partial N/\partial t$ in the E region continuity equation, the electron production remaining at the time of total optical eclipse would generate a much larger proportional error in α. Furthermore, the radiation is probably more intense from various active regions on the sun and the production function would not be the smoothly varying geometrical function originally assumed. Values for α between 10^{-8} and 10^{-7} cm^3/sec are usually adopted for the E region, and are somewhat smaller in the F1 region. Thus eclipse results fall in the lower portion of this range.

The various eclipse measurements of α become more consistent with each other and also with the results from entirely different methods (e.g., nocturnal decay and "sluggishness") when a two-ion mixture is considered (Bowhill, 1961). If the ions have distinctly different values of α, one ion will decay more rapidly, resulting in a diminishing recombination coefficient with time. Bowhill suggests that NO^+ and O_2^+ are these ions and that the latter may decay most rapidly. After sunset, the NO^+/O_2^+ ratio should increase and this seems to be borne out by the rocket ion spectrometer results of Fig. 17.

Eclipse results in the F2 region are more difficult to interpret than those at lower altitudes. Near the peak, little or no effect may be observed and movements resulting from diffusion or electromagnetic drift may also be important. The most successful analysis has been made by Van Zandt, Norton and Stonehocker (1960) for the October 1958 eclipse at Danger Island. They made several simplifying assumptions which appear to be rather well satisfied by the results. They have first assumed that temperature changes and all movement terms are negligible. Since Danger Island is at a magnetic latitude of only 11 deg, vertical diffusion is certainly slow. Also, their calculations have been made only at altitudes greater than 280 km, where the loss of electrons is believed to be linearly related to the electron concentration (βN). Furthermore, these altitudes are all well above the production peak and have small optical depths. Thus, the production rate at any fixed height is approximately constant without dependence on $\cos \chi$ for control days; on the eclipse day, q need only be multiplied by the uneclipsed portion of the sun's disk. The radiation principally responsible for F2 ionization is in

the UV, and it is believed to originate more uniformly across the disk, rather than partly in active regions and in the corona. This eliminates one of the principal difficulties encountered at lower altitudes. Within these assumptions, the continuity equation for the F2 region can be written

$$\frac{\partial N/\partial t}{N(h,t)} = q(h)\left[\frac{\phi(h,t)}{N(h,t)}\right] - \beta(h) \qquad \text{(IV-7)}$$

Since $q(h)$ is relatively constant well above the production peak as discussed earlier and $\beta(h)$ should be nearly constant if temperature changes are negligible, Eq. (IV-7) is of the form $y = qx - \beta$. The values of y and x can be determined experimentally as a function of time at any fixed altitude, and we may expect a graph of y vs x to be approximately linear, with a slope of $q(h)$ and y intercept equal to $\beta(h)$. Van Zandt et al (1960) have made these calculations at each 10 km height interval between 290 km and 450 km and obtained rather good consistency throughout the range. Their results may be expressed mathematically as

$$q(h) = 880 \exp\left[(300 - h)/186\right] \text{ elec/cm}^3\text{/sec} \qquad \text{(IV-8)}$$

$$\beta(h) = 6.8 \times 10^{-4} \exp\left[(300 - h)/103\right] \text{ sec}^{-1} \qquad \text{(IV-9)}$$

where h is measured in kilometers.

Although this value of β is much greater than that obtained by Ratcliffe et al (1956) from nighttime $N(t)$ curves at times of moderate sunspot numbers, Fig. 23 shows that these two results are reasonably consistent. At the time of the Danger Island eclipse, the sunspot number was almost as high as has ever been recorded; hence, as discussed in Sec. IV-4, large values of β are to be expected. If the scale height in Eq. (IV-8) is associated with atomic oxygen, and that in (IV-9) with molecular nitrogen or molecular oxygen, a temperature of over 3000 °K is deduced, but this would seem to be rather excessive, since other evidence favors values of 2000 °K to 2500 °K at sunspot maximum.

6. Ionospheric Irregularities

The preceding sections dealt with only the large-scale or "background" distribution of ionization. But, superimposed on this background, small-scale irregularities of ionization seem to exist at every level in the ionosphere. The basic properties to be measured are their size and shape, intensity (i.e., fractional deviation of electron density) and their direction and speed of motion. The measurements are, however, liable to be influenced by instrumental selection. For instance, a spectrum of irregularities may exist at a particular level, of which only certain components will be recorded by any particular equipment. Some information about irregularities is given by standard ionograms or $h'(f)$ curves, and by continuous recordings of phase heights at fixed frequencies, or $h'(t)$ curves. These are particularly useful for the detection of large "travelling ionospheric disturbances," to be discussed later in this section.

Irregularities are also detected because of their ability to scatter radio waves. Signals at frequencies of 50 to 100 Mc/s, too high to be reflected from a smooth ionosphere even at oblique incidence, may be received at distances of a thousand kilometers from the transmitter, having been scattered from irregularities in the D region at 80 to 90 km (Bailey, Bateman and Kirby, 1955). This forward scatter is of practical importance, but most of the scientific study of the irregularities themselves has been conducted with more specialized techniques. One of these is the reflection method of Mitra (1949), which uses a pulse transmitter at a frequency of a few Mc/s, and three receivers in a triangle, spaced roughly one radio wavelength apart. Another method makes use of a radio star as the source and amplitude fluctuations produced by the ionosphere are again observed with spaced receivers. This latter method detects mainly irregularities in the F region, whereas the reflection method can be used to study the normal E layer by day, and has been applied to E_S ionization at night. If a suitable radio frequency is chosen, it can also be used to study the F layer. If the fading is caused by the steady drift of irregularities in the ionosphere, then the records from each receiver are similar, but there are systematic

time delays between the appearance of particular features (such as maxima and minima of signal strength) on the different records, from which the drift velocity of the irregularities can be determined.

This simple "time-delay" approach is only valid if the ionospheric irregularities possess certain statistical properties. It has largely been superseded by a more sophisticated analysis which treats fading statistically (Briggs, Phillips and Shinn, 1950; Phillips and Spencer, 1955; Bowhill, 1961). First, it should be noted that the wavefield at the ground is formed by diffraction from an irregular "screen" in the ionosphere. This "screen" consists of irregularities which impose phase variations on the wavefront of the downcoming radio wave. If the variations are "deep," in the sense that the phase deviations exceed one radian in the width of one Fresnel zone, the pattern at the ground is smaller in scale than the screen, but it may retain the general shape and orientation of the irregularities (Hewish, 1951; Fooks and Jones, 1961). For a "shallow" screen, in which the phase changes are less than a radian in a horizontal distance of one Fresnel zone, the amplitude pattern on the ground should be very similar in size and shape to the structure of the irregularities in the ionosphere. The distinction between these two cases therefore depends on both the wavelength and the altitude of the irregularities. The velocity of the wave pattern at the ground is equal to the drift velocity in the ionosphere in the radio-star scintillation method and twice as great for the reflection method.

To describe the shape and size of the irregularities in the screen, use is made of the autocorrelation function of the electron density distribution. In the two-dimensional case, this function may depend on direction and it is generally assumed that the irregularities can be described in terms of a "characteristic ellipse," whose radius in any direction is the distance in which the correlation falls to the value 1/2. The shape, size and orientation of this ellipse provides the information about the ionospheric irregularities.

Since the pattern of the irregularities may change as it moves, another parameter V_C has been defined which is zero if the pattern drifts without

change. If V_C is comparable to the drift velocity V of the pattern, it implies that random changes in the pattern contribute to the observed fading as much as does the bodily drift, and this appears to be the situation usually encountered.

All these quantities can be determined from sets of fading records by a complicated procedure known as "full correlation analysis." This has been applied by Fooks and Jones (1961) who compare the results with those of a simpler analysis developed by Yerg (1956) and the straightforward "time-delay" approximation described earlier. They further discuss the circumstances under which the simpler methods can give meaningful results. The time-delay method seems to lead to overestimates of drift velocity. Moreover, if the irregularities are elongated, the simple time-delay method tends to emphasize motions normal to the axis of elongation, and thus give incorrect results concerning the direction of drift.

The reflection method of Mitra has been used to study drifts in many parts of the world. Most of the data have been analyzed only by simple procedures, such as the time-delay method. Deduced drift velocities are typically a few decameters per second, but the details of their magnitudes and directions are extremely complicated and consistent patterns do not always emerge. Survey articles, with references, have been given by Briggs and Spencer (1954), Shimazaki (1959), and Rawer (1963).

The irregularities in the E and lower F region are often quoted as being a hundred meters or so in dimension. Probably there exists a distribution of excess electron density which contains a broad spectrum of spatial periods. When "correlation ellipses" are computed, the ratios of their major axes are generally found to lie in the range from 1.5 to 2. The irregularities are thus not greatly elongated, and the directions of elongation do not seem to follow a very clear-cut pattern. The ratio V_C/V which, as previously stated, measures the relative importance of random change and bodily drift in producing fading is sometimes small and sometimes large, but its median value is near unity. Typical irregularities are thought to contain a fractional deviation of electron density, $\Delta N/N$, of a few percent. Fooks (1962) has quoted a figure of 2 percent for irregularities in the E layer and lower F layer by day.

The irregularities principally responsible for radio-star scintillations are located in the F region, at heights of 250 km and above. On occasion they are above the level of the F2 peak and are therefore inaccessible to conventional ground-based sounding, although they can be studied by satellite techniques such as beacon transmissions and the topside sounder.

Early observations of radio-star scintillations at 3.7 m wavelength (81 Mc/s) showed that records obtained from spaced receivers showed good correlation for spacings up to a few kilometers, but for spacings of 200 km, the occurrences of scintillation at the two sites are related but the scintillations themselves are quite uncorrelated (Smith, Little and Lovell, 1950). This indicated a terrestrial (presumably ionospheric) origin of the scintillations. By using diffracting screen theory, Hewish (1952) was able to estimate an altitude of 400 km and dimensions of several kilometers for irregularities producing scintillations at 6.7 m wavelength (45 Mc/s). Steady drift velocities of 100 m/sec or more, were found. Later work on nighttime scintillation has tended to confirm Hewish's conclusions in general, but some scintillation at low elevation angles has been associated with E_S ionization (Wild and Roberts, 1956) and E region irregularities (Chivers and Greenhow, 1959).

There seems to be general agreement that irregularities in the F region are considerably elongated in the direction of the geomagnetic field lines. Axial ratios as great as 10:1 have been reported, and under these circumstances it is difficult to deduce reliable north-south components of velocity.

It is sometimes possible to make continuous observations of a circumpolar radio star. The amount of scintillation may then depend on the elevation of the source above the horizon. At low elevations, scintillations become more severe because of the greater length of the slant ray path in the ionosphere and because irregularities are further from the observer. Since the ray path from a source at low elevation intersects the F region a thousand kilometers or so from the observing point, latitudinal variations of the severity and frequency of scintillation may be studied.

In order to make a statistical study of the occurrence of scintillation, it is necessary to assign numerical indices to describe the amount of scintillation or the degree of spreading. This tends to be somewhat subjective, though it is possible for individual observers to achieve consistency in the analysis of a long series of records. Prolonged series of observations, extending over several years, have been made in Britain (Briggs, 1964; Chivers, 1960) and in West Africa (Koster and Wright, 1960). Scintillations occur mainly at night, but are sometimes observed by day. It is not clear whether the apparent seasonal variations observed in Britain are real, or result from the dependence of scintillation on the zenith angle of the radio source. But it is clear that scintillations are more common at sunspot maximum than at sunspot minimum, although this is the opposite of the solar-cycle dependence of spread F. It has also been found from satellite observations that the regions producing scintillations are quite dependent on magnetic latitude (Yeh and Swenson, 1959; Kent, 1961). A comprehensive survey of the effects of the ionosphere on radio-wave propagation, including absorption, refraction and scintillation is given by Lawrence et al (1964).

Large irregularities may be detected as distortions of ionogram traces or of high-frequency backscatter patterns. A particular type, known as "travelling ionospheric disturbances," produces "kinks" in the "o" and "x" traces near the F2 cusps on an ionogram, and these gradually move down toward lower frequencies (Munro and Heisler, 1956; Munro, 1957). These are believed to be wavefronts of distrubances, many hundreds of kilometers in extent, which may travel for horizontal distances of 3000 km or more, with speeds of up to 10 km/min. The apparent vertical motion seen on ionograms can be accounted for if the wavefronts are supposed to be inclined to the vertical. Hines (1960) interprets these disturbances as gravity waves in the atmosphere. Because they travel so far and last for so long, it seems that their energy must be trapped in some kind of horizontal duct or "waveguide." If this "ducting" results from large scale wind circulations, as discussed by Hines (1963), then it may be possible to account for the preferred directions of motion noted by Munro. The energy is probably trapped at heights around 100 km,

but some upward leakage occurs and causes the observed effects in the F region.

Spreading of F region traces on ionograms has been divided into two main types. One is "range spreading," in which multiple traces are seen at frequencies well below f_oF2, and which seems to be prevalent at lower latitudes. The other is "frequency spreading," in which the high-frequency ends of the traces are branched or blurred. This is the type most commonly seen at higher latitudes, and the range of frequencies covered by the "spreading" gives an indication of the deviation of electron density, ΔN, present in the irregularities. Spread F indices have been defined empirically and used for statistical studies, including comparisons with the empirical indices used for radio-star scintillations. Published bulletins of ionospheric data contain information about the occurrence of spread F, but scaling practices are known to vary and care must be exercised in the use of such data for detailed statistical studies. On account of their availability, they have been widely used for studies of worldwide occurrence of spread F. Among these may be mentioned the work of Shimazaki (1959) and Singleton (1960, 1962).

From such studies it has been found that spread F occurs most frequently in equatorial and auroral latitudes, less frequently in temperate and polar regions. Spread F occurrence is positively correlated with magnetic disturbance at high latitudes but negatively at low latitudes. At low latitudes the phenomenon appears to be closely connected with the increase of height of the F layer after sunset. It has been suggested by Martyn (1959) that there is a causal connection between these phenomena. Singleton further finds that probability of occurrence is negatively correlated with F2 layer critical frequency. This appears to hold also for the solar-cycle variation at temperature latitudes. Thus spread F is less common at sunspot maximum than at sunspot minimum, opposite to the behavior of radio-star scintillation. This has been used as evidence against the view that the phenomena are closely related (Chivers, 1960), but Briggs (1964) thinks that at sunspot maximum the greatest degree of irregularity occurs above the F2 peak, where it cannot produce effects on bottomside ionograms.

Ionograms obtained from the Alouette topside sounder have also given considerable information about the distribution of spread F. Calvert and Schmid (1964) found that it occurred most frequently at low latitudes, during the night and mid-morning, and at high latitudes, at any hour. It was found to be less common at middle latitudes.

Much study has been devoted to the detailed form of spread F echoes on ionograms, both bottomside and topside, and the way in which they are related to the geometry of the irregularities. This naturally involves wave propagation calculations in an irregular medium. Considerable success has been achieved in relating field-aligned irregularities associated with equatorial spread F to the "ducts" which guide the radio waves transmitted by Alouette. In circumstances when multiple reflections occur, waveguide calculations have proved fruitful in explaining features observed on ionograms (Calvert and Cohen, 1961; Pitteway and Cohen, 1961; Muldrew, 1963).

7. Sporadic E

Ionosondes often detect dense layers or patches of ionization in the E region, at heights of 100 km to 120 km, which do not seem to be related to the normal daytime E layer. This phenomenon is known as "sporadic E" or "Es" because it does not show any regular behavior. Sometimes Es appears in sheets which completely hide the overlying F layer. At other times it may be patchy and partially transparent to waves reflected from higher layers.

In their comprehensive survey article, Thomas and Smith (1959) adopt the IGY definition of a sporadic E reflection as an E region echo characterized by one or more of the following:

random time of occurrence,
partial transparency (echoes also obtained from higher layers),
variation of penetration frequency with transmitter power,
virtual height independent of frequency.

Much of the work carried out on Es has necessarily consisted of classification and tabulation of data. For this purpose, several types

of Es have been defined, which are mostly distinguished by the appearance of the Es traces on ionograms; sketches of these are shown in the Thomas and Smith review cited above. A more recent review, containing many original papers, has been published by Smith and Matsushita (1962).

Sporadic E is studied with the aid of vertical incidence ionograms, oblique incidence ionograms and fixed frequency recordings. Backscatter methods are also useful, particularly if a steerable antenna is used so that the motions of individual Es patches can be followed (Peterson, Egan and Pratt, 1959). Rockets have been flown through Es layers, and data obtained from propagation and probe techniques have indicated the presence of very thin layers of dense ionization at heights of 100 to 130 km. There is some evidence that these occur at a series of "preferred" heights, at intervals of about 6 km (Pfister and Ulwick, 1958; Gringauz, 1958; Smith, 1962).

The parameters used to describe Es include the critical frequencies f_oEs and f_xEs. Es traces often do not show the usual "cusps" and sometimes a "top frequency" at which reflections are obtained, f_tEs, is used (Bibl, Busch, Rawer and Suchy, 1955). In many cases it may be assumed that f_tEs = f_xEs. The "blanketing frequency" f_bEs is the lowest frequency at which echoes from higher layers are received through the Es layer. Generally f_bEs < f_tEs, so that the Es layer is partially transmitting over a (small) range of frequency. Sometimes the Es layer completely blankets all layers above it, and thus prevents observation of the F layer. Another parameter is the virtual height h'Es which is usually independent of frequency over most of the trace, in which case it should be nearly equal to the actual height of the base of the Es layer.

Many surveys of Es occurrence do not distinguish between different types, but merely assess the frequency with which some arbitrary criterion, such as f_tEs > 5 Mc/s, is met. In temperate latitudes, occurrence of this condition has a probability of about 50 percent around noon in summer, and there are lesser peaks of occurrence near noon in winter and midnight in summer. Diurnal minima of occurrence are found near sunrise and sunset, and seasonal minima at the equinoxes. In addition, variations with longitude may exist.

"Patches" of Es may be tens or hundreds of kilometers in extent, and drift with velocities of order 50 m/s. There seems to be little correlation between mid-latitude Es and magnetic activity. Some connection between Es and thunderstorms has been suggested (Rastogi, 1957), and certain E region echoes (not necessarily within the major Es categories) have been attributed to meteoric ionization (Naismith, 1954).

It is difficult to see how sources of ionization could be sufficiently localized to produce Es, except perhaps for energetic charged particles, which seem more likely to be associated with high latitude Es, rather than the mid-latitude types. Any such source would have to operate for the observed lifetime of Es patches, which may persist for some hours, since the mean lifetime of ions in the E region is only a few minutes. Consequently, most attention has been given to explanations involving a redistribution of existing ionization rather than the production of extra ionization.

It does not seem that ordinary turbulence could produce the strong nonuniformities of ionization present in Es. Dungey (1956) showed that a vertical gradient of the horizontal wind velocity (that is, a wind shear) could cause irregularities, and Whitehead (1961) has shown that shears of east-west wind velocity can be very effective in producing thin layers of ionization. This theory seems promising, especially since rocket experiments reveal the existence of strong shears (see also Hines, 1964). Moreover, the theory can explain the connection between Es occurrence and the strength of the horizontal geomagnetic field component (Heisler and Whitehead, 1960). It has been shown that gravity waves in the neutral atmosphere may be the source of the wind shears necessary to this theory of Es (Axford, 1963).

In high latitudes, one type of Es is associated with aurora (Knecht, 1956). Other types are strongly associated with magnetic disturbance, and their geographical and temporal distribution shows interesting patterns (Thomas, 1962b) which suggest that direct particle bombardment is responsible for production of Es ionization.

Near the magnetic equator, a distinctive type of "equatorial" Es is observed, which is patchy and transparent to waves reflected from higher layers. It is strongly associated with the "electrojet" current

(Sec. VI) which flows along the magnetic equator by day (Skinner and Wright, 1957) and, like the electrojet, it is subject to some lunar control (Matsuchita, 1957). The equatorial Es irregularities appear to be aligned with the geomagnetic field (Bowles, Cohen, Ochs and Balsley, 1960), and it has been suggested that they are caused by plasma instabilities arising from the flow of the large electrojet current (Farley, 1963).

8. Artificial Disturbances

The availability of rockets has led to several methods in which modifications to the naturally-occurring ionosphere are possible. A number of rocket flights have released various chemicals including sodium, aluminum oxide, and cesium at altitudes within the D and E regions. The objectives of a series of flights in 1960 (Project Firefly) were the study of the motions, luminescence, and decay of regions of high electron density (Gallagher, 1963) which describe these results, An interesting collection of ionograms relating to these experiments has been presented by Wright (1964). The wind velocities are found to range up to 70 m/s in the E region on many occasions and at times to exceed 150 m/s. Usually, there is also a variation of both speed and direction with altitude; the resulting wind shear may well lead to the sporadic E layers as we discussed in the preceding section.

The radial growth of the artificial ion-electron clouds which are produced by these chemical releases permits the appropriate diffusion coefficients to be calculated. Zimmerman and Champion (1963) find the measured values for the diffusion of lithium, sodium or cesium through molecular nitrogen to be a factor of two to four smaller than theoretical values at altitudes between 100 and 150 km.

The explosion of nuclear bombs at high altitudes also generates a variety of geophysical effects which have been used to study the upper atmosphere. The great release of energy will obviously produce greatly enhanced ionization over a considerable volume and a visual aurora may be observed at the magnetic conjugate point owing to the dumping of high energy electrons trapped in the earth's field. Other electrons may "mirror" at higher altitudes and continue to precess about the earth in

"shells" for periods of months or even years. The synchrotron radio emission from these electrons has been measured and is the source of considerable concern to some radio astronomers (Peterson and Hower, 1963; Ochs et al, 1963). VLF and hydromagnetic waves are launched at the time of the explosion and the propagation of these waves may be studied all around the globe. These and other phenomena are described in the "Collected Papers on the Artificial Radiation Belt from the July 9, 1962, Nuclear Detonation" (1963).

V. RELEVANT ASPECTS OF GEOMAGNETISM

1. Introduction

Any discussion of the ionosphere would be quite incomplete without consideration of the terrestrial magnetic field. In Sec. III-5 we found that in the "transport regime" above the F2 peak, plasma diffusion was constrained to follow the earth's magnetic field lines, and this fact was included in evaluation of the diffusion coefficient in the continuity equation.

A number of the experimental techniques described earlier rely on magnetic field effects. The polarization rotation produced by the Faraday effect was measured in propagation experiments with satellites and moon echoes. The received spectrum from incoherent scatter was found to be greatly modified by the presence of a magnetic field.

In addition to these reasons for studying the earth's magnetic field, there are several phenomena which have not yet been considered. It appears that tides and thermal expansion of the neutral atmosphere generate a sufficient emf by dynamo action to drive currents and produce additional polarization fields which can move the plasma in the ionosphere. The height at which the electron-neutral collision frequency equals the gyromagnetic frequency determines the altitude of maximum conductivity, and thereby the currents which flow in response to the induced emf's. We shall also describe "magnetic storms" which are usually accompanied by auroras and ionospheric deviations as large as ±50 percent from the normal electron density values.

One of the earliest experiments related to geomagnetism was published in 1600 by Queen Elizabeth's physician, William Gilbert, and it provided considerable insight into the nature of the earth's magnetic field. As described by Chapman (1951), Gilbert "cut a spherical piece of the naturally magnetized mineral called lodestone, and examined the distribution of direction of the magnetic force over its surface by means of tiny magnetized needles freely pivotted. He saw that the distribution of dip agreed with what was known of the earth's field. Hence, he concluded that the earth itself is a great magnet, similar to his magnetized

sphere except in size." We can now show mathematically that the external field of a uniformly magnetized sphere is identical to that of a dipole of appropriate magnitude placed at the center of the sphere. Since we find, as did Gilbert, that this does provide a reasonable first-order fit to the observed field near the earth's surface, we will want to consider the dipole field in more detail a little later.

By 1635 Gellibrand had discovered the secular variation in declination at London, and observations since then suggest a cyclic "wandering" of the magnetic declination and inclination with a period of about 500 years. The secular variation in the magnitude of the field has only been studied for a little over a century, since instruments to measure the absolute magnitude were not devised until the nineteenth century.

Another major advance was made in 1722 by Graham, who was a clockmaker in London. He discovered the regular diurnal variations of the compass needle and also the larger perturbations which occur at times of magnetic storms. Further work by Celsius and Wilcke showed that magnetic disturbances are quite widespread and well correlated with the visible auroras. Surprisingly, it was still another century before Schwabe in 1843 noted the periodicity of the sunspot number. It was soon established that this periodicity is reproduced in the frequency of magnetic disturbance.

In 1882 Balfour Stewart connected these magnetic variations with the region we now identify as the ionosphere. He argued that the diurnal variations were produced by currents flowing in the upper atmosphere in regions of appreciable conductivity. He also indicated that these currents could be driven by electric fields induced by motion of the air across the earth's magnetic field lines and this is essentially the position maintained today. The presence of the ionosphere was further implied by Marconi's high-frequency trans-Atlantic communication in 1901, but "direct" measurements were not made until about 1925 by Breit and Tuve and by Appleton, as we discussed earlier.

The strength of the earth's field is now measured at numerous magnetic observatories located all over the globe. The standard components which are recorded on magnetograms are usually: (a) northward X;

eastward Y; downward Z; or (b) easterly declination $D = \arctan(Y/X)$; horizontal intensity $H = (X^2 + Y^2)^{1/2}$; vertical intensity $V = |Z|$. Sometimes the dip angle or inclination, $I = \arctan(Z/H)$, is also given.

Further details of a historical nature are given by Chapman in "Solar Plasma, Geomagnetism and Aurora" (1963). Probably the best discussion of the entire area is found in the two-volume edition of Chapman and Bartels, "Geomagnetism" (1940).

2. The Geomagnetic Field

In many cases, a very convenient way to describe a field is with a "potential function." Since the currents which produce the main field of the earth do not flow across the earth's surface (measured atmosphere to ground currents average about 10^{-12} amps/m^2, which are too small to produce significant magnetic fields), the field is "curl-free" at the surface, $\nabla \times \underline{B} = 0$, and it therefore may be obtained from a scalar potential, $\underline{B} = -\nabla V$. Since $\nabla \cdot \underline{B} = 0$ also, we see that the potential function V satisfies Laplace's equation. The solution to this equation in spherical coordinates is well known to be a product of three functions, each containing only one of the variables, colatitude (θ) increasing southward, longitude (ϕ) increasing eastward and radial distance (r) increasing outward. It is written as

$$V = a \sum_{n=1}^{\infty} \left(\frac{a}{r}\right)^{n+1} \sum_{m=0}^{n} P_{n,m}(\cos\theta) \left[g_n^m \cos m\phi + h_n^m \sin m\phi\right] \qquad (V\text{-}1)$$

In this equation $P_{n,m}(\cos\theta)$ is the associated Legendre polynomial of degree n and order m, and a is the earth radius. We have ignored a radial solution proportional to $(r/a)^n$, which restricts our results to the region $r > a$ and assumes that the currents producing the fields are inside the earth's surface. This assumption has been verified to within 0.1 percent, which is as close to zero as may be determined from presently available magnetic data. The index $n = 0$ is missing because this would correspond to an unrealistic magnetic monopole. The index m

increases only to n, since $P_{n,m}(\theta) = 0$ for $m > n$. We see that the index n determines the order of the magnetic multipole, e.g., $n = 1$ gives a dipole potential, $n = 2$ gives a quadrupole potential, etc.

The orthogonality relation for associated Legendre polynomials gives

$$\int_{-1}^{+1} P_{n,m}(x)\, P_{n',m}(x)\, dx = \begin{cases} 0 & \text{for } n' \neq n \\ \dfrac{2}{(2n+1)} \dfrac{(n+m)!}{(n-m)!} & \text{for } n' = n \end{cases} \qquad \text{(V-2)}$$

in which $x \equiv \cos\theta$. We can see that when $n = n'$, the value of the integral is very strongly dependent on the choice of m. This would eventually be reflected in the values of g_n^m and h_n^m when these coefficients are evaluated by comparison with magnetic observations. To overcome this defect, Schmidt is credited with introducing a partially normalized Legendre polynomial (see Chapman and Bartels, 1940) defined by

$$P_n^m(x) = P_{n,m}(x) \qquad \text{for } m = 0$$

$$P_n^m(x) = \left\{ \frac{2(n-m)!}{(n+m)!} \right\}^{1/2} P_{n,m}(x) \qquad \text{for } m > 0 \qquad \text{(V-3)}$$

Equation (V-1) may be rewritten in terms of $P_n^m(x)$ instead of $P_{n,m}(x)$, and the coefficients g_n^m and h_n^m will have different numerical values owing to the normalization. It should also be noted that these polynomials can be obtained from the ordinary Legendre polynomials $P_n(x)$, since

$$P_{n,m}(x) = (1 - x^2)^{m/2} \frac{d^m P_n(x)}{dx^m} \qquad \text{(V-4)}$$

When we consider a single magnetic dipole at the earth's center, oriented along the line of the geographic poles, these equations become

very simple. In this case $n = 1$, $m = 0$ and $P_1^0(x) = P_{1,0}(x) = P_1(x) = \cos\theta$. Thus

$$V = a\, g_1^0 \left(\frac{a}{r}\right)^2 \cos\theta \qquad \text{(V-5)}$$

Since $\underline{B} = -\nabla V = -\hat{1}_r(\partial V/\partial r) - \hat{1}_\theta(1/r)(\partial V/\partial\theta) - \hat{1}_\phi(1/r \sin\theta)(\partial V/\partial\phi)$, we may obtain the magnetic field components by differentiation. Usually the values of $Z = (\partial V/\partial r)$, radially downward, $X = (1/r)(\partial V/\partial\theta)$, northward, $Y = -(1/r \sin\theta)(\partial V/\partial\phi)$, eastward are those obtained. For the potential (V-5) we obtain

$$X = -\, g_1^0 \left(\frac{a}{r}\right)^3 \sin\theta = X_1^0$$

$$Y = 0 \qquad \text{(V-6)}$$

$$Z = -2g_1^0 \left(\frac{a}{r}\right)^3 \cos\theta = Z_1^0$$

and

$$|\underline{B}| = (X^2 + Y^2 + Z^2)^{1/2}$$

$$= g_1^0 \left(\frac{a}{r}\right)^3 (1 + 3\cos^2\theta)^{1/2}$$

Another useful parameter is the magnetic dip angle I, defined by

$$\tan I = \frac{Z}{(X^2 + Y^2)^{1/2}} = 2\cot\theta \qquad \text{(V-7)}$$

for the simple dipole field. The value of g_1^0 may be identified with the southward component of the field strength (more precisely, the magnetic induction) at the equator and, for the earth, $g_1^0 \approx -0.305$ gauss $= -3.05 \times 10^{-5}$ webers/m^2.

It is impossible to fit the earth's field very well with a single dipole term as we have considered above. As the next better approximation, we can let $n = 1$ and $m = 1$, which generate two additional terms in the potential expression. We find $P_1^1(x) = P_{1,1}(x) = \sin\theta$, and

$$V = a\left(\frac{a}{r}\right)^2 \left\{g_1^0 \cos\theta + \left(g_1^1 \cos\phi + h_1^1 \sin\phi\right) \sin\theta\right\} \qquad \text{(V-8)}$$

The first term in the bracket corresponds to (V-5) while the second term provides two new contributions to each of X, Y and Z. Physically, these may be considered to be generated by two additional orthogonal dipoles placed at the center of the earth but with their axes in the plane of the equator. From $(-\nabla V)$, we obtain

$$\left.\begin{aligned} X_1^1 &= \left(\frac{a}{r}\right)^3 \cos\theta \left(g_1^1 \cos\phi + h_1^1 \sin\phi\right) \\ Y_1^1 &= \left(\frac{a}{r}\right)^3 \left(g_1^1 \sin\phi - h_1^1 \cos\phi\right) \\ Z_1^1 &= -\left(\frac{a}{r}\right)^3 2 \sin\theta \left(g_1^1 \cos\phi + h_1^1 \sin\phi\right) \end{aligned}\right\} \qquad \text{(V-9)}$$

The terms in Eqs. (V-9) and (V-6) must be added as appropriate to obtain the fields produced by potential (V-8). The effect of g_1^1 and h_1^1 is to incline the total dipole term to the geographic pole by an amount

$$\alpha = \tan^{-1}\left[\frac{\left(g_1^1\right)^2 + \left(h_1^1\right)^2}{\left(g_1^0\right)^2}\right]^{1/2} \qquad \text{(V-10)}$$

Thus, the potential (V-8) could be produced by a single dipole inclined at an angle α to the geographic pole and with an equatorial field

strength $\left[\left(g_1^0\right)^2 + \left(g_1^1\right)^2 + \left(h_1^1\right)^2\right]^{1/2}$. For the earth, the single dipole equivalent would be tipped by about 11.5° toward 70° W longitude and have an equatorial field strength of about 0.312 gauss.

For $n > 1$, additional multipoles contribute to V. Finch and Leaton (1957) have computed the first 48 terms in Eq. (V-1) (through $m = 6$, $n = 6$) for epoch 1955 and their first eight terms are given in Table IV below. The dipole term clearly predominates and the higher order multipoles are not only smaller in magnitude, but they also diminish more rapidly with altitude. However, even this model cannot give any representation of the local variations of the geomagnetic field, as only features whose scale is of order one-sixth of the earth's radius can be accurately described by formulas involving only $m \leq n \leq 6$.

TABLE IV. FINCH AND LEATON COEFFICIENTS
(values in gauss)

$g_1^0 = -0.3055$	
$g_1^1 = -0.0227$	$h_1^1 = +0.0590$
$g_2^0 = -0.0152$	
$g_2^1 = +0.0303$	$h_2^1 = -0.0190$
$g_2^2 = +0.0158$	$h_2^2 = +0.0024$

A significant improvement can be obtained, while retaining a simple mathematical form, by using "eccentric dipole coordinates" (Cole, 1963). In this model, the dipole is moved away from the earth center (about 400 km toward the western Pacific) to obtain a better world-wide fit to the magnetic field.

3. Regular Variations

We have already noted that the magnetic elements (X, Y, Z) undergo a regular diurnal oscillation about their mean values. Figure 25

shows the solar daily magnetic variation, or Sq, for quiet days in the 1922-1933 equinoctial periods at various latitudes (Vestine et al, 1947). The more obvious features include the phase reversal in ΔY and ΔZ (but not ΔX) across the equator and the large increase in ΔX near the equator. The latter feature is evidence of the equatorial electrojet, previously discussed in connection with ionospheric conductivities.

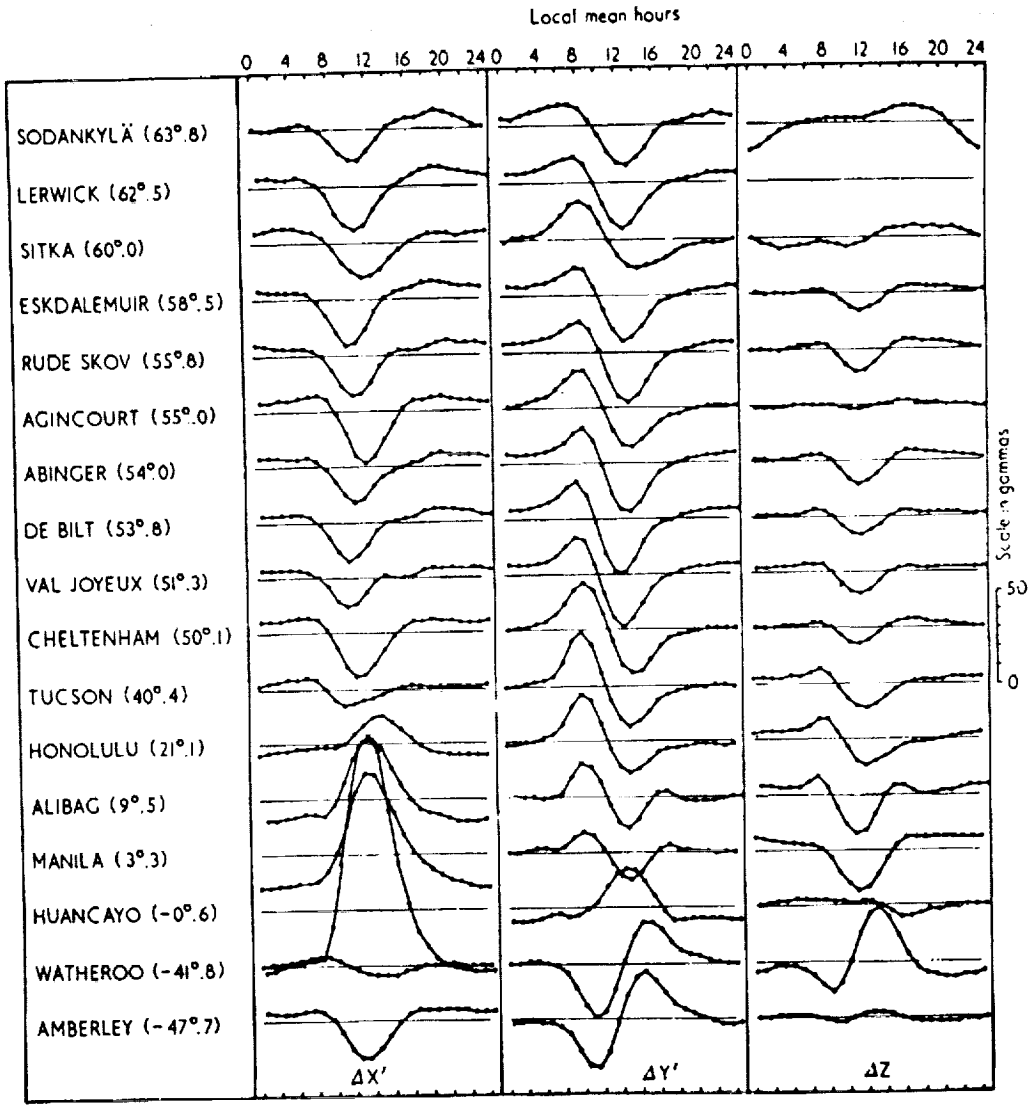

FIG. 25. THE Sq VARIATION IN ΔX, ΔY AND ΔZ AT VARIOUS LATITUDES (after Vestine, 1960).

It is again convenient to find a scalar magnetic potential from which these variations may be calculated. The starting point is usually with data such as shown in Fig. 25, from which a Fourier series is calculated to represent the diurnal variation at each station. Then it is assumed that the same series is applicable at all points along the circle of latitude through the station under consideration. This permits the variable in the Fourier series (time) to be related to the variable in the spherical harmonics (longitude). The procedure is unfortunately rather complicated, but it is explained very carefully in Chapter XX of Chapman and Bartels (1940). The analysis is further complicated by the necessity of separating the potential into internal and external parts. Chapman found the external part of the potential to exceed the internal part by about 2.5 to 1.0. The latter is presumably produced by currents within the earth induced by currents in the ionosphere.

Another very convenient way to represent the source of the regular magnetic variations is by a current sheet, flowing on the surface of a sphere above the earth. This surface is usually assumed to be at an altitude of about 100 km where the maximum conductivity is found. The current density can be expressed directly in terms of the magnetic potential (or vice versa), as shown by Chapman and Bartels. The current systems which they have found required to produce the external part of the Sq variation for sunspot minimum, equinoctial conditions, is shown in Fig. 26. Current flows parellel to the streamlines with 10,000 amperes between each line.

The main features of Fig. 25 can be related to the current system of Fig. 26 by inspection. We remember that an eastward sheet current above the ground will produce a northward magnetic field at the surface, etc. Therefore, between the latitudes of about ±40 deg, the eastward daytime current produces a positive ΔX component, as can be seen at Alibag and Honolulu. At higher latitudes, however, the phase reverses to a negative ΔX (southward) by day. The transition occurs near the current focus at the latitudes of Tucson and Watheroo. The current sheet does not include the equatorial electrojet required to explain the large variation at Huancayo. A narrow current belt along the magnetic dip

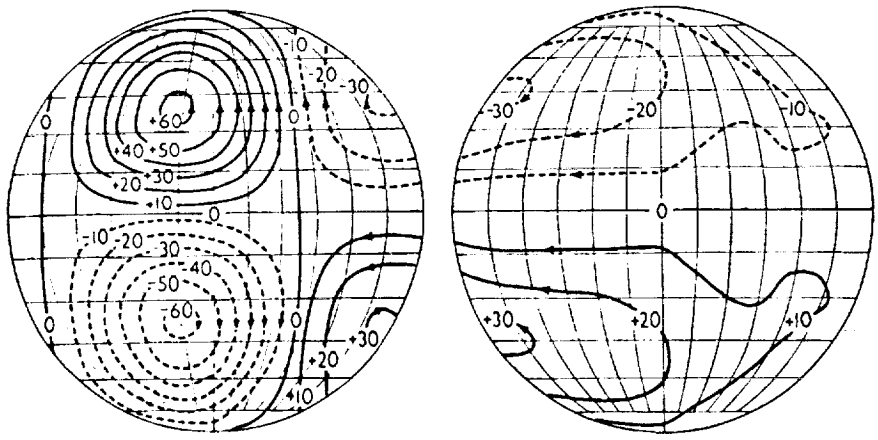

FIG. 26. THE OVERHEAD CURRENT SYSTEM CORRESPONDING TO THE EXTERNAL PART OF Sq FOR SUNSPOT MINIMUM, EQUINOCTIAL CONDITIONS (after Chapman and Bartels, 1949).

equator could be added to produce this feature. The ΔY variation implied by Fig. 26 should be eastward prior to about 1100 local time and westward in the afternoon for northern latitudes and reversed in the southern hemisphere and this is also observed in Fig. 25. The ΔZ variations are not understood quite so easily, since they must be produced by currents removed from the point in question since overhead currents produce horizontal variations only. The vertical variations are most pronounced near the current focus because the counter-clockwise current flow produces an upward magnetic field near the focus in the northern hemisphere while a positive ΔZ is produced in the southern hemisphere near Watheroo. At night, the current densities are much smaller owing to the reduced conductivity in the E region.

A similar magnetic variation can be found with the fundamental period of a lunar day, about 24.8 hours. The magnitude of the lunar (L) variation is much smaller than the solar (Sq) variation, being on the order of $\pm 4\gamma$. Also, the predominant mode is a <u>semidiurnal</u> variation as is found in ocean tides, rather than the predominant diurnal period in Sq. This is particularly important since the L variation is presumably induced by tides alone while the Sq variation may be produced by both solar gravitational tides and by thermal expansion.

4. Storm Variations

In addition to the regular Sq and L variations discussed above, there are sudden and sometimes rather large disturbances of the magnetic field which are observed all over the world. As these transient amplitude fluctuations grow larger, the "magnetic activity" is said to increase and the period may then be identified as a "magnetic storm."

The degree of magnetic activity is determined by an examination of the magnetograms obtained from the various observatories. For each station individually, according to its own average activity, a K index scale is assigned which varies between 0 and 9. The index is not linear but varies quasi-logarithmically with magnetic disturbance. The qualification for K = 9 might be a disturbance of about 300γ for a low latitude (but not equatorial) station, 500γ for a mid-latitude station and 2000γ for a station in the auroral zone. We remember that 1 gauss is equivalent to $10^5\gamma$ or 10^{-4} webers/m^2. The K indices from a set of observatories are then combined to yield a "planetary" figure, Kp, for every 3-hour interval of each day. The Kp scale is determined to an accuracy of 1/3 unit, running as: 0o, 0+, 1-, 1o, 1+, 2-, ..., 8+, 9-, 9o. The maximum value 9o has been recorded only on a few occasions.

The range of variation in gammas for each of the elements (D, H, V) or (X, Y, Z) at each station may also be scaled from the magnetograms. The greatest range in each three-hour interval is called (a) and it is from (a) that the K index was assigned. The arithmetic sum of the (a's) at 12 representative stations yields a planetary value (a_p) and its daily average is published as A_p. The planetary figures Kp and A_p are computed in De Bilt, Holland and are published in several places, such as the National Bureau of Standards Publication, CRPL-F(B) series.

The days on which magnetic storms occur may follow the observation of a solar flare on the sun or at times of high solar activity. These flares or emitting regions are believed to eject streams of charged particles with velocities on the order of 300 to 1000 km/sec which then require two to five days to reach the earth. The interaction of the charged particles with the earth's atmosphere and magnetosphere then produces the magnetic storm, but the manner in which this is done is

still an area of active debate and research. The arrival of the solar plasma is many times revealed by a "sudden commencement" observed nearly simultaneously all over the world.

The disturbed value of a magnetic element (we will use X as an example, but any of the other elements may be treated similarly) is defined by $\Delta X_D = X_{obs} - X_q$, where X_{obs} is the observed value and X_q is the quiet day value, including the regular Sq and L variations. The values of ΔX_D depend not only on "storm time" τ, which is the number of hours elapsed after the commencement of the storm, but also on the colatitude θ and longitude λ of the observing station. The disturbed value is usually split into two parts: (a) the Dst or storm time variation, which is the average value of ΔX_D around a circle of constant latitude and (b) the SD solar daily disturbance or the DS disturbance local-time inequality. All of these three quantities vary with storm time, and are defined by

$$\Delta X_D = Dst + DS = Dst + SD \qquad (V\text{-}11)$$

The SD description was first developed when it was thought that the longitude variation of ΔX_D maintained a fixed orientation in solar time. It is now known that the phase and amplitude of the longitude (or local time) variation changes during the course of a storm, and the quantity DS has therefore been defined (Akasofu and Chapman, 1964). These authors now consider that "SD is merely the mean of DS over a day," but it would appear that SD could be the average of DS over any convenient interval. These relations have been expressed as

$$X_D = a_o + \sum_n c_n \sin (n\lambda + \mathcal{E}_n) \qquad (V\text{-}12)$$

where

$$Dst \equiv a_o$$

$$DS \equiv \sum_n c_n \sin (n\lambda + \mathcal{E}_n)$$

The evaluation of these coefficients at any latitude requires either the observation of many storms of comparable intensity at a single station or the observations of several stations at the same latitude for a single storm. Ideally, both of these approaches will lead to the same result, but some differences are to be expected in practice owing to local variations, different storm characteristics, etc.

These quantities have been defined with a particular model of a magnetic storm in mind, although there is no assurance that this model is correct in any detail. The Dst variation, which is the same all around a circle of latitude, must be produced by a current loop encircling the globe. Observations suggest that the main phase is produced by such a ring current flowing from east to west and perhaps at an altitude of several earth radii (Akasofu and Chapman, 1961). The DS variation would be produced by currents flowing in the lower ionosphere, particularly intense near the auroral zone and presumably related to the influx of particles in these regions.

VI. DYNAMO THEORY

1. Atmospheric Oscillations

The dynamo theory was first suggested by Stewart (1882) to account for the daily variations of the geomagnetic field and developed quantitatively by Schuster (1908). Although there are serious difficulties with some aspects of it, the theory may be partially correct and we shall review it here. A good account has been given by Hines (1963). The basic stages in the discussion are as follows:

(1) The sun and moon produce tidal forces in the atmosphere, the periods being fractions of the solar day (24 hr) and lunar day (24.8 hr).

(2) These forces set up standing waves in the atmosphere below 100 km, which result in (primarily horizontal) air motions.

(3) There may be a natural resonance of the atmosphere of about 12 hr period, which selectively amplifies the solar semi-diurnal component.

(4) The motion of the air across the geomagnetic field induces electromotive forces, which drive currents at levels where the electrical conductivity is appreciable (principally in the E region), thus causing the solar quiet-day and lunar magnetic variations.

(5) Because of the vertical and horizontal variations of conductivity, currents cannot flow freely in all directions; and polarization charges are thereby set up, modifying the flow of current.

(6) The electrostatic fields associated with these charges are transmitted to the F region, via the highly-conducting geomagnetic field lines, where they cause electromagnetic drifts.

Stages (1) to (3) come within the field of atmospheric dynamics and may be thought of as the "mechanical" side of the dynamo theory, which is shown on the left of Fig. 27. The "electrodynamic" side comprises stages (4) to (6).

Let us now review the mechanical side in greater detail. First, we note that the 12-hr oscillation is observed to be the dominant component of the pressure oscillations at ground level. At low latitudes, the 12-hr oscillation is about 1 mb in amplitude and is visible on ordinary barograms, though in middle latitudes it is concealed by the

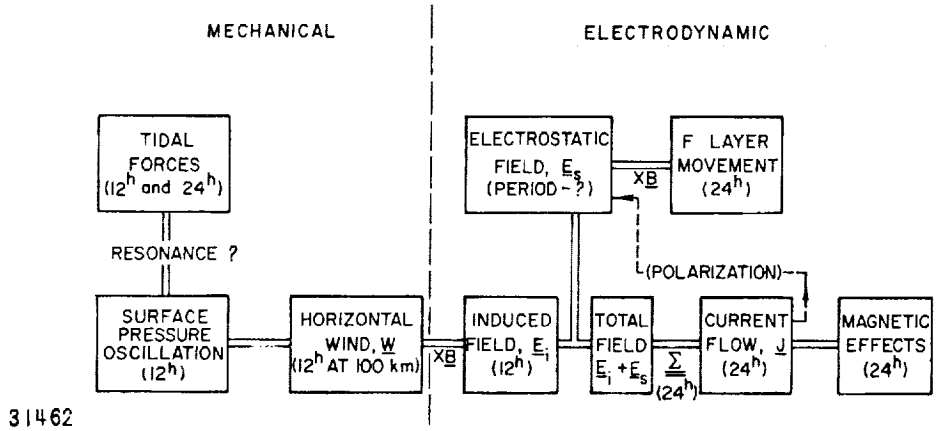

FIG. 27. BLOCK DIAGRAM OF THE DYNAMO THEORY, SHOWING (LEFT) ITS MECHANICAL AND (RIGHT) ITS ELECTRODYNAMIC ASPECTS. The predominant period of the variation is indicated in parenthesis, but other components may also be of appreciable size. Only a small fraction of the total current $\underline{J}$ is required to establish and maintain the electrostatic field, $\underline{E}_s$.

irregular meteorological variations. Some typical amplitudes of pressure oscillations are as follows:

	Tropics	Mid-latitudes
Solar diurnal	0.8 mb	0.3 mb
Solar semidiurnal	1.3 mb	0.4 mb
Lunar semidiurnal	0.08 mb	0.03 mb

For gravitational tides which have a fundamental semidiurnal period, the lunar driving force (period 12.4 hr) exceeds the solar force (period 12 hr). This is consistent with the observed domination of ocean tides by the moon, and we might expect the same situation to apply in the atmosphere. However, there is also a solar driving force arising from the periodic input of thermal energy. This has a fundamental 24-hr period but its harmonics (12-hr, 8-hr, 6-hr, etc.) might have appreciable amplitude. Even so, it is not obvious why the 12-hr period should predominate.

To overcome this difficulty, it was suggested that the atmosphere has a natural period of oscillation close to 12 hr, which amplifies the solar semidiurnal oscillation but is too selective to respond to the lunar

12.4-hr oscillation (Thomson, 1882). Although this coincidence is possible, it might seem too good to be true since resonance is rare in nature. But before we can discuss it further, we must consider how the atmosphere responds to these periodic driving forces. The energy, both thermal and gravitational, is introduced primarily into the lower atmosphere, where the density is greatest. The pressure oscillations are propagated upwards, and increase in amplitude because of the upward decrease of density. Provided no energy is dissipated, the energy density (proportional to ρW^2 where W is the amplitude of the oscillatory wind velocity) is independent of height; thus, $W \propto \rho^{-1/2}$. Now ρ decreases by a factor of about 10^6 between the surface and 100 km, so there is a considerable upward increase of W, known as "tidal amplification." A consequence of this amplification is that the fractional oscillations of pressure and density, $\Delta p/p$ and $\Delta\rho/\rho$, increase upward. At the ground $\Delta p/p \sim 10^{-3}$ but at 100 km, this ratio would approach unity, but for the limitations set by other processes.

The upward progress of the tidal wave is interrupted by partial reflection, which occurs at heights where the temperature gradient is negative. This reflection is expected to be so pronounced in the mesosphere at about 60 to 80 km that a system of standing waves is established and most of the oscillatory energy is trapped below the mesopause. There is, however, some upward leakage of energy which is dissipated at greater heights through various processes. One reason for the dissipation is the tidal amplification discussed above, because the simple linear wave theory holds only where $\Delta p/p \ll 1$. The tidal wave then "breaks" and its energy is degraded into smaller scale motion, ultimately being lost in viscous and electrical resistive damping. Figure 28 shows the amplitude and phase of $\Delta p/p$ for the solar semidiurnal oscillation, as a function of height (Weeks and Weekes, 1947). There is a node at about 30 km, and the phase gradient above 80 km is connected with the leakage of energy from the top of the system.

The trapping of tidal energy below the mesopause gives rise to the possibility of resonant oscillations, which we mentioned earlier. The work in this field has been reviewed by Wilkes (1949). The resonant periods are very sensitive to the temperature profile and so should

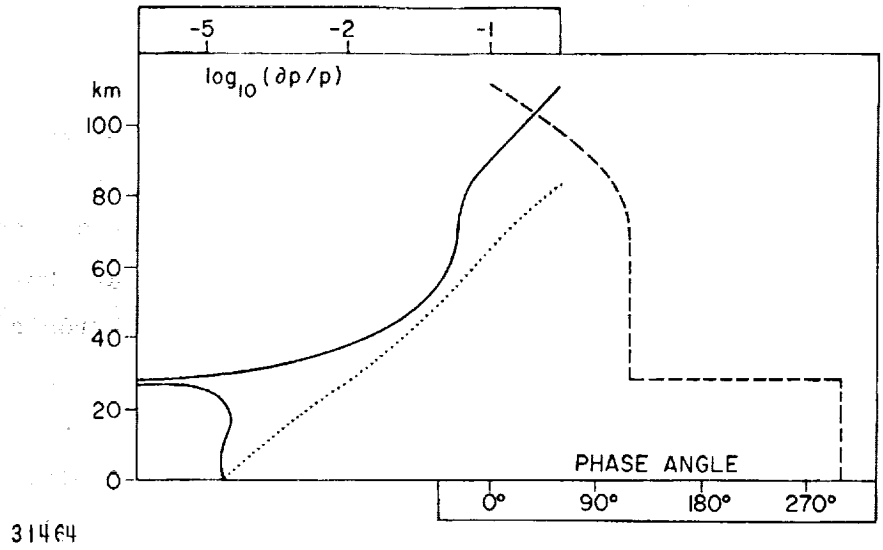

FIG. 28. AMPLITUDE (SOLID LINE) AND PHASE ANGLE (BROKEN LINE) OF THE SEMIDIURNAL PRESSURE VARIATION, AS A FUNCTION OF HEIGHT, AFTER WEEKES AND WILKES (1947). The dotted curve shows a growth amplitude given by exp (z/2). The departure of the solid line from this curve near 30 km represents a node in the standing wave pattern, produced by internal reflections from the ground and the mesosphere.

vary with position and time. In addition, the reflection of energy is affected by winds in the stratosphere and mesosphere (Charney and Drazin, 1961); thus the calculations of resonant periods are very uncertain. There may well be a broad resonance at a period of about ten hours, which would have some effect in increasing the ratio of the 12-hr to the 24-hr oscillation, but the theory that a sharp resonance exists near the 12-hr period now appear untenable. Small and Butler (1961, 1963) have computed the response of the atmosphere to a thermal tide arising from absorption of solar ultraviolet radiation in the ozonosphere, and find the semi-diurnal component to exceed the diurnal.

As with ocean tides, the tidal velocities in the atmosphere are principally horizontal. At the ground, the tidal wind velocities are only of order 0.05 m/s and are thus very difficult to detect in the presence of much larger meteorological winds, but at 100 km the velocities have amplitudes of about 50 m/s, as measured by drifts of meteor trails.

2. Conductivities

Before we can discuss the flow of current resulting from dynamo action, we must deal with the electrical conductivity of the ionosphere, which is anisotropic because of the geomagnetic field. We shall derive the results obtained by Baker and Martyn (1952, 1953), Chapman (1956) and others.

We will start by investigating the motions of the charged particles, and use the following symbols: mass m, charge $\epsilon(\pm)$, electronic charge $-e$, angular gyrofrequency $\omega = Be/m$, collision frequency with neutral particles ν. Suffixes i and e are used for positive ions and electrons. We ignore negative ions, since they probably do not play an important role at the heights where conductivities are large, at any rate by day.

Consider first a particle subject only to collisions and a force $\underline{F}$. We are primarily concerned with electrical forces for which $\underline{F} = \epsilon\underline{E}$. If each particle has a constant probability of collision, ν per unit time, and has (on average) zero velocity after each collision, we may write the drift velocity as $\underline{v} = k\underline{F}$, in which k is the mobility of the particle. The effect of collisions is then represented as a constant retarding force $m\nu\underline{v}$. Then the equation of motion in electric and magnetic fields is

$$m\, d\underline{v}/dt = \epsilon\underline{E} + \epsilon\underline{v} \times B - m\nu\underline{v} \qquad \text{(VI-1)}$$

If $\underline{E} \parallel \underline{B}$, the motion is unaffected by the presence of the magnetic field. For the more interesting case of $\underline{E} \perp \underline{B}$, the motions are as indicated in Fig. 29, where for convenience, we have omitted the last term in (VI-1) and assumed that the particle is brought to rest at equal intervals, $1/\nu$. The trajectories are then cycloidal, and are shown for different values of ν/ω. Both ions and electrons move in the direction $\underline{E} \times \underline{B}$ if $\nu/\omega = 0$, and in general, their motion is inclined at an angle $[\arctan(\omega/\nu)]$ to E.

To obtain the actual mobilities, we find the average drift velocities, over periods long compared with both $1/\nu$ and $1/\omega$, by setting $d\underline{v}/dt = 0$ in (VI-1). Hence, in a cartesian coordinate system in which $\underline{B}$ is directed along the z axis,

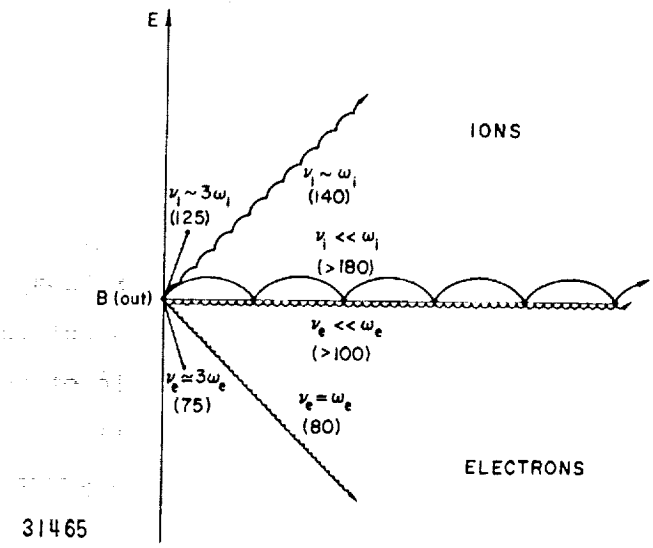

FIG. 29. IDEALIZED TRAJECTORIES FOR ELECTRONS AND IONS SUBJECT TO AN ELECTRIC FIELD IN THE PLANE OF THE DIAGRAM AND A MAGNETIC FIELD DIRECTLY OUT OF THE PLANE. Charged particles are assumed to collide with neutral particles at regular intervals $1/\nu$, and to possess zero velocity after each collision. In order to show both electronic and ionic gyrations, the diagrams are drawn as though $\omega_e/\omega_i \cong 10$ (instead of $\cong 10^4$ as in reality). All the trajectories refer to equal intervals of time, namely 5 ionic (or 50 electronic) gyroperiods. Numbers in brackets refer to approximate heights, in kilometers, at which the conditions occur. In general, the head of the vector representing $\underline{v}_i$ or $\underline{v}_e$ lies on a semicircle.

$$0 = \epsilon E_x + \epsilon v_y B - m\nu v_x$$

$$0 = \epsilon E_y - \epsilon v_x B - m\nu v_y \qquad \text{(VI-2)}$$

$$0 = \epsilon E_z - m\nu v_z$$

By solving these equations for v_x, v_y, v_z we find three different components of the mobility. The solution can be compactly written in terms of a tensor mobility $\underline{\underline{k}}$, which satisfies the equation $\underline{v} = \epsilon \underline{\underline{k}} \cdot \underline{E}$. It is

$$\underline{\underline{K}} = \begin{bmatrix} k_t & -k_h & 0 \\ k_h & k_t & 0 \\ 0 & 0 & k_0 \end{bmatrix} \qquad \text{(VI-3)}$$

where the suffixes "0," "t," "h" denote "direct" (or "longitudinal"), "transverse," and "Hall." Note that the charge ϵ is not included in $\underline{\underline{K}}$, so that according to our definition $\underline{\underline{K}}$ is the ratio of <u>velocity</u> to <u>force</u>. This is applicable whether the force is electrical or mechanical, and is found more convenient here than a quantity defined as a ratio of <u>velocity</u> to <u>electric field</u>.

If we define $\omega = Be/m$ (always positive) we can write each component in two forms, one of which includes B explicitly. Because the Hall current flows in the direction of $\underline{B} \times \underline{E}$ in the ionosphere, whereas the ions and electrons actually drift in the direction of $\underline{E} \times \underline{B}$, the quantity k_h in the preceding equation is negative for ions and positive for electrons.

"Direct" $\quad (\|\underline{B}, \|\underline{E}),\ k_0 = \dfrac{1}{m\nu} = \dfrac{1}{Be}\dfrac{\omega}{\nu}$

"Transverse" $\quad (\perp\underline{B}, \|\underline{E}),\ k_t = \dfrac{1}{m\nu}\dfrac{\nu^2}{\nu^2 + \omega^2} = \dfrac{1}{Be}\dfrac{\nu\omega}{\nu^2 + \omega^2}$

"Hall" (- for ion, + for electrons) $\quad (\perp\underline{B}, \perp\underline{E}), \pm k_h = \dfrac{1}{m\nu}\dfrac{\omega\nu}{\nu^2 + \omega^2} = \dfrac{1}{Be}\dfrac{\omega^2}{\nu^2 + \omega^2}$

At any given height in the ionosphere, ω/ν is not the same for ions as for electrons. The height variation of the mobilities for one kind of carrier is shown in Fig. 30, in which altitude is measured from the level where $\nu = \omega$ and the logarithmic mobility scale is referred to the value $1/Be$.

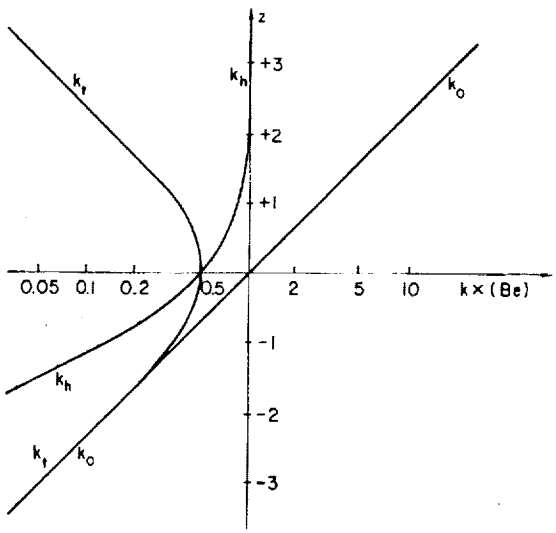

31463

FIG. 30. MOBILITIES FOR A SINGLE CHARGED SPECIES, AS A FUNCTION OF REDUCED HEIGHT z. It is assumed that the collision frequency $\nu \propto e^{-z}$ and that the gyrofrequency ω is height independent. The level $z = 0$ is taken where $\nu = \omega$. The longitudinal, transverse and Hall mobilities (k_0, k_t, k_h) are plotted in units of $1/Be$. The combination of two such diagrams, one each for electrons and ions, placed at their appropriate heights, gives the conductivity per ion pair (Fig. 31).

To find the electrical direct-current conductivity $\underline{\underline{\sigma}}$, we combine the ionic and electronic motions, using the equations

$$\underline{j} = \underline{\underline{\sigma}} \cdot \underline{E} = Ne(\underline{v}_i - \underline{v}_e) \qquad \text{(VI-4)}$$

where $\underline{j}$ is the current density and N the electron and ion concentration. It is customary to define four components of conductivity as,

"Longitudinal" or "Direct": $\sigma_0 = Ne^2(k_{0e} + k_{0i})$

"Transverse" or "Pedersen": $\sigma_1 = Ne^2(k_{te} + k_{ti})$

"Hall": $\sigma_2 = Ne^2(k_{he} + k_{hi})$

"Cowling": $$\sigma_3 = \left(\sigma_1^2 + \sigma_2^2\right)/\sigma_1$$

These conductivities are all positive quantities. The electron and ion contributions to σ_2 are of opposite sign, but as we shall see, $|k_{he}| \geq |k_{hi}|$ at all heights in the ionosphere.

Three of these appear in the tensor expression for $\underline{\underline{\sigma}}$, which follows from these definitions and the expression for $\underline{\underline{k}}$:

$$\underline{\underline{\sigma}} = \begin{bmatrix} \sigma_1 & -\sigma_2 & 0 \\ \sigma_2 & \sigma_1 & 0 \\ 0 & 0 & \sigma_0 \end{bmatrix} \qquad \text{(VI-5)}$$

whereas the Cowling conductivity appears at a later stage in the theory. The vertical variations of these quantities are sketched in Fig. 31, in which the contributions of the ions and electrons are shown in units of Ne/B. The resulting sums are thus conductivities <u>per ion pair</u>, and should be multiplied by the electron density profile to obtain the actual vertical variation of each σ.

The important levels in the diagram are defined by $\omega_e = \nu_e$ (about 80 km in the actual ionosphere), $\omega_i\omega_e = \nu_i\nu_e$ (about 105 km) and $\omega_i = \nu_i$ (about 140 km). We assume $(\nu_i/\omega_i) \cong 1000\ (\nu_e/\omega_e)$, this ratio being relatively independent of height. Peaks of σ_1/N occur at the levels $\omega_e = \nu_e$ and $\omega_i = \nu_i$, but the former does not give an actual peak of σ_1 because of the very low value of N at 80 km. Numerical values of the conductivities have been given by Chapman (1956).

Baker and Martyn (1953) have discussed the "effective" or "layer" conductivities in the actual ionosphere. These arise because of the limited vertical extent of the conducting layer in the E region. If an electric field is generated in the ionosphere by dynamo action, the resulting current $\underline{\underline{\sigma}} \cdot \underline{E}$ may contain a vertical component. If so, charge will accumulate at the boundaries of the conducting layer because the current cannot flow into the region of low conductivity. These "polarization" charges will modify the electric field $\underline{E}$ until the resulting

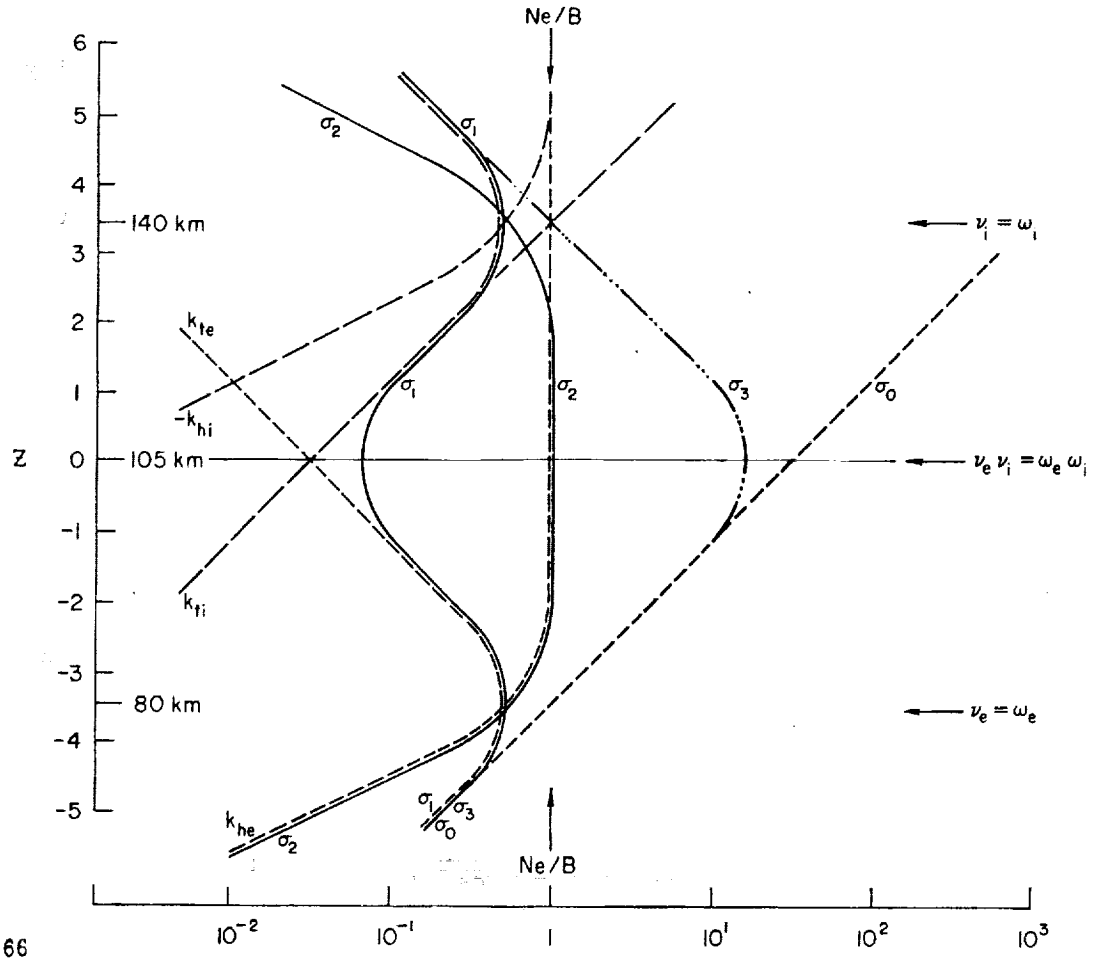

FIG. 31. CONDUCTIVITIES PER ION PAIR $(\sigma_0, \sigma_1, \sigma_2, \sigma_3)$ PLOTTED ON A LOGARITHMIC SCALE RELATIVE TO THE VALUE Ne/B, AS A FUNCTION OF REDUCED HEIGHT z FOR AN IDEALIZED ISOTHERMAL MODEL ATMOSPHERE. It is assumed that collision frequency $\nu \propto e^{-z}$ and gyrofrequency ω is independent of z, for both positive ions and electrons; also that $\nu_i\omega_e/\nu_e\omega_i \cong 1000$ (independent of height), this being a reasonable value for the actual ionosphere. The zero of z is the level where $\nu_i \nu_e = \omega_i\omega_e$, and the important levels where $\nu_i = \omega_i$ and $\nu_e = \omega_e$ are therefore situated at $z = \pm 1/2 \ln(1000)$; also shown are the approximate altitudes at which they occur in the actual ionosphere.

flow is horizontal. Therefore, when we impose the condition of zero vertical current, we can eliminate the vertical electric field from the equations, and we find that the 3×3 tensor $\underline{\underline{\sigma}}$ can be replaced by a 2×2 tensor $\underline{\underline{\sigma}}'$, representing the "layer conductivity" whose components

depend on the magnetic dip angle I. From this point on, we use coordinates x, y for the magnetic southward and eastward directions, and denote the dip angle by I. Then we can write the layer conductivity as

$$\underline{\sigma}' = \begin{bmatrix} \sigma_{xx} & \sigma_{xy} \\ -\sigma_{xy} & \sigma_{yy} \end{bmatrix} \qquad \text{(VI-6)}$$

where

$$\sigma_{xx} = \frac{\sigma_0 \sigma_1}{\sigma_0 \sin^2 I + \sigma_1 \cos^2 I} \approx \frac{\sigma_1}{\sin^2 I}$$

$$\sigma_{xy} = \frac{\sigma_0 \sigma_2 \sin I}{\sigma_0 \sin^2 I + \sigma_1 \cos^2 I} \approx \frac{\sigma_2}{\sin I} \qquad \text{(VI-7)}$$

$$\sigma_{yy} = \frac{\sigma_2^2 \cos^2 I}{\sigma_0 \sin^2 I + \sigma_1 \cos^2 I} + \sigma_1 \approx \sigma_1$$

The approximations given at the right arise because generally $\sigma_0 \gg \sigma_1$ or σ_2, but they are not valid near the magnetic equator where $I = 0$, and where we have

$$\sigma_{xx} = \sigma_0, \quad \sigma_{xy} = 0, \quad \sigma_{yy} = \left(\sigma_1^2 + \sigma_2^2\right)/\sigma_1 = \sigma_3 \qquad \text{(VI-8)}$$

Two consequences follow from these latter results. First, the very high conductivity $\sigma_{xx} = \sigma_0$ along the field lines insures that these lines are approximately electric equipotentials. Second, the east-west conductivity σ_{yy} at the equator is extremely large, being the "Cowling" conductivity σ_3 which is comparable to σ_0. This highly conducting strip along the magnetic equator carries a large current known as the "equatorial electrojet," which is confined to the region a few degrees in width, where $\sigma_0 \sin^2 I \ll \sigma_1 \cos^2 I$.

The simple model of the dynamo region is therefore a relatively thin, horizontally stratified layer. The effects of the currents as observed at the ground can most conveniently be calculated with the use of "integrated layer conductivities," $\Sigma_1 \equiv \int \sigma_1 dh$ and $\Sigma_2 \equiv \int \sigma_2 dh$, where the integration is made vertically through the conducting region. Since the major part of the conductivity is found in the E region, Σ_1 and Σ_2 are approximately proportional to $N_m E$. At night, they become small because the E layer almost disappears.

We should also consider the effects of a force due to a wind of velocity $\underline{W}$ in the neutral air, as Martyn (1953z) and Weekes (1957) have done. We may take the force exerted as $\underline{F} = \underline{W} m\nu$, as in Eq. (VI-1). If $\underline{W}$ is parallel to the magnetic field, the plasma moves with velocity $\underline{v} = k\underline{F} = (1/m\nu)\ \underline{W}\ m\nu = \underline{W}$. However, all the other components of the tensor mobility $\underline{\underline{k}}$ depend on (ν/ω) or $(\nu/\omega)^2$ and thus decrease rapidly upwards. At heights above the E layer a wind is ineffective in moving ionization across the field lines, whereas an electric field $\underline{E}$ is much more effective since it causes the ionization to drift with the velocity $\underline{E} \times \underline{B}/B^2$. In the D region, where $\nu \gg \omega$ for ions and electrons, winds rather than electric fields are effective in moving ionization. In the E region, both winds and fields produce motion of ions and electrons in different directions, thereby generating electric currents.

3. Motions in the Ionosphere and Magnetosphere

The discussion up to this point may be summarized with the two equations

$$\underline{J} = \underline{\underline{\Sigma}}' \cdot \underline{E}_t \qquad \text{(VI-9)}$$

$$\underline{E}_t = \underline{E}_i + \underline{E}_s = \underline{W} \times \underline{B} - \nabla\phi \qquad \text{(VI-10)}$$

The horizontal sheet current $\underline{J}$ flows in response to the total electric field $\underline{E}_t$, which is composed of an induced part $(\underline{W} \times \underline{B})$ and an electrostatic part, $-\nabla\phi$, which was established in order to require the current flow to be horizontal. Observations of the magnetic field strength at

the ground permit the current flow to be calculated from Ampere's circuital relations. If horizontal variations can be neglected, the southward (x) and eastward (y) components of magnetic field $\underline{H}$ (or induction $\underline{B}$) and layer current density $\underline{J}$ are related by

$$-\frac{1}{2} J_y = H_x = B_x/\mu_o$$

$$\frac{1}{2} J_x = H_y = B_y/\mu_o \qquad \text{(VI-11)}$$

The numerical factor in these equations should be about 3/4, instead of 1/2, because of the contribution of currents induced in the ground by the overhead current systems. Detailed analysis shows that ground currents cause about one-third of the observed magnetic effect, though the proportion is not the same for the different magnetic components (Chapman and Bartels, 1940). If the ground were a perfect conductor, and complications due to horizontal variations and the earth's curvature were neglected, the ground and ionospheric currents would be equal and opposite, and would contribute equally to the observed magnetic variations. The coefficients in Eqs. (VI-11) would then be 1.

If there are electrostatic fields in the E region, they must exist also in the F region owing to the very high conductivity parallel to $\underline{B}$. Hence, the E and F regions are electrically "coupled," as suggested by Martyn (1947) and investigated by Farley (1959) and others. It is believed that E region fields are accurately "mapped" into the F region, even for scale sizes down to a few kilometers. Above the E region, only the electrostatic component of the electric field is present, because the tidal winds are thought to be damped out by viscosity. Hence, the electric field acts on the ionization in the F region, causing it to drift with the velocity

$$\underline{v} = \frac{\underline{E}_s \times \underline{B}}{B^2} \qquad \text{(VI-12)}$$

This has been likened to an electric "motor" running without load, as the "back emf" $\underline{v} \times \underline{B}$ set up by the drift of ionization across the field lines, just balances the applied field $\underline{E}_s$. Actually, a small current flows, because the electron and ion drift velocities are not precisely equal, implying that some energy is expended in collisions and in overcoming gravity. The vertical component of the F region drift velocity is produced by the eastward electric field component E_y and is given by $v_z = (E_y/B) \cos I$.

Dynamo theory, as condensed into Eqs. (VI-9) to (VI-12), is perhaps deceptively simple. In practice, there are numerous difficulties in the application of this theory, such as the interaction of the drifting plasma with the neutral atmosphere (Cowling, 1945; Hirono and Kitamura, 1956; Dougherty, 1961), which can reduce the vertical velocity v_z of the plasma.

We now wish to extend our discussion to higher heights, and introduce some concepts used in some modern theories of magnetic storms, which provide an alternative way of looking at the motions of ionizations. Since the geomagnetic field lines above the E region are (almost) electric equipotentials, the electrostatic fields which cause F layer "motor" drifts must also permeate the magnetosphere. At these levels the fields $\underline{B}$ and $\underline{E}$ and the ionization drift velocity $\underline{v}$ satisfy the so-called "freezing-in" equations

$$0 = \underline{E} + \underline{v} \times \underline{B}$$

$$\underline{v} = \underline{E} \times \underline{B}/B^2 \qquad \text{(VI-13)}$$

The second of these has already appeared as the F region motor equation (VI-12).

The "freezing-in theorem" is of very general application to the magnetosphere, stellar atmospheres, and ionized interstellar matter. It is valid whether or not the electric field $\underline{E}$ is purely electrostatic (i.e., derivable from a potential Φ), providing its time variation is slow enough. Basically, the theorem states that the ionized matter and magnetic field moves in such a way that

(i) a set of charged particles, if connected by a field line, remain so connected at all times.

(ii) any given tube of ionization bounded by a set of field lines, always encloses the same magnetic flux.

The proof of these statements is somewhat involved, and has been given by Dungey (1958) and by others. Since a "line of force" is an abstraction and not a physical object, its "motion" is somewhat arbitrary. In elementary magnetostatics, "lines of force" are visualized as being fixed in space; yet the result (i) just quoted entitles us to identify a field line by the material situated on it, so that its motion is taken to be that of the material. We then think of the effect of a transverse electrostatic field as a translation of the field line itself, with velocity $\underline{E} \times \underline{B}/B^2$, in which all charged particles participate. This applies strictly only to thermal particles, but holds to some extent for energetic particles.

In the atmosphere, the translational motion of magnetic field lines can take place in such a way that $\underline{B}$ does not change with time. In the case in which the field is electrostatic, this must always be the case, because then

$$\partial \underline{B}/\partial t = \text{curl } \underline{E} = \text{curl grad } \Phi = 0 \qquad \text{(VI-14)}$$

There is then a "circulation" or "convection" in three dimensions (Gold, 1959), which is possible because the presence of the nonconducting lower atmosphere enables the field lines in the upper atmosphere to move independently of those in the solid earth.

The motions of field lines are opposed by frictional collision forces acting on the ions in the E region, since $\nu_i > \omega_i$ below about 140 km and the ions are not "frozen in" to the magnetic field. But since $\nu_e \ll \omega_e$ in the dynamo region, the electrons are "frozen in," and do take part in the motion of the field lines. Thus, the ions and electrons in the F region drift with the same velocity as the electrons in the E region, apart from small differences due to the vertical changes of $\underline{B}$. All have the cycloidal types of motion shown in Fig. 30, for the case $\nu \ll \omega$ and move along electric equipotentials. In the E region,

the relative motions of ions and electrons represent an electric current and the ion-neutral collisions represent joule loss. This is just another way of looking at the motions from which the conductivities were derived.

This description implies that any current flowing in the E layer is accompanied by motions of ionization in the F region and magnetosphere. Conversely, if any motion of ionization normal to $\underline{B}$ is set up in the magnetosphere by external causes, it will produce corresponding motions of the F region ions and electrons and will set up electron currents in the E region, which will dissipate energy. The circulatory motion in the magnetosphere, however, is frictionless because of the absence of collisions, but has to take place in such a way that the field lines are merely interchanged and the field is not distorted in shape. The magnetospheric circulation does not directly produce any magnetic variations at the ground; these result indirectly from the E region currents and induced earth currents, in which the energy is eventually dissipated.

4. Observational Data

It is useful to keep in mind the orders of magnitude of the various parameters of importance to the dynamo theory. Some of these are listed in Table V, and a more detailed discussion of the observational results is given below.

Barometric oscillations have been analyzed in detail, but the comparison between ground-level and dynamo region conditions involves calculation of the tidal amplification factor and phase variations, using an atmospheric model such as done for Fig. 28. As we have discussed earlier, this has not been a particularly fruitful approach to wind determinations.

Drifts of meteor trails can be observed by radar technqiues, and give winds in the neutral air at 80 - 110 km height, but the data are limited to a few locations. A long series of measurements has been made at Jodrell Bank (53° N) where the amplitude of the 12-hr oscillation is somewhat greater than that of the 24-hr wind (Greenhow and Neufeld, 1961); whereas at Adelaide (35° S) the 24-hr component is more pronounced (Elford, 1959).

TABLE V. SOME ORDERS OF MAGNITUDE OF QUANTITIES IN DYNAMO THEORY

Pressure oscillations:	1 mb at ground, or 1 part in 1000. At 100 km, probably about 1 part in 10.
Wind velocities at 100 km, W	50 m/sec
Total geomagnetic field, B	1/2 gauss $= 5 \times 10^4$ gammas
Daily Sq variation at ground	20 gammas
Currents (total in each vortex of Sq system)	10^5 amperes
Layer current density	30 amp/km
Induced field, E_i	10^{-3} volts/m
Vertical drift velocity of F region ionization, v_z	10 m/sec
Daytime integrated conductivities (nearly all contributed by E region)	$\int \sigma_1 \, dh \cong 10$ mhos
	$\int \sigma_2 \, dh \cong 20$ mhos
	$\int \sigma_3 \, dh \cong 200$ mhos

Quantities	E Region (100 km)	F Region (300 km)
Daytime electron density (N)	10^5 cm^{-3}	10^6 cm^{-3}
Neutral gas concentration (n)	10^{13}	10^9 cm^{-3}
Ratio n/N	10^8	10^3
Ratio of N (day/night)	30	5
ω_e/ν_e	30	10^4
ω_i/ν_i	0.02	300

E layer drifts have been measured at various stations. Early results were reviewed by Briggs and Spencer (1954) and an analysis of IGY data given by Shimazaki (1959). A more recent survey has been given by Rawer (1963). Strong semidiurnal components are found, whose vectors generally rotate clockwise with advancing time in the northern hemisphere, and counterclockwise in the southern hemisphere. Diurnal components comparable to the semidiurnal ones, have been reported but their detection

necessitates inclusion of data from nighttime E_s layers, which may not be strictly comparable with the normal E layer data.

F layer drifts are also reviewed in the papers quoted above. When the velocities are subjected to harmonic analysis, the diurnal component is found to predominate. Often there are fairly abrupt changes near sunrise and sunset, which perhaps arise from the changes of E region conductivity accompanying the formation and disappearance of the E layer.

Magnetic variations of the D, H, Z elements on quiet days follow a regular latitudinal pattern and can be represented by overhead current systems (see Figs. 25 and 26). The dominant period of variation is 24 hr, doubtless because of the variation of E region conductivity. These daily variations contain an unknown "zero level" which unfortunately cannot be separated from the earth's main field, so that variations of each component are conventionally measured from its average level throughout 24 hr. However, it would seem much more probable that the real zero levels are near the nighttime values, since the nighttime conductivity is so small. This is one of the major problems in relating magnetic variations to dynamo currents, although it could be resolved by determining the nighttime currents by means of a sensitive rocket-borne magnetometer.

The calculations required in dynamo analysis can be approached from two standpoints. One is to solve the equations on a local scale, inserting observed values of the local magnetic variations and comparing them with other data. The most that can be said in this regard is that limited agreement is sometimes obtained between the E region data, meteor winds, and ground-level pressure oscillations; but that it is difficult to relate F layer drifts to the other data.

To some extent, this may be due to the difficulty of separating the electric field into its "induced" and "electrostatic" components. Another (and more basic) difficulty is that the "thin sheet" approach to dynamo theory fails if the wind velocity $\underline{W}$ varies considerably with height through the conducting regions. There are strong indications that it does, and that the height variations may be too irregular to enable any meaningful "average" velocity to be defined.

The other approach is to assume that a steady state exists and to solve the equations on a global scale to obtain the layer current density $\underline{J}$, electrostatic potential Φ and wind velocity $\underline{W}$. Not only must these quantities satisfy the dynamo equations at all points of the conducting layer, but in addition the current continuity equation, div $\underline{J} = 0$, must be satisfied everywhere. Fortunately, it then becomes possible to separate the "induced" and "electrostatic" components by procedures which make use of the identity curl grad $\Phi \equiv 0$. In addition, some dynamical constraint on the wind velocity must be assumed. It is generally assumed that the wind velocity $\underline{W}$ can be derived either from a scalar potential (the terms "scaloidal" and "irrotational" being used a describe this case) or from a vector potential ("toroidal" or "solenoidal"). The latter approach, however, seems to lead to difficulties at the poles of rotation. In addition, the Coriolis forces arising from the earth's rotation introduce considerable complications, so are often neglected.

All calculations are based on models for the conductivity $\underline{\underline{\Sigma}}$. Since E region electron density changes by a factor of 30 (or more) between day and night, $\underline{\underline{\Sigma}}$ undergoes a variation which is predominantly diurnal, but contains higher harmonics. Lunar tidal calculations are simpler because the moon does not affect the conductivity, provided the data are averaged in such a way as to remove the solar effects.

The calculations of Baker (1953) and Fejer (1953) proceed in the "forward" direction, left to right in Fig. 27. They neglect the diurnal variation of conductivity and therefore obtain only semidiurnal magnetic effects and drifts from their assumed semidiurnal pressure variations. Several of the Japanese workers start with the magnetic Sq data and proceed in the reverse direction (e.g., H. Maeda, 1955; Hirono and Kitamura, 1956; Kato, 1956). The computed E region winds turned out to be predominantly diurnal, whereas the observational data we quoted earlier (meteor trails, E region drifts, barometric oscillations) suggest that semidiurnal variations dominate.

Considering the uncertainties that arise in discussing just the dynamo region itself, it is not too surprising that the extension of the theory to F region drifts gives few firm conclusions. A number of F2

layer phenomena are attributed to electromagnetic drifts, sometimes because no other explanation is available. We can see that drifts might be important by a simple order-of-magnitude argument, by which we expect a vertical drift velocity to cause noticeable effects at the F2 peak if it moves ionization through one scale height H in a period equal to its average lifetime $1/\beta$. Thus $v \sim H\beta = 50 \text{ km} \times 10^{-4} \text{ sec}^{-1} = 5 \text{ m/sec}$, say. Velocities deduced from dynamo theory are generally larger than this, so should be of importance.

To determine the actual effect of the drift on the electron density $N(h,t)$, one must solve the continuity equation with drift and diffusion included. This is complicated but has been attempted for some idealized conditions. Some conclusions relating to "day equilibrium" and "night stationary" layers were mentioned in Sec. III-6, but so far little success has been achieved in relating calculated and observed drifts to detailed time variations of the F2 layer.

It may have been noted that the principal unknown in all of the calculations is the electrostatic field, $\underline{E}_s$. If this could be computed or measured with confidence, the applicability of dynamo theory would be much better established. Unfortunately, it is extremely difficult to measure this quantity <u>in situ</u>, because its magnitude is on the order of 1 mv/m. Rocket and satellite potentials are typically 100 to 1000 times larger and quite variable due to photoemission, induced potential and other perturbing factors.

VII. STORMS AND THEIR IONOSPHERIC EFFECTS

1. Synopsis of Storm Effects

The events known as magnetic storms comprise a very complicated sequence of phenomena. Our account is necessarily condensed, and is largely devoted to ionospheric effects. We must caution that most of our statements are subject to reservations of one sort or another. Most of the theories are tentative, and individual storms vary so much that exceptions may be found to almost any description of the observed phenomena.

Magnetic storms are initiated by solar disturbances. Most severe storms have a sudden commencement (SC) which takes place 1 to 2 days after a solar chromospheric flare, though often there is difficulty in associating storms with particular flares and it may be that some SC storms originate differently. Another type of storm, generally less severe, is not associated with flares. These storms start gradually and tend to recur at intervals of 27 days, the period of solar rotation as viewed from the earth. They have been attributed to periodic immersion of the earth in particle streams emitted, more or less continuously, from active areas on the sun which became known as (magnetic) M regions. Since M regions could not be positively identified with visual phenomena on the solar disk, even though they must persist for some months, they remained somewhat hypothetical. It has been suggested (Piddington, 1964) that M region storms are associated with certain features in the interplanetary magnetic field. These rotate with the sun, hence causing a 27-day recurrence, but there need be no association between the storms and visible features on the solar disk. M region storms are most common during the declining part of the solar cycle. SC-type storms are most frequent at sunspot maximum, when large solar flares are commonest.

Table VI shows some storm phenomena, with notes on their durations and possible causes; some of these are reasonably well established but others are quite speculative. Any numerical values quoted are intended to be mere orders of magnitude, characteristic of strong (but not exceptional) storms. Timewise, the phenomena fall into two categories. Those

listed under (1) and (2) in Table VI, accompany the visual flare, and involve electromagnetic radiation travelling at the speed of light. Effects (3) to (7), which comprise the storm proper, depend on the much slower propagation of clouds of solar plasma. A typical delay time of 1-1/2 days between the flare and the SC implies a speed of $\sim 10^3$ km/s from the sun to the earth. But solar cosmic-ray increases and PCA events listed under (2), begin not long after the flare and seem to be due to solar protons propagating at velocities of up to 10^5 km/s.

The storm sudden sudden commencement (SC) is thought be be caused by the impact of a shock wave which precedes the plasma cloud on the magnetosphere of the earth. The disturbances are then propagated to the earth in the form of hydromagnetic waves. There are differences of order 1 min in the time of SC at different places, presumably due to the travel time of the waves. Sometimes an impulse resembling an SC is observed, but no storm ensues, in which case the term "sudden impulse" (SI) is used.

In a typical magnetic storm, the SC is followed by an "initial" or "positive" phase lasting a few hours. During this time the geomagnetic field intensity is increased, the "stormtime" component Dst(H) being positive. This is probably due to the compression of the geomagnetic field by the solar plasma. After a few hours the main phase sets in, in which Dst(H) becomes negative and the field is depressed for a day or so. This reduction can be represented as the field of a "ring current" which is oppositely directed to the main geomagnetic field, the location and nature of which constitutes one of the central problems of storm theory. Dst(H) reaches its greatest negative values about 18 - 36 hr after the SC (soonest in great storms). There are often irregular fluctuations of fields during the initial and main phases, but after 1-1/2 - 2 days the storm passes to the recovery phase and the field returns smoothly to normal, with an exponential time constant of a day or so.

The amplitude of the Dst magnetic field is greatest in low latitudes, and decreases polewards. This is opposite to the field of the current systems associated with the DS disturbance local-time inequality. This field is most intense at auroral latitudes, where it exceeds Dst, but

TABLE VI. STORM PHENOMENA

Disturbance	Outline of Phenomenon	Timing and Duration	Possible Cause
Solar Flare	Eruption in solar chromosphere		
(1) Solar Phenomena			
Optical	Enhanced $H\alpha$ emission over fraction ($\leq 10^{-3}$) of solar disk	1/2 hour	
Ultraviolet	Ly α (1216 Å) and He II (304 Å) enhanced by order of 10 percent	All start simultaneously	
X rays	Strong emission in 1 - 10 Å range		
Radio frequencies (Type IV, Type II, III)	Several types of emissions covering all observable wavelengths	(Complicated line dependences and frequency drifts)	Some types initiated by plasma (ejected from flare) travelling through corona
(2) Geophysical Phenomena			
Sudden ionospheric disturbance (SID)	Effects in sunlit hemisphere Strong absorption; anomalous VLF reflection; effects in F region	Accompanies visual flare, persists ~1/2 hour	D region ionization increased by X rays
Magnetic bay	Sudden "bay" or "crochet" (~20γ)	Accompanies visual flare	Increase of ionospheric currents because of enhanced conductivity
Solar cosmic rays	Latitude dependent increase	Starts about 1/2 hour after flare	Protons $\leq$100 Mev
Polar cap absorption (PCA)	Intense radiowave absorption in magnetic polar regions	Starts few hours after flare	Protons 1 - 10 Mev
Magnetic Storm			
(3) Geomagnetic Field	Interaction of low energy plasma, produced by flare, with the earth		
Sudden commencement (SC)	Impulsive increase of field (10γ)	Impulsive: simultaneous (to within ~1 min) over the earth	Impact of plasma "front" on boundary of magnetosphere
Initial phase	Field increased; Dst(H) ~ +20γ	2 - 6 hours	Compression of field by impinging plasma
Main phase	Field depressed; Dst(H) ~ -50γ Strong daily variations are superimposed on this stormtime behavior; SD(H) ~30γ	1-2 days	Orbiting charged particles in magnetosphere give "ring current"
Recovery phase	Field returns exponentially to normal	Time constant ~1 day	Particles removed by collisions (charge exchange) with neutral atoms

TABLE VI. (Continued)

Disturbance	Outline of Phenomenon	Timing and Duration	Possible Cause
(4) Energetic Particle Phenomena			
Forbush cosmic ray decrease	(Galactic) Cosmic ray intensity temporarily reduced	~1/2 hour before SC	Particle trajectories perturbed by the solar plasma "front" as it approaches the earth
Radiation belts	Outer Van Allen belts initially depleted during storm, then replenished		Acceleration mechanism probably related to that of auroral particles
(5) Aurora	Auroral activity is intensified, and occurs at lower latitudes than the normal auroral zone		Excitation probably due to electrons (tens of kev) accelerated by (unknown) mechanism in vicinity of earth
Mid-latitude red arcs	Enhanced [OI] 6300 Å emission in bands some thousands of km long oriented along magnetic latitudes ~500 km wide, and situated at ~400 km altitude	Stable for many hours Associated with magnetic disturbance, not necessarily with SC-type storms	Corpuscular bombardment Electron heating by electric fields
(6) Atmospheric Effects	Drag on satellites increases, because density at great heights is increased by a rise of thermospheric temperature	Persists for some days Starts soon after SC (time resolution in data is few hours)	Absorption of hydromagnetic waves; corpuscular heating; joule heating
(7) Ionospheric Effects			
Blackout, storm E_s at high latitudes	Enhanced absorption, E_s ionization, following regular ("spiral") geographical distributions	Strong Universal Time and local-time dependences	Precipitation of electrons of few kev
Long term changes in D region	Diurnal variation of VLF phase is abnormal	Persists for >10 days	Possible chemical changes in atmosphere
Mid- and low latitude F region changes of electron density	f_oF2 increased during first day of storm then generally depressed, but sometimes increased, especially in low latitudes	Effects last for many days, with strong daily variations	Temperature changes; increase of loss coefficient; electromagnetic movements

decreases towards low latitudes, where Dst is the dominant storm variation. In general, the variation observed at any station is a complicated combination of DS and Dst, which depends on the local time at which the SC occurs.

In early stages of a storm, the DS system changes rapidly, but after some hours it settles into a pattern which remains nearly fixed with respect to the sun, and gradually decays as the storm progresses. Once these patterns are established, the harmonic components of the DS variation at any station maintain almost constant phases in local time, though the amplitudes decay gradually. A comprehensive study of weak, moderate and great magnetic storms has been made by Sugiura and Chapman (1958).

Much of the interest in geomagnetic storms is centered on the aurora, cosmic rays and the radiation belts. These are included under (4) and (5) in Table VI, but we do not propose to discuss them further here. The mid-latitude red arcs are a fairly recently discovered phenomenon, which promise to be of considerable interest in relation to upper atmosphere processes. An account of many of their known properties has been given by Roach and Roach (1963).

The increase of satellite drag during storms is almost certainly due to an increase of atmospheric temperature. A detailed analysis of this effect has been given by Jacchia (1961, 1963) who find that the temperature in the upper thermosphere increases by 1.0 to 1.5 °K per unit of A_p. It has been suggested that joule heating by DS currents is responsible for these temperature increases in the neutral atmosphere (Cole, 1962). The connection between current flows and the electric fields which might cause mid-latitude "red arcs" has been discussed by Carleton and Megill (1964). So far, it has not been possible to assess the relative importance of this mechanism, corpuscular heating, and other possible causes of heating such as absorption of hydromagnetic waves (Dessler, 1959). Waves of periods around 1 sec are strongly absorbed in the ionosphere (Karplus, Francis and Dragt, 1962); there seems to be no evidence that the intensity of such waves incident on the ionosphere from above is sufficient to account for the heating.

2. Storm Effects in the Lower Ionosphere

Disturbances of the lower ionosphere during storms are most pronounced in high latitudes. This scarcely surprising, because of the known precipitation of energetic particles in the auroral zone. Some effects, however, occur at other latitudes.

It is well known that radio communications are affected during magnetic disturbance, the terms "fadeout" and "blackout" being in common use. Though part of the difficulties in ionospheric propagation arise from decreased F2 critical frequencies, to be discussed in the next section, they are largely due to D region absorption. Reid and Collins (1958) showed that high latitude absorption comprises three distinct types of phenomena which we list here. Their "type numbers" are not now in general use but are sometimes found in the literature.

Type I is the "short wave fadeout" (SWF), part of the "sudden ionospheric disturbance" (SID) which accompanies solar flares (Dellinger, 1937). This is observed all over the sunlit hemisphere, so is not particularly a "high-latitude" phenomenon.

Type II is the "auroral absorption" which accompanies the main phase of geomagnetic storms. It is associated with visual auroras or those detected by radar, and its positional distribution has been found to follow well-defined "spiral" patterns, as we shall see later.

Type III is the "polar cap absorption" (PCA) which begins a few hours after solar flares--and thus, well before the storm SC--and persists for some days, with pronounced diurnal variations. Maps showing the development of PCA have been published by Obayashi (1959, 1960).

The "sudden ionospheric disturbance," SID, which accompanies solar flares, is associated with a number of other phenomena which begin simultaneously, including:

SWF: Short wave fadeout or "Type I" absorption. Waves reflected from the E and F layers are strongly attentuated by enhanced ionization in the D region.

SCNA: Sudden cosmic-noise absorption. A fairly large flare may cause a 2 db increase in absorption or even more at a frequency of 25 Mc/s (Bhonsle, 1960).

SPA: Sudden phase anomaly. The change of phase of long waves reflected at oblique incidence indicates a drop of several kilometers in the height of reflection (Bracewell et al, 1951; Bracewell and Straker, 1949).

SEA: Sudden enhancement of atmospherics recorded at frequencies around 20 kc/s (Ellison, 1953; Bureau, 1937). Like the SPA, this indicates a change of VLF propagation conditions.

SFE: or crochet: Magnetic solar flare effect. A disturbance of the geomagnetic field, attributed to increased ionospheric conductivity, which leads to increased current flow.

All these effects indicate an increase of electron density in the D region, perhaps by a factor of ten in a major flare. The fact that they begin at the time of visual sighting of the flare implies that they are due to electromagnetic, rather than corpuscular, radiation. The fact that ionization is produced at lower heights than usual provides strong evidence that the radiation is harder (i.e., possesses a smaller absorption cross-section) than that responsible for the normal D layer. It is known that solar X ray emission is greatly enhanced during a flare, whereas Ly α emission is only slightly increased.

With regard to the magnetic crochet, we recall that the conductivity per ion pair is so small below 80 km that huge changes of electron density would be required to enable sizable electric currents to flow. Thus, it may be that the currents producing the crochet flow in the E region, and this might be connected with the increase of f_oE which has been reported on occasions (Taubenheim, 1957). But information on electron density changes above the D region, during solar flares, is rather incomplete, largely because of absorption in the D region.

Solar flare phenomena were observed in an extreme form during the famous event of February 23, 1956. A few minutes after the start of the flare, which was accompanied by an intense SID on the sunlit side of the earth, a worldwide increase of cosmic rays was observed and strong D region disturbances occurred in the dark hemisphere. Many papers on this event have appeared, and a summary of the observations has been given by Bailey (1959).

During the main phase of storms, the lower ionosphere is not drastically affected at middle latitudes. There is some evidence that the

critical frequency f_oE is depressed by a few percent (Sato, 1957). D region absorption is almost unaffected, but there are abnormal diurnal variations of amplitude and phase of low frequency waves (<300 kc/s) reflected from the ionosphere (Bracewell et al, 1953). Belrose has found that these persist for two weeks or more after the storm (Ratcliffe and Weekes, 1960), and similar long-lived phenomena have been reported after a nuclear explosion (Brady et al, 1964). Thus, the D region may possess a long time constant for recovery from storm effects.

An early description of high-latitude storm effects was based on observations at Tromsö during the Second Polar Year of 1932/33 (Appleton et al, 1937). In recent years, much study has been devoted to the distribution of "polar blackouts" and storm sporadic E, using routine tabulations of ionospheric parameters such as f_oEs and f_{min} (the minimum frequency at which ionospheric echoes are received, this being determined principally by absorption). The occurrence of these phenomena shows marked maxima at certain times of day, which vary from station to station. On polar maps plotted in magnetic coordinates, "isochrons" can be drawn to join points at which the maxima occur simultaneously (in Universal Time), and these are found to be spiral in form (Agy, 1954; Thomas, 1962). A similar spiral pattern has been found for magnetic activity at high latitudes (Nikol'skii, 1961), and for auroral activity.

Originally, these were interpreted as Störmer spirals, which are the locus of precipitation of charged particles originating in a distant source and deflected by the geomagnetic field (Störmer, 1917). If this were correct, then the sense of the spiral would indicate that blackouts and storm Es are produced by positively and negatively charged particles, respectively. However, it is now clear that Störmer's theory is not applicable to particles in the required range of energy, because their density must be high enough for interactions between particles to be important. The Störmer theory neglects such interactions and is probably valid only for high-energy cosmic ray particles whose motion is influenced only by the geomagnetic field. Instead, the explanation of the observed spirals has become a part of modern theories of geomagnetic storms.

3. Storm Effects in the F Region

Solar flare effects in the F layer have proved difficult to detect, and were considered to be absent by Berkner and Wells (1937). This probably implies that the effects produced by a flare lasting (say) half an hour are no larger than the random variations of N_mF2 in such a period, which might be 10 percent. Knecht and Davies (1961) have reviewed a few cases in which increases in N_mF2 have been observed. These increases range from 20 to 50 percent and generally disappear within about one hour. The Orbiting Solar Observatory recorded a 14 percent increase in the intensity of solar HeII 304 Å radiation during a fairly large (Class 3) flare (Lindsay, 1963), so the F2 layer effects may well be due to increased photoionization.

In contrast to these rather elusive flare effects, changes in the F layer during a storm are profound. The critical frequency f_oF1 is not greatly affected; Sato (1957) found a slight decrease of about 0.3 Mc/s (which implies a reduction of about 10 percent in N_mF1). We may take this to indicate that the production rate q is not greatly changed during a storm, as we might indeed expect. But the reduction of F2 layer electron density sometimes results in the F1 "cusp" becoming visible on ionograms at times when it would not normally be seen. This is probably due to the reduction of electron density in the overlying F2 layer, which would tend to make the F1 ledge more conspicuous, as we discussed in Sec. III-4.

During storms, the h'(f) curves for the F2 layer are greatly changed. The critical frequencies f_oF2 are usually reduced and the virtual heights h' greatly increased, sometimes attaining values of 600 km or more. These were originally thought to indicate real changes in the height of the F2 layer, but this interpretation was shown to be false when the N(h) profiles were computed (Thomas and Robbins, 1958). The real height of the F2 layer is actually the same, to within about ±20 km, on storm days and quiet days. The great virtual heights occur because the disturbed electron density distributions are such that the virtual height integral, $h' = \int \mu'(f,N)\, dh$, takes very large values. We say that the waves reflected from the F2 layer suffer very large

"group retardation" below the height of reflection. If follows that increase of h'F2 should be regarded only as a sensitive indicator of F layer disturbance. Many authors have used semiempirical measures of F2 layer height (deduced from ionograms by assuming parabolic N(h) profiles, or from published maximum-usable frequencies), but it is not clear that these parameters give reliable information about h_mF2.

The storm changes in f_oF2 can be analyzed in terms of the SD and Dst variations originally applied to magnetic parameters. This was done by Martyn (1953x; 1953y), and a more extensive analysis was carried out by Matsushita (1959), who used data for 109 storms at 38 observatories situated in eight latitude zones. Matsushita's Dst curves are reproduced in Fig. 32.

In the Zones 1 - 3 (geomagnetic latitudes 45 deg to 60 deg) the Dst curves are positive for the first few hours and then become negative, reaching a greatest depression of 30 percent in N_mF2 (for strong storms) about 24 hr after the SC. In geomagnetic latitudes 20 deg to 45 deg, the "positive" phase lasts longer and the "negative" phase is weaker (~10 percent depression of N_mF2). In low latitudes, there is no negative phase and Dst is weakly positive (+5 percent to +10 percent in N_mF2) throughout the storm.

It seems therefore that ionospheric storms can be either positive or negative, according to whether N_mF2 is increased or decreased from mean quiet day values. Positive storms appear to be more common in winter (Sato, 1957). Negative storms generally possess an initial positive phase, so that the curves of Dst (N_mF2) possess a superficial resemblance to magnetic Dst(H) curves. However, we may note that the positive phase lasts longer in the N_mF2 variation than in the magnetic field variation. Some detailed studies have been presented by Appleton and Piggott (1952), by J. W. King (1961) and by Benkova (1961). Generally, the greatest depressions of N_mF2 are observed on the day after the greatest disturbance of the magnetic field.

In addition to the Dst components, there are SD (local-time) components of the variation, which display fairly complicated changes of amplitude and phase, especially during the earlier parts of the storm, but gradually die away in the recovery phase.

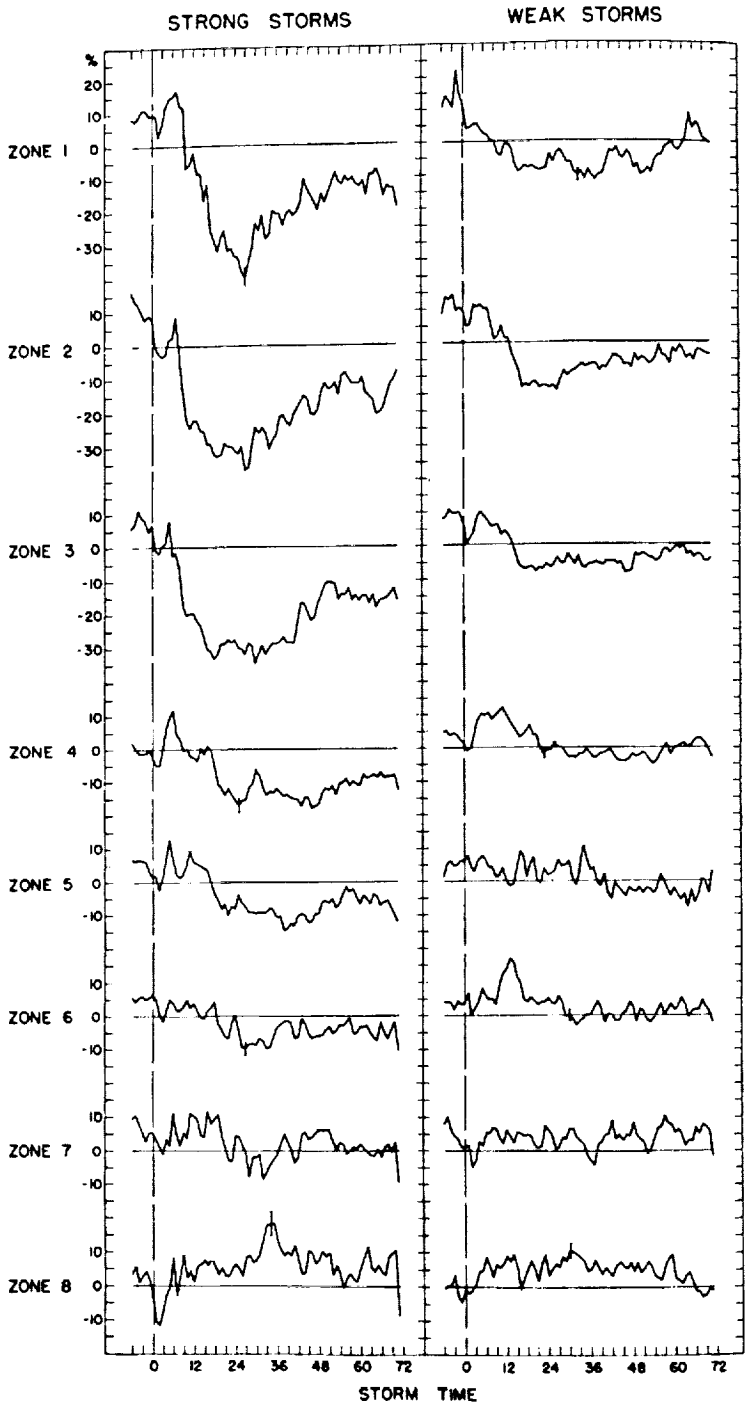

FIG. 32. Dst VARIATIONS OF N_mF2 IN EACH OF EIGHT LATITUDE ZONES FOR STRONG AND WEAK MAGNETIC STORMS WHICH EXHIBIT SUDDEN COMMENCEMENTS. The ordinate is the approximate percentage deviation from the quiet day behavior vs storm time. The zone number is shown in parenthesis between the applicable geomagnetic latitudes: 60°(1)55°(2)50°(3)45°(4)40°(5)30°(6)20°(7)10°(8) -10° (Matsushita, 1959).

Satellite and moon-echo observations show that the total electron content $\int Ndh$ is generally reduced during storms, though probably to a lesser extent than the peak electron density (Lawrence et al, 1963). This would imply that the F2 layer is slightly thicker during storms, although Titheridge (1964) finds little change. The reduction of total electron content was extremely pronounced during a severe storm in November 1960 (Taylor, 1961). In addition, the electron content increased much more slowly after sunrise on the disturbed day than on quiet days. It had previously been known that $dN(h)/dt$ and dN_m/dt were reduced during storms, and the total content observations show that the reduction cannot be interpreted in terms of a mere redistribution of ionization. Therefore, the observations suggest that the storm interfered with the F2 layer photochemical processes in some manner. However, the prime cause of these effects must be explained by more comprehensive theories of geomagnetic storms (Sec. VII-4).

These F region storm effects present many unsolved problems. We can do no more than review briefly some possible explanations, which include "thermal expansion," "photochemical changes" and "electromagnetic drift" theories. Very possibly, all of these contribute to F layer storm phenomena.

Early papers (Berkner, Wells and Seaton, 1939) attributed the depression of electron density to thermal expansion of the F region, this being largely suggested by the increase of F2 layer virtual height, which is now known to be misleading. Although satellite drag studies have shown that the atmosphere is indeed heated during storms, this explanation is probably inadequate, and could not account for the occurrence of positive storms in which N_mF2 increases. A more recent discussion has been given by Matuura (1963).

Thermal expansion of the F region would be expected to cause some increase in h_mF2 and a modest decrease in N_mF2. If it were the main process, there should then be a correlation between the storm changes of N_mF2 and h_mF2 which has not, in fact, been shown to exist. In order to explain large decreases of N_m, it has been suggested that the loss coefficient is enhanced, either because of a postulated temperature

dependence of the ion-atom interchange coefficient (Yonezawa, 1963) or by changes of atmospheric composition which increase the proportion of molecular gases in the F region (Seaton, 1956; Kamiyama, 1960). Such a change might conceivably occur if dynamic processes in the vicinity of 100 km were enhanced such as to increase turbulence and raise the upper limit of mixing of molecular gases (O_2 and N_2) with atomic oxygen, as discussed by King (1962).

The drift theory of Martyn (1953y) attributes storm effects to electromagnetic movements, produced by the electric fields associated with the storm current systems. Although this seems quite a reasonable concept, the detailed calculations have not led to a really satisfactory model. This is because they resemble a complicated chain which contains weak links in the form of unproven assumptions. It has very much in common with the "dynamo theory scheme" of Fig. 27. The drift calculations can be divided into three main stages:

(a) Computation of ionospheric storm current systems from the magnetic data. This requires assumptions about the contribution of induced ground currents to the magnetic effects.

(b) Calculation of electric fields driving these currents, by inserting conductivities, and then the derivation of F region drift velocities by assuming transmission of the electric field up the geomagnetic field lines. On the simplest theory, these velocities are $\underline{v}_D = \underline{E}_S \times \underline{B}/B^2$.

(c) Insertion of the drift velocity $\underline{v}_D$ into the continuity equation and calculation of the resulting change of electron density. In general, the vertical component of $\underline{v}_D$ would be expected to produce the greatest effects, but these are likely to be modified by the effects of ion-drag (Baker and Martyn, 1953).

We do not further discuss (a) and (b) here, because the problems arising are very similar to those discussed earlier. One simplification exists, however, because the storm electric fields are unlikely to be produced by dynamo action, but are probably entirely electrostatic in nature, so that no separation of the field is necessary. Regarding (c), there have been considerable doubts about even the sense of changes of N produced by given drifts, because of the complexity of the F layer continuity equation. Maeda and Sato (1959) attributed the occurrence of positive and negative storms at different latitudes to a latitude-dependent combination of quiet day and storm (Sq and DS) drift velocities.

Complete solutions of the F2 layer continuity equation with time-varying drift, diffusion and photochemical processes, will doubtless be developed. One can obtain some idea of the effects of drifts quite simply. An upward drift transports ionization into a region of lower loss, thus prolonging the average lifetime of ionization. Thus, during the day, upward movements would certainly increase the total electron content $\int Ndh$, and would probably increase N_m. A downward movement would have opposite effects. At night, once a "stationary" layer were established, upward or downward movement would alter the effective rate of decay of the layer.

Some authors attribute ionospheric DS effects to DS currents, and ionospheric Dst effects to Dst ring-currents, the latter being suggested by the superficial similarity of typical Dst(H) and Dst ($N_m F2$) curves. In our opinion, the similarity may be accidental. Most of the Dst ring current is thought to flow at geocentric distances of several earth radii, and the presence of Dst current in the ionosphere has not been established. Because conductivities and production rates are different by day and by night, a periodically-varying drift velocity with average value of zero can produce an average non-zero change of electron density. In this way a periodic (DS) current system in the ionosphere can give rise to both Dst and DS effects in $N_m F2$. This is consistent with the argument that there are differences in the magnetic SD variations for ionospherically positive or negative storms (Rishbeth, 1963).

4. Theories of Geomagnetic Storms

In the last section, we saw that no detailed explanation yet exists of how the storm effects in the ionosphere arise. But the problem of accounting for the geomagnetic phenomena is perhaps more basic. We can only attempt to summarize some of the theories which have been advanced.

The most obvious features of the magnetic disturbance are the storm-time Dst decrease of the field, which can be represented by a ring current, and the auroral zone electrojets which belong to the DS current system. There is a case for saying that the electrojets are associated with the prime cause of the DS currents, and that DS currents outside

the auroral zone largely represent return flows of current which complete the circuit; though Akasofu and Chapman (1964) have presented evidence for a different view.

If the DS auroral electrojets are to be produced by wind-driven dynamo action within the atmosphere, there must exist very localized wind systems (with velocities ~1 km/s) or strong enhancements of ionospheric conductivity (Nagata and Fukushima, 1952; Cole, 1960). The latter seems more plausible, because the electron density in the auroral zone is certainly enhanced by ionization produced by incoming charged particles, especially during storms. In the absence of any other driving mechanism, the currents would have to be sustained by abstracting more power from the atmospheric tides than is absorbed under quiet conditions. Since the height-integrated current density in the jets is of order 3 amp/m for an intense storm, as compared to a quiet-day current density of 0.1 amp/m in the mid-latitude ionosphere, the increase in conductivity would have to be roughly 30:1 if no other driving mechanism existed. It is not clear whether the DS currents could arise purely by this means, without any active driving mechanism being present, so it seems reasonable to look for driving mechanisms within the auroral zones, or in the parts of the magnetosphere linked by field lines to the auroral zones. The review by Nagata (1963) discusses these possibilities.

The pioneer development of geomagnetic storm theory was carried out by Chapman and Ferraro (1931 and later papers). They solved idealized mathematical problems in relation to the interaction of neutral ionized streams projected from the sun with the geomagnetic dipole field. They found that oppositely charged particles tend to be deviated towards opposite sides of the earth; some particles might enter captured orbits and would give rise to a westward ring current far outside the earth. This might produce the Dst decrease of magnetic field, but it is not so clear how the DS current systems arise.

Though historically important, the Chapman-Ferraro theory is inadequate because it treats interplanetary space as a vacuum, ignoring both the ionized interplanetary matter, which may be regarded as an extension of the solar corona, and the conducting plasma in the earth's magnetosphere. Disturbances can be transmitted rapidly through the magnetosphere

in the form of hydromagnetic waves, and most modern theories use this idea in one form or another. There is little doubt that the magnetic SC is caused by the arrival of a shock wave preceding the solar plasma cloud, and is transmitted to the earth's surface as a hydromagnetic wave. Then the initial phase Dst increase of the geomagnetic field is ascribed to a sustained pressure exerted by the impinging solar stream.

In some theories, it is supposed that solar plasma streams interact with the magnetosphere as they sweep past it, and that the main phase Dst decrease and the DS current systems arise from the interaction. Thus, Piddington (1960) attributes the main phase Dst decrease to an outward force exerted on the geomagnetic field by the solar stream, which causes field lines to be drawn out into a geomagnetic "tail." He regards the DS fields as arising initially from transmission to the earth of hydromagnetic "twist" waves generated in the vicinity of the magnetopause.

Axford and Hines (1961) envisage a gigantic circulation in the magnetosphere, driven by frictional interaction with the solar wind at the magnetopause. Because the plasma is frozen to the magnetic field lines, the circulation takes the form of a "convection" of field lines, as described in Sec. VI-5. Figure 33 shows the proposed form of the electric equipotentials, which are also streamlines of the convective motion, in the earth's equatorial plane. The pattern at ionospheric heights is then obtained by mapping the streamlines along geomagnetic field lines.

The solar wind interaction generates turbulence in the outer magnetosphere, and the turbulent material is conveyed by the circulation into the interior of the magnetosphere. The regions in which turbulence is expected to be present, when mapped along magnetic field lines, correspond to a band which resembles the locus of peak magnetic and auroral activity, and the high-latitude ionospheric phenomena described in Sec. VII-2.

We have devoted some space to a description of the Axford and Hines theory, as its concepts overlap to some extent those of other theories. Nevertheless, there are essential differences between different theories which we have not attempted to bring out.

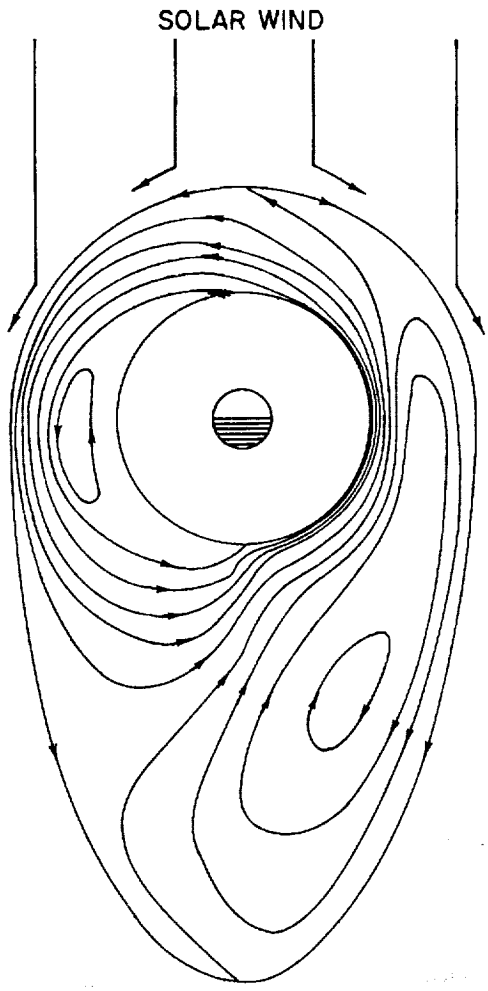

FIG. 33. STREAMLINES OF THE MAGNETOSPHERIC CONVECTION IN THE EARTH'S EQUATORIAL PLANE. The curves also represent electric equipotentials, and are obtained by combining a symmetrical pattern caused by interaction between the solar wind and the outer magnetosphere, and an asymmetric pattern caused by rotation of the magnetosphere. An additional circulation may exist in the inner magnetosphere (after Axford and Hines, 1961).

In reality, the magnetosphere contains not only the thermal plasma but also a wide spectrum of energetic particles. Low energy particles take part in the circulation, but high energy particles trapped in the geomagnetic field describe "mirror" orbits, and produce a "ring current" because they precess around the earth. Of course, no sharp distinction exists between "low" and "high" energies, though for rough calculations 1 kev might be taken as the dividing line. In principle, the precession

of energetic ions and electrons can give rise to a ring current which could produce the Dst field in the main phase of a storm. The mechanisms by which particles enter and escape from the belts form a very active field of experimental and theoretical research.

Kern (1962) has suggested that, should asymmetries exist in the distribution of charged particles, a separation of charge would occur which might be capable of producing the DS current system. The mechanism proposed by Fejer (1963) does not require any asymmetry, but requires the trapped radiation to contain a slight preponderance of particles of one sign (e.g., protons). Electrical neutrality of the magnetosphere as a whole is then preserved by a slight excess of oppositely charged particles (e.g., electrons) in the low energy plasma which takes part in the large-scale circulation of the magnetosphere. Because the paths of high-energy and thermal particles, when projected into the equatorial plane, are different, electric fields are set up, and are neutralized by flow of current along geomagnetic field lines and through the polar ionosphere. If the sign of the excess charges is as indicated above, the theory can qualitatively account for the flow of the polar electrojet current. More recently, Fejer (1964) has extended his analysis to the calculation of worldwide DS current systems resulting from this mechanism. Promising results have been obtained with a relatively crude model, in which diurnal variations of ionospheric conductivity are neglected.

We may safely say that, in spite of the great progress achieved in recent years, the problems posed by geomagnetic storms will remain of interest for many years to come. Indeed, the same can be said for upper atmosphere physics as a whole, as we have tried to show in this account.

BIBLIOGRAPHY

	Ref.
Abelson, P. H. and T. C. Hoering - "Carbon Isotope Fractionation in Formation of Amino Acids by Photosynthetic Organisms" Proc. Nat'l Acad. Sci. U. S., 47, 1961, p. 623.	Sec. I-2
Agy, V. - "Geographical and Temporal Distribution of Polar Blackouts" J. Geophys. Res., 59, 1954, pp. 499-512.	Sec. VII-2
Aikin, A. C. - "The Sunrise Absorption Effect Observed at Low Frequencies" Journal of Atmospheric and Terrestrial Physics, 23, Dec 1961, pp. 287-300.	Sec. IV-1
Aikin, A. C. and M. Nicolet - "The Formation of the D Region of the Ionosphere" Journal of Geophysical Research, 65, 5, May 1960, p. 1469.	Sec. I-4 Sec. III-4 Sec. IV-1 Fig. 20
Akasofu, S. and S. Chapman - "On the Asymetric Development of Magnetic and Storm Fields in Low and Middle Latitudes" Planet. Sp. Sci., 12, 1964, pp. 607-626.	
Akasofu, S. and S. Chapman - "The Ring Current, Geomagnetic Disturbance, and the Van Allen Radiation Belts" J. Geophys. Res., 66(5), 1961, pp. 1321-1350.	Sec. V-4
Allen, C. W. - "Critical Frequencies, Sunspots, and the Sun's Ultra Violet Radiation" J. Geophysical Research, 53, 1948, pp. 433-448.	Sec. IV-2 Sec. IV-4
Antonova, L. A. and Ivanov-Kholodnyy - "Corpuscular Hypothesis for the Ionization of the Night Ionosphere" Geomag. and Aeronomy (English Edition) USSR, 1(2), 1961, pp. 149-156.	Sec. III-3 Sec. IV-3
Appleton, E. V. and M. A. F. Barnett - "Local Reflection of Wireless Waves from the Upper Atmosphere" Nature, 115, 7 Mar 1925, pp. 333-334.	Sec. II-1
Appleton, E. V. - "A Note on the 'sluggishness' of the Ionosphere" Journal of Atmospheric and Terrestrial Physics, 3, 1953, pp. 282-284; Proc. Roy. Soc. A162, 1937, p. 451 (also).	Sec. IV-2 Sec. IV-4
Appleton, E. V., et al - "British Radio Observations during the Second International Polar Year" Phil. Trans. Roy. Soc., 236, 1937, pp. 191-259.	Sec. VII-2

Appleton, E. V. and M. A. F. Barnett - "On Some Direct Evidence for Downward Atmospheric Reflection of Electric Rays" Proc. Roy. Soc., 109, 1925, pp. 621-641. Sec. II-1

Appleton, E. V., et al - "The Detection of the S_q Current System in Ionospheric Radio Sounding" Journal of Atmospheric and Terrestrial Physics, 7, 4/5, Oct 1955, pp. 292-295. Sec. IV-2

Appleton, E. V. and W. R. Piggott - "Ionosphere Absorption Measurements during a Sunspot Cycle" J. Atmospheric and Terrestrial Physics, 5, 1954, pp. 141-172. Sec. IV-1

Appleton, E. V. and W. R. Piggott - "The Morphology of Storms in the F2-Layer of the Ionosphere. I. Some Statistical Relationships" J. Atmos. Terr. Phys., 2, 1952, pp. 236-252. Sec. VII-3

Arima, Y. and T. Yonezawa - "On the Seasonal and Non-Seasonal Annual Variations and the Semi-Annual Variations in the Noon and Midnight Electron Densities of the F2 Layer in Middle Latitudes" Journal Radio Res. Labs., 6, 1959, pp. 293-309. Sec. IV-3

Axford, W. I. - "The Formation and Vertical Movement of Dense Ionized Layers in the Ionosphere Due to Neutral Wind Shears" Journal of Geophysical Research, 68, 3, 1 Feb 1963, p. 769. Sec. IV-7

Axford, W. I. and C. O. Hines - "A Unifying Theory of High-Latitude Geophysical Phenomena and Geomagnetic Storms" Can. J. Phys., 39, 1961, pp. 1433-1464. Sec. VII-4 Fig. 3

Bailey, D. K. - "Abnormal Ionization in the Lower Ionosphere Associated with Cosmic-Ray Flux Enhancements" Proceedings of the IRE, 47, 2, Feb 1959, pp. 255-266. Sec. III-3 Sec. VII-2

Bailey, D. K., et al - "Radio Transmission at VHF by Scattering and other Processes in the Lower Ionosphere" Proc. IRE, 43, 1955, pp. 1181-1230. Sec. IV-6

Baker, W. G. - "Electric Currents in the Ionosphere. II. The Atmospheric Dynamo" Phil. Trans. Roy. Soc., A246, 1953, pp. 295-305. Sec. VI-4

Baker, W. G. and D. F. Martyn - "Conductivities of the Ionosphere" Nature, 170, 1952, pp. 1090-1092. Sec. VI-2

Baker, W. G. and D. F. Martyn - "Electric Currents in the Ionosphere. I. Conductivity" Phil. Trans. Roy. Soc., A246, 1953, pp. 281-294. — Sec. VI-2, Sec. VII-3

Balsley, B. B., et al - "Radio Echoes from Field-Aligned Ionization Above the Magnetic Equator and Their Resemblance to Auroral Echoes" J. of Geophys. Res., 65, 6, June 1960, pp. 1853-1855. — Sec. IV-7

Barron, D. W. and K. G. Budden - "The Numerical Solution of Differential Equations Governing the Reflexion of Long Radio Waves from the Ionosphere. III" Proc. Roy. Soc., A249, 1960, pp. 387-401. — Sec. IV-1

Barron, D. W., et al - "A Theory of Incoherent Scattering of Radio Waves by a Plasma. II. Scattering in a Magnetic Field" Proc. Roy. Soc., A263, 1961, pp. 238-258. — Sec. II-5

Barron D. W. and H. Rishbeth - "Equilibrium Electron Distributions in the Ionospheric F2 Layer" Journal of Atmospheric and Terrestrial Physics, 18, 2/3, Jun 1960, pp. 234-252. — Sec. III-6

Barrington, R. E. and E. Thrane - "The Determination of D-Region Electron Densities from Observations of Cross-Modulations" Journal of Atmospheric and Terrestrial Physics, 24, 1962, p. 31. — Sec. II-3

Bartels, J. and S. Chapman - "Geomagnetism" Clarendon Press - Oxford, 1940. — Sec. V-1, Sec. V-2, Sec. V-3, Sec. VI-3

Bartman, F. L., et al - "Upper-Air Density and Temperature by the Falling-Sphere Method," Journal of Applied Physics, 27(7), 1956, pp. 706-712. — Sec. 1-7

Bates, D. R. - "Charge Transfer and Ion-Atom Interchanging Collisions" Proc. Phys. Soc., A68, 1954, pp. 344-345. — Sec. III-3

Bates, D. R. - "A Suggestion Regarding the Use of Rockets to Vary the Amount of Atmospheric Sodium." Journal of Geophysical Research, 55, 1950, pp. 347-349. — Sec. 1-7

Bates, D. R. and M. Nicolet - "Ion-Atom Interchange" Journal of Atmospheric and Terrestrial Physic, 18, 1, Apr 1960, pp. 65-70. — Sec. III-4

Bauer, S. J. - "Some Implications of a Direct Measurement of the Hydrogen and Helium Ion Distribution in the Upper Atmosphere" Journal of Geophysical Research, 69, 3, Feb 1964, pp. 553-555. Sec. IV-3

Becker, W. and W. Dieminger - "Uber die Haufigkeit und die Struktur der E2-Schicht der Ionosphare" Naturwissenschaften, 31, 1950, pp. 90-91. Sec. IV-2

Bedinger, J. F., et al - "Study of Sodium Vapor Ejected into the Upper Atmosphere" Journal of Geophysical Research, 63(1), 1958, pp. 19-29. Sec. 1-7

Bellchambers, W. H. and W. R. Piggott - "The Ionosphere Over Halley Bay" Proc. Roy. Soc., 256, 1960, pp. 200-218. Sec. IV-3

Ben'kova, N. P. - "Ionospheric Investigations in the USSR" Geomagnetism & Aeronomy, I, 1, 1961, pp. 2-17. Sec. VII-3

Berkner, L. V., et al - "Ionospheric Effects Associated with Magnetic Disturbances" J. Geophys. Res., 44, 1939, pp. 283-311. Sec. VII-3

Berkner, L. V. and H. W. Wells - "Further Studies of Radio Fade-Outs" J. Geophys. Res., 42, 1937, pp. 301-309. Sec. VII-3

Bevan, H. C., et al - "A Long Term Variation in the Relationship of Sunspot Numbers to E-Region Character Figures" J. of Atmospheric and Terrestrial Physics, 21, 1961, pp. 167-173. Sec. VI-3

Beynon, W. J. G. and G. M. Brown - "Geomagnetic Distortion of Region-E" Journal of Atmospheric and Terrestrial Physics, 14, 1/2, Apr 1959, pp. 138-166. Sec. IV-2

Bhonsle, R. V. - "Study of Solar Flares using Cosmic Radio Noise on 25 Mc/s at Ahmedabad " Proc. Indian Acad. Sci., 51 (4), 1960, pp. 189-201. Sec. VII-2

Bibl, K., et al - "La Nomenclature Ionospherique et les Conventions pour le Depouillement" Journal of Atmospheric and Terrestrial Physics, 6, 2/3, Mar 1955, pp. 69-87. Sec. IV-7

Blumle, L. J. and R. J. Fitzenreiter - "Analysis of Topside Sounder Records" J. Geophys. Res., 69, 3 Feb 1964, pp. 407-415. Sec. II-2

Bowhill, S. A. - "The Formation of the Daytime Peak of the Ionospheric F2-Layer" Journal of Atmospheric and Terrestrial Physics, 24, June 1962, pp. 503-519. Sec. III-6

Bowhill, S. A. - "Statistics of a Radio Wave Diffracted by a Random Ionosphere" J. Res. NBS 65D (3), 1961, pp. 275-292. Sec. IV-6

Bowhill, S. A. - "The Effective Recombination Coefficient of an Ionosphere Containing a Mixture of Ions" Journal of Atmospheric and Terrestrial Physics, 20, 1, Feb 1961, pp. 19-30. Sec. IV-2 Sec. IV-5

Bowles, K. L. - "Incoherent Scattering by Free Electrons as a Technique for Studying the Ionosphere and Exosphere: Some Observations & Theoretical Considerations" J. of Research - National Bureau of Standards, 65D, 1, 1961, pp. 1-14. Sec. II

Bowles, K. L., et al - "Radio Echoes from Field-Aligned Ionization above the Magnetic Equator and Their Resemblance to Auroral Echoes" Journal of Geophysical Research, 65, 6, Jun 1960, p. 1853. Sec. IV-8

Bowles, K. L., et al - "On the Absolute Intensity of Incoherent Scatter Echoes from the Ionosphere" J. of Research, National Bureau of Standards, 66D, 4, 1962, pp. 395-407. Sec. II

Bowles, K. L. and T. E. Van Zandt - "Use of the Incoherent Scatter Technique to Obtain Ionospheric Temperatures" Journal of Geophysical Research, 65, 9, Sep 1960 pp. 2627-2628. Sec. II-5

Brace, L. H., et al - "Ionosphere Electron Temperature Measurements and Their Implications" Journal of Geophysical Research, 68, 19, 1 Oct 1963, p. 5397. Sec. IV-1

Bracewell, R. N. and W. C. Bain - "An Explanation of Radio Propagation at 16 KC/Sec in Terms of Two Layers below E-Layer" J. Atmospheric and Terrestrial Physics, 2, 1952, pp. 216-225. Sec. II-4 Fig. 8

Bracewell, R. N., et al - "The Ionospheric Propagation of Low- and Very-Low-Frequency Radio Waves over Distances Less than 1000 Km" Proc. Instn. Elect. Engrs., 98-III, 1951, pp. 221-236. Sec. IV-1 Sec. VII-2

Bracewell, R. N. and Owen K. Garriott - "Satellite Studies of the Ionization in Space by Radio" Advances in Geophysics, 8, Academic Press, 1961. Sec. II-3

Bracewell, R. N. and T. W. Straker - "The Study of Solar Flares by Means of Very Long Radio Waves" Mon. Not. R. Astr. Soc., 109, 1949, pp. 28-45. Sec. VII-2

Bradbury, N. E. - "Ionization, Negative-Ion Formation, and Recombination in the Ionosphere" Terrestrial Magnetism & Atmospheric Electricity, 43, 1, Mar 1938, pp. 55-66. Sec. III-5

Brady, A. H., et al - "Long-Lived Effects in the D Region after the High-Altitude Nuclear Explosion of July 9, 1962" J. of Geophysical Research, 69, 9, 1 May 1964, pp. 1921-1924. Sec. VII-2

Breit, G. and M. A. Tuve - "A Radio Method for Estimating the Height of the Ionosphere Conducting Layer" Nature, 116, 2914, 25 Sept 1925, p. 357. Sec. II-1

Briggs, B. H. - "The Diurnal and Seasonal Variations of Spread-F Ionospheric Echoes and the Scintillations of a Radio Star" Journal of Atmospheric and Terrestrial Physics, 12, 2/3, 1958, pp. 89-99. Sec. IV-7

Briggs, B. H. - "Observations of Radio Star Scintillations and Spread-F Echoes over a Solar Cycle" Journal of Atmospheric and Terrestrial Physics, 26, 1, Jan 1964, pp. 1-23. Sec. IV-6

Briggs, B. H., et al - "The Analysis of Observations on Spaced Receivers of the Fading of Radio Signals" Proc. Phys. Soc., 63, 1950, pp. 106-121. Sec. IV-6

Briggs, B. H. and H. Rishbeth - "An Analogue Solution of the Continuity Equation of the Ionospheric F Region" Proc. Phys. Soc., 78, March 1961, pp. 409-422. Sec. III-6

Briggs, B. H. and M. Spencer - "Horizontal Movements in the Ionosphere" Rep. Progr. Phys., 17, 1954, pp. 245-280. Sec. IV-6 Sec. VI-4

Brown, J. and E. J. Schaefer - "Additional Rocket-Borne Mass Spectrometer Measurements of the Dissociation of Oxygen" Journal of Geophysical Research, 69, 1 April 1964, pp. 1455-1456. Sec. I-4

Budden, K. G. - "A Method for Determining the Variation of Electron Density with Height (N(z) curves) from Curves of Equivalent Height Against Frequency (h',f) curves)," The Physics of the Ionosphere, Phys. Soc., 1955. Sec. II-2

Budden, K. - Phys. Soc. Ionosphere Conf. 1955, p. 332 — Sec. II-2

Bureau, R. - "Abnormalities of the Ionosphere and Bright Solar Eruptions" Nature, 139, 1937, pp. 110-111. — Sec. VII-2

Butler, S. T. and K. A. Small - "The Solar Semidiurnal Atmospheric Oscillation" Journal of Geophysical Research, 66, 11,Nov 1961, pp. 3723-3725; Proc. Roy. Soc. A274, 1963, p. 91. — Sec. VI-1

Byram, E. T., et al - "Attempt to Measure Night Helium Glow - Evidence for Metastable Molecules in the Ionosphere" Journal of Geophysical Research, 66, 7, Jul 1961, p. 2095. — Sec. IV-3

Calvert, W. and R. Cohen - "The Interpretation and Synthesis of Certain Spread-F Configurations Appearing on Equatorial Ionograms" J. of Geophys. Res., 66, 10, Oct 1961, pp. 3125-3140. — Sec. IV-6

Calvert, W. and G. B. Goe - "Plasma Resonances in the Upper Ionosphere" J. Geophys. Res., 68, 22, Nov 1963, pp. 6113-6120. — Sec. II-2

Calvert, W. and C. W. Schmid - "Spread-F Observations by the Alouette Topside Sounder Satellite" J. of Geophys. Res., 69, 9, 1 May 1964, pp. 1839-1852. — Sec. IV-6

Carleton, N. P. and L. R. Megill - "Excitation by Local Electric Fields in the Aurora and Airglow" J. Geophys. Res., 69, 1, Jan 1964, pp. 101-122. — Sec. VII-1

Chamberlain, J. W. - "Planetary Coronae and Atmospheric Evaporation" Planet. Space Sci., 11, 1963, pp. 901-960. — Sec. I-6

Chamberlain, R. T. - "Physics of Aurora and Airglow" Academic Press, New York, 1959. — Sec. III-4

Chamberlin, Rollin T. - "Geological Evidence on the Evolution of the Earth's Atmosphere" The Atmospheres of the Earth and Planets, ed. G. P. Kuiper, University of Chicago Press, 1949, pp. 250-259. — Sec. I-2

Champion, K. S. W. and S. P. Zimmerman - "Transport Processes in the Upper Atmosphere" Journal of Geophysical Research, 68, 10, 15 May 1963, p. 3049. — Sec. IV-8

Chapman, S. - "The Atmospheric Height Distribution of Band-Absorbed Solar Radiation" Proc. Phys. Soc. 51, 1939, pp. 93-109. Sec. III-2

Chapman, S. - "The Earth's Magnetism" Methuen Monograph (2nd ed.) 1951, p. 17. Sec. V-1

Chapman, S. - "The Electrical Conductivity of the Ionosphere: A Review" Nuovo Cimento, Suppl. 4, Series 10, 1956, pp. 1385-1412. Sec. VI-2

Chapman, S. - "Upper Atmospheric Nomenclature" J. Atmos. Terr. Phys., 1(2), 1950, pp. 121-124. Sec. I-1

Chapman, S. - "Solar Plasma, Geomagnetism and Aurora" Geophysics, the Earth's Environment, pp. 373-502. Sec. V-1

Chapman, S. - "The Outermost Ionosphere" Journal of Atmospheric and Terrestrial Physics, 15, 1/2, Sep 1959, pp. 43-47. Sec. I-5

Chapman, S. and V. C. A. Ferraro - "A New Theory of Magnetic Storms" Terrestrial Magnetism & Atmospheric Electricity, 36, 2, Jun 1931, p. 77. Sec. VII-4

Chapman, S. and M. Sugiura - "A Study of the Morphology of Magnetic Storms" Technical Reports from the Geophysical Institute, University of Alaska, 1956, 1958. Sec. VII-1

Charney, J. G. and P. G. Drazin - "Propagation of Planetary-Scale Disturbances from the Lower into the Upper Atmosphere" J. of Geophys. Res., 66, 1, Jan 1961, pp. 83-109. Sec. VI-1

Chivers, H. J. A. - "Observed Variations in the Amplitude Scintillations of the Cassiopeia (23N5A) Radio Source" Journal of Atmospheric and Terrestrial Physics, 19, 1, Sep 1960, pp. 54-64. Sec. IV-6

Chivers, H. J. A. and J. S. Greenhow - "Auroral Ionization and the Absorption and Scintillation of Radio Stars" Journal of Atmospheric and Terrestrial Physics, 17, 1/2, Dec 1959, pp. 1-12. Sec. IV-6

Cohen, R. and M. L. V. Pitteway - "A Waveguide Interpretation of 'Temperate-Latitude Spread F' on Equatorial Ionograms" J. of Geophys. Res., 66, 10, Oct 1961, pp. 3141-3156. Sec. IV-6

Cole, K. D. - "Eccentric Dipole Coordinates" Aust. J. Phys. 16(3), 1963, pp. 423-429. Sec. V-2

Cole, K. D. - "A Dynamo Theory of the Aurora and Magnetic Disturbance" Aust. J. Phys., 13, 1960, pp. 484-497. Sec. VII-4

Cole, K. D. - "Joule Heating of the Upper Atmosphere" Aust. J. Phys., 15, 1962, pp. 223-235. Sec. VII-1

Collins, C. and G. C. Reid - "Observations of Abnormal VHF Radio Wave Absorption at Medium and High Latitudes" J. Atmos. Terr. Phys., 14, 1958, pp. 63-81. Sec. VII-2

Cowling, T. G. - "The Electrical Conductivity of an Ionized Gas in a Magnetic Field, with Applications to the Solar Atmosphere and the Ionosphere" Proc. Roy. Soc., 183, Series A, 1945, pp. 453-470. Sec. VI-3

Crain, Cullen M. - "Ionization Loss Rates Below 90 Km" Journal of Geophysical Research, 66, 4, Apr 1961, pp. 1117-1126. Sec. III-4

Crawford, F. W. and R. F. Mlodnosky - "Langmuir Probe Response to Periodic Waveforms" J. of Geophysical Research, 69, 13, 1 Jul 1964, pp. 2765-2773. Sec. II

Croom, Robbins & Thomas - "blue book", Cavendish Laboratory Report, 1959a. Sec. IV Fig. 22

Croom, Sheila, et al - "Variation of Electron Density in the Ionosphere with Magnetic Dip" Nature, 185, 1960, pp. 902-903. Sec. IV-3

Croom, Sheila, et al - "Two Anomalies in the Behavior of the F2 Layer of the Ionosphere" Nature, 184, 1959, pp. 2003-2004. Sec. IV-3

Cummack, C. H. - "The Thermal Balance of the Ionospheric F-Region" Journal of Atmospheric and Terrestrial Physics, 24, Aug 1962, pp.691-699. Sec. I-5

Cummack, C. H. - "Extensions of the 'Chapman' Theory of Layer Formation" Journal of Geophysical Research, 66, 6, Jun 1961, p. 1685. Sec. III-2

Cummack, C. H. - "Evidence of Some Geomagnetic Control on the F1 Layer" Journal of Atmospheric and Terrestrial Physics, 22, 2, Oct 1961, pp. 157-158. Sec. IV-2

Dalgarno, A. - "Ambipolar Diffusion in the F-2 Layer" Journal of Atmospheric and Terrestrial Physics, 12, 2/3, 1958, pp. 219-220. Sec. III-5

Davies, K. and R. W. Knecht - "Solar Flare Effects in the F Region of the Ionosphere" Nature, 190, 27 May 1961, pp. 797-798. Sec. VII-3

Dellinger, J. H. - "Sudden Ionospheric Disturbances" J. Geophys. Res., 42, 1937, pp.49-53. Sec. VII-2

de Mendonca, F. and O. K. Garriott - "A Comparison of Methods Used for Obtaining Electron Content from Satellite Observations" J. Geophys. Res., 68 (17), 1963, pp. 4917-4927. Sec. II-3

Dessler, A. J. - "Ionospheric Heating by Hydromagnetic Waves" J. Geophys. Res.,64, 1959, pp. 397-401. Sec. VII-1

Dieminger, W. - "Uber Die Ursache der Excessiven Absorption in der Ionosphare an Wintertagen" Journal of Atmospheric and Terrestrial Physics, 2, 1952, pp. 340-349. Sec. IV-1

Dieminger, W. - "Transient Fine Structure of the E-Layer" Journal of Atmospheric and Terrestrial Physics, 16, 1/2, Oct 1959, p. 179. Sec. IV-2

Donahue, T. M. and G. E. Thomas - "Lyman α Scattering in the Earth's Hydrogen Geocorona, 2" J. of Geophys. Res., 68, 9, 1 May 1963, pp. 2661-2667; Planet. Space Sci., 10, 1963, pp. 65-72. Sec. I-6

Dougherty, J. P. - "On the Influences of Horizontal Motion of the Neutral Air on the Diffusion Equation of the F-Region" J. Atmos. and Terr. Phys., 20, 1961, pp. 167-176. Sec. III-5

Dougherty, J. P. and D. T. Farley - "A Theory of Incoherent Scattering of Radio Waves by a Plasma" Proc. Roy. Soc., A259, 1960, pp. 79-99. Sec. II-5

Dragt, A. J., et al - "The Attenuation of Hydromagnetic Waves in the Ionosphere" Planet. Space Sci., 9, 1962, pp. 771-785. Sec. VII-1

Duncan, R. A. - "The Behavior of a Chapman Layer in the Night F2 Region of the Ionosphere, Under the Influence of Gravity, Diffusion and Attachment" Aust. J. Phys., 9, 1956, pp. 436-439. Sec. III-6

Duncan, R. A. - "The Equatorial F-Region of the Ionosphere" Journal of Atmospheric and Terrestrial Physics, 18, 2/3, Jun 1960, pp. 89-100. Sec. IV-3

Duncan, R. A. - "Photometric Observations of 5577A and 6300A Airglow during the IGY" Aust. J. Phys., 13, 1960, pp. 633-637. Sec. III-4

Dungey, J. W. - "The Effect of Ambipolar Diffusion in the Night-time F Layer" Journal of Atmospheric and Terrestrial Physics, 9, 2/3, Aug/Sep 1956, pp. 90-102. Sec. III-6

Dungey, J. W. - "The Influence of Geomagnetic Field on Turbulence in the Ionosphere" Journal of Atmospheric and Terrestrial Physics, 8, 1/2, Feb 1956, pp. 39-42. Sec. IV-7

Egan, R. D., et al - "The IGY Three-Frequency Backscatter Sounder" Proc. IRE, 47(2), 1959, pp. 300-314. Sec. IV-7

Elford, W. G. - "A Study of Winds Between 80 and 100 km in Medium Latitude" Planetary Space Sci. 1, 1959, pp. 94-101. Sec. VI-4

Ellison, M. A. - "The Hα Radiation from Solar Flares in Relation to Sudden Enhancements of Atmospherics on Frequencies Near 27 kc/s" J. Atmos. Terr. Phys., 4, 1953, pp. 226-239. Sec. VII-2

Elterman, Louis - "The Measurement of Stratospheric Density Distribution with the Searchlight Technique" Terr. Mag., 56(4), 509, 1951. Sec. 1-7

Elterman, Louis - "Seasonal Trends of Temperature, Density and Pressure to 67.6 km Obtained with the Searchlight Probing Technique" Terr. Mag., 59 (3), p. 351, 1954. Sec. I-7

Elwert, Gerhard - "The Distribution of X-rays Emitted by the Solar Corona and the Residual Intensity during Solar Eclipses" Journal of Atmospheric and Terrestrial Physics, 12, 2/3, 1958, pp. 187-199. Sec. IV-5

Epstein, E. S. and C. Young - "Atomic Oxygen in the Polar Winter Mesosphere[1,2]" J. of the Atmospheric Sciences, 19, 6, Nov 1962, pp. 435-443. Sec. IV-3

Evans, J. V. - "The Electron Content of the Ionosphere" J. Atmos. Terr. Phys., 11(4), 1957, pp. 259-271. Sec. II-3

Evans, J. V. - "Diurnal Variation of Temperature of the F Region" Journal of Geophysical Research, 67, 12, Nov 1962, pp. 4914-4920. Sec. II-5

Evans, J. V. and G. N. Taylor - "The Electron Content of the Ionosphere in Winter" Proc. Roy. Soc. A263, 1961, pp. 189-211. Sec. IV-3

Farley, D. T., Jr. - "A Theory of Electrostatic Fields in a Horizontally Stratified Ionosphere Subject to a Vertical Magnetic Field" J. Geophys. Res., 64, 1959, pp. 1225-1234. Sec. VI-3

Farley, D. T., Jr. - "Artificial Heating of the Electrons in the F Region of the Ionosphere" Journal of Geophysical Research, 68, 22, 15 Jan 1963, p. 401. Sec. II-5 Sec. IV-7

Faucher, G. A., et al - "Upper-Atmosphere Density Obtained from Measurements of Drag on a Falling Sphere" Journal of Geophysical Research, 68(11), 1963, pp. 3437-3450. Sec. I-7

Fejer, J. A. - "Semidiurnal Currents and Electron Drifts in the Ionosphere" J. Atmos. Terr. Phys. 4, 1953, pp. 184-203. Sec. VI-4

Fejer, J. A. - "Theory of the Geomagnetic Daily Disturbance Variations" J. Geophys. Res., 69, 1, Jan 1964, pp. 123-137. Sec. VII-4

Fejer, J. A. - "Theory of Auroral Electrojets" J. Geophys. Res., 68, 8, Apr 1963, pp. 2147-2157. Sec. VII-4

Fejer, J. A. - "The Interaction of Pulsed Radio Waves in the Ionosphere" Journal of Atmospheric & Terrestrial Physics, 7, 1955, p. 222. Sec. II-3

Fejer, J. A. - "Scattering of Radio Waves by an Ionized Gas in Thermal Equilibrium" Canadian Journal of Physics, 38, 1960, pp. 1114-1133. Sec. II-5

Ferraro, V. C. A. - "Diffusion of Ions in the Ionosphere" Terrestrial Magnetism & Atmospheric Electricity, 50, 1945, pp. 215-222. Sec. III-5

Ferraro, V. C. A. - "The Coefficient of Diffusion of Ions in the F2 Regions" Journal of Atmospheric and Terrestrial Physics, 11, 1957, pp. 296-298. Sec. III-5

Fooks, G. F. - "Ionospheric Irregularities and the Phase Paths of Radio Waves" J. of Atmos & Terrestrial Physics, 24, Nov 1962, pp. 937-947. Sec. IV-6

Fooks, G. F. and I. L. Jones - "Correlation Analysis of the Fading of Radio Waves Reflected Vertically from the Ionosphere" Journal of Atmospheric and Terrestrial Physics, 20, 4, Apr 1961, pp. 229-242. Sec. IV-6

Friedman, H. - "The Sun's Ionizing Radiations" Physics of the Upper Atmosphere, ed. J. A. Ratcliffe, Academic Press, 1960, p. 134. Fig. 14 Sec. III

Gardner, F. F. and J. L. Pawsey - "Study of the Ionospheric D-Region Using Partial Reflections" Journal of Atmospheric and Terrestrial Physics, 3, 1953, pp. 321-344. Sec. II-3

Garriott, O. K. and H. Rishbeth - "Effects of Temperature Changes on the Electron Density Profile in the F2 Layer" Planetary and Space Science, 11, 6, Jun 1963, pp. 587-590. Sec. I-3 Sec. III-6

Gliddon, J. E. C. and P. C. Kendall - "A Mathematical Model of the F2 Region" Journal of Atmospheric and Terrestrial Physics, 24, Dec 1962, pp. 1073-1099. Sec. III-6

Gliddon, J. E. C. and P. C. Kendall - "The Effects of Diffusion and of Attachmentlike Recombination on the F2 Region" Journal of Geophysical Research, 65 8, Aug 1960, p. 2279. Sec. III-6

Gold, T. - "Motions in the Magnetosphere of the Earth" J. Geophys. Res., 64, 1959, pp. 1219-1224. Sec. VI-3 Sec. VII-4

Goldberg, R. A., et al - "Geomagnetic Control of the Electron Density in the F Region of the Ionosphere" J. of Geophys. Res., 69, 3, 1 Feb 1964, pp. 417-427. Sec. IV-3

Goody, R. M. and J. F. Noxon - "Observation of Day Airglow Emission" Journal of the Atmospheric Sciences, 19, 4, 1962, pp. 342-343. Sec. III-4

Gordon, W. E. - "Incoherent Scattering of Radio Waves by Free Electrons with Applications to Space Exploration by Radar" Proc. IRE, 46, 1958, pp. 1824-1829. Sec. II-4

Greenhow, J. S., et al - "The Electron Scattering Cross-Section in Incoherent Backscatter" Journal of Atmospheric & Terrestrial Physics, 25, 1963, p. 197. Sec. II-5

Hagfors, T. - "Density Fluctuations in a Plasma in a Magnetic Field, with Applications to the Ionosphere" J. Geophys. Res., 66(6), 1961, p. 1699. Sec. II-5

Hakura, Y. and T. Obayashi - "Enhanced Ionization in the Polar Ionosphere Associated with Geomagnetic Storms" J. Atmos. Terr. Phys., 18, 1960, pp. 101-122. Sec. VII-2

Hanson, W. - "Electron Temperatures in the Upper Atmosphere" Space Research, Proc. Int. Space Sci. Symp. 3rd, Washington, 1962, pp. 282-302. Sec. II-4

Hanson, W. B. - "Upper-Atmosphere Helium Ions" Journal of Geophysical Research, 67, 1, Jan 1962, pp. 183-188. Sec. III-5

Hanson, W. B., et al - "Atmospheric Density Measurements with a Satellite-Borne Microphone Gage" Journal of Geophysical Research, 67, 4, Apr 1962, p. 1375. Sec. I-7

Hanson, W. B. and I. B. Ortenburger - "The Coupling between the Protonosphere and the Normal F Region" Journal of Geophysical Research, 66, 5, May 1961, pp. 1425-1435. Sec. III-1 Sec. IV-3

Hanson, W. B. and T. N. L. Patterson - "Diurnal Variation of the Hydrogen Concentration in the Exosphere" Planetary and Space Science, 11, 9, Sep 1963, pp. 1035 1052. Sec. I-6 Sec. IV-3

Harris, I. and W. Priester - "Time-Dependent Structure of the Upper Atmosphere" Journal of the Atmospheric Sciences, 19, 4, 1962a, NASA, TN-D1444, 1962b. Sec. I-3 Sec. I-4 Fig. 3

Harris, Isadore and Wolfgang Priester - "Theoretical Models for the Solar-Cycle Variation of the Upper Atmosphere" Journal of Geophysical Research, 67, 12, Nov 1962, pp. 4585-4591. Sec. I-5 Sec. III-3

Haselgrove, Jenifer, et al - "The Electron Distribution in the Ionosphere over Slough - I. Quiet Days" Journal of Atmospheric and Terrestrial Physics, 12, 1958, pp. 46-56. Sec. II-2 Sec. IV-2 Sec. IV-3

Heisler, L. H. and G. H. Munro - "Divergence of Radio Rays in the Ionosphere" Aust. J. Phys., 9, 1956, pp. 359-372. Sec. IV-6

Heisler, L. H. and J. D. Whitehead - "Longitude Effect in Temperate Zone Sporadic E and the Earth's Magnetic Field" Nature, 187, 1960, pp. 676-677. Sec. IV-7

Heppner, J. P. and L. H. Meredith - "Nightglow Emission Altitudes from Rocket Measurements" Journal of Geophysical Research, 63, 1, Mar 1958, pp. 51-65. Sec. III-4

Herzberg, Luise- "The Possible Importance of Nitric Oxide Formation during Polar-Cap Ionospheric Absorption Events" Journal of Geophysical Research, 65, 10, Oct 1960, pp. 3505-3508. Sec. IV-1

Hewish, A. - "The Diffraction of Radio Waves in Passing through a Phase-Changing Ionosphere" Proc. Roy. Soc., A209, 1951, pp. 81-96. Sec. IV-6

Hewish, A. - "The Diffraction of Galactic Radio Waves as a Method of Investigating the Irregular Structure of the Ionosphere" Proc. Roy. Soc., A214, 1952, pp. 494-514. Sec. IV-6

Hines, C. O. - "Internal Atmospheric Gravity Waves at Ionospheric Heights" Canad. J. Phys., 38, 1960, pp. 1441-1481. Sec. IV-6

Hines, C. O. - "The Formation of Midlatitude Sporadic E Layers" J. of Geophys. Res., 69, 5, 1 Mar 1964, pp. 1018-1019. Sec. IV-7

Hinteregger, H. E. and K. Watanabe - "Photoionization Rates in the E and F Regions" Journal of Geophysical Research, 67, 3, Mar 1962, p. 999. Sec. III-2 Sec. III-3

Hinteregger, H. E. and K. Watanabe - "Photoionization Rates in the E and F Regions, 2" Journal of Geophysical Research, 67, 9, Aug 1962, pp. 3373-3392 Sec. I-4 Fig. 13

Hirono, M. and T. Kitamura - "A Dynamo Theory in the Ionosphere" J. Geomag. Geoelec, 8, 1956, pp. 9-23. Sec. VI-3

Hirsh, A. J. - "The Electron Density Distribution in the F Region of the Ionosphere" Journal of Atmospheric and Terrestrial Physics, 17, 1/2, Dec 1959, pp. 86-95. Sec. III-4

Hoffman, J. H., et al - "Neutral Composition of the Atmosphere in the 100- to 200- Kilometer Range" Journal of Geophysical Research, 69, 5, 1 Mar 1964, p. 979. Sec. I-5

Holmes, Julian C., et al - "Ion Composition of the Arctic Ionosphere" Journal of Geophysical Research, 63, 2, Jun 1958, pp. 443-444. Sec. III-4

Holt, O. - "Some Experimental Studies of the Ionospheric D Region at High Latitudes" NDRE Report, 46, Jul 1963. Sec. II-3 Fig. 6

Hower, G. L. and A. M. Peterson - "Synchrotron Radiation from High Energy Electrons" Journal of Geophysical Research, 68, 3, 1 Feb 1963, p. 723. Sec. IV-8

Hulburt, E. O. - "Ionization in the Upper Atmosphere of the Earth" Phys. Rev., 31, 1928, pp. 1018-1037. Sec. III-5

Hulburt, E. O. and M. H. Johnson - "Diffusion in the Ionosphere" Phys. Rev., 79, 1950, pp. 802-807. Sec. III-5

Hultqvist, B. - "On the Height Distribution of the Ratio of Negative Ion and Electron Densities in the Lowest Ionosphere" Journal of Atmospheric and Terrestrial Physics, 25, 5, May 1963, pp. 225-240. Sec. IV-1

Hultqvist, Bengt and Johannes Ortner - "The Height of the Polar Cap Absorption Layer" Arkiv for Geofisik, 3, 1961, p. 419. Sec. IV-1

Hultqvist, B. and J. Ortner - "Strongly Absorbing Layers Below 50 Km" Planetary and Space Science, 1, 1959, pp. 193-204. Sec. IV-1

Hunt, D. C. and T. E. Van Zandt - "Photoionization Heating in the F Region of the Atmosphere" Journal of Geophysical Research, 66, 6, Jun 1961, pp. 1673-1682. Sec. I-5

Hynek, D. P. and V. C. Pineo - "Spectral Widths and Shapes and Other Characteristics of Incoherent Backscatter from the Ionosphere Observed at 440 Mc/s during a 24-Hour Period in May, 1961" J. Geophys. Res., 67(13), 1962, pp. 5119-5129. Sec. II-5

Jacchia, L. G. - "A Working Model for the Upper Atmosphere" Nature, 192, 23 Dec 1961, pp. 1147-1148. Sec. VII

Jacchia, Luigi G. - "A Variable Atmospheric Density Model from Satellite Accelerations" Journal of Geophysical Research, 65(9), 1960, pp. 2775-2782. Sec. I-5 Sec. I-7

Johnson, F. S. - "Pressure and Temperature Equalization at 200 km Altitude" Journal of Geophysical Research, 65(8), 1960, pp. 2227-2232. Sec. I-7

Johnson, C. Y., et al - "Ion Composition of the Arctic Ionosphere" J. Geophys. Res., 63(2), 1958, pp. 443-444. Sec. III Fig. 17

Kelso, J. M. - "A Procedure for the Determination of the Vertical Distribution of the Electron Density in the Ionosphere" Journal of Geophysical Research, 57, 1952, pp. 357-367. Sec. II-2

Kendall, P. C. - "Geomagnetic Control of Diffusion in the F2-Region of the Ionosphere" - I The Form of the Diffusion Operator, Journal of Atmospheric and Terrestrial Physics, 24, Sep 1962, pp. 805-811. Sec. III-5

Kent, G. S. - "High Frequency Fading of the 108 Mc/s Wave Radiated from an Artificial Earth Satellite as Observed at an Equatorial Station" J. Atmos. Terr. Phys., 22, 1961, pp. 255-269. Sec. IV-6

Kern, J. W. - "A Charge Separation Mechanism for the Production of Polar Auroras and Electrojets" J. of Geophysical Research, 67, 7, Jul 1962, pp. 2649-2665. Sec. VII-4

King, G. A. M. - "The Dissociation of Oxygen and High Level Circulation in the Atmosphere" J. of the Atmospheric Sciences, 21, 3, May 1964, pp. 231-237. Sec. IV-3

King, G. A. M. - "The Ionospheric F Region during a Storm" Planetary and Space Science, 9, 1962, pp. 95-100. Sec. VII-3

King, G. A. M. - "The Seasonal Anomalies in the F-Region" Journal of Geophysical Research, 66, 12, Dec 1961, pp. 4149-4154. Sec. IV-3

King, G. A. M. - "Relation Between Virtual and Actual Heights in the Ionosphere" Journal of Atmospheric and Terrestrial Physics, 11, 1957, pp. 209-222. Sec. II-2

King, J. W. - "Investigations of the Upper Ionosphere Deduced from Top-Side Sounder Data" Nature, 197, 16 Feb 1963, pp. 639-641. Sec. IV-3

King, J. W. - "Magnetic Effects in the F-Region of the Ionosphere" J. of Atmospheric & Terrestrial Physics, 21, 1961, pp. 26-34. Sec. VII-3

King-Hele, D. G. - "Improved Formulae for Determining Upper-Atmosphere Density from the Change in a Satellite's Orbital Period" Planetary and Space Science, 11, 3, Mar 1963, pp. 261-268. Sec. I-7

Knecht, R. W. - "Relationships between Aurora and Sporadic-E Echoes at Barrow, Alaska" Journal of Geophysical Research, 61, 1, Mar 1956, pp. 59-69. Sec. IV-7

Knecht, R. W. - "Observations of the Ionosphere over the South Geographic Pole" Journal of Geophysical Research, 64, 9, Sep 1959, pp. 1243-1250. Sec. IV-3

Knecht, R. W. and T. E. Van Zandt - "Some Early Results from the Ionospheric Top-Side Sounder Satellite" Nature, 16 Feb 1963, pp. 641-644. Sec. IV-3

Koster, J. R. and R. W. Wright - "Scintillation, Spread F, and Transequatorial Scatter" Journal of Geophysical Research, 65, 8, Aug 1960, p. 2303. Sec. IV-6

Kuiper, G. P. - "Survey of Planetary Atmospheres" The Atmospheres of the Earth and Planets, ed. G. P. Kuiper, University of Chicago Press, 1949, pp. 304-345. Sec. I-2

Lagow, H. E., et al - "Arctic Atmospheric Structure to 250 km" Planetary Space Sciences, 2, 1959, pp. 33-38. Sec. I-7

Lawrence, R. S., et al - "The Total Electron Content of the Ionosphere at Middle Latitudes near the Peak of the Solar Cycle" J. of Geophys. Res., 68, 7, 1 Apr 1963, pp. 1889-1898. Sec. II

Lawrence, R. S., et al - "A Survey of Ionospheric Effects upon Earth-Space Radio Propagation" Proc. IEEE 52(1), 1964, pp. 4-27. Sec. IV-6

Lerfald, G. M., et al - "Derivation of Electron-Density Profiles in the Lower Ionosphere Using Radio Absorption Measurements at Multiple Frequencies" Journal of Geophysical Research, 68, 12, Jun 1963, pp. 3581-3588. Sec. II-3

Little and Leinbach - "Some Measurements of High-Latitude Ionospheric Absorption Using Extra-terrestrial Radio Waves" Proc. IRE, 46, 1958, p. 334; Proc. IRE, 47, 1959, pp. 315-320. Sec. II-3

Little, C. G., et al - "Origin of the Fluctuations in the Intensity of Radio Waves from Galactic Sources" Nature, 165, 1950, pp. 422-423. Sec. IV-6

Lockwood, G. E. K. and G. L. Nelms - "Topside Sounder Observations of the Equatorial Anomaly in the 75° W Longitude Zone" J. of Atmos. & Terrest. Physics, 26, 5, May 1964, pp. 569-580. Sec. IV-3

Long, A. R., et al - "The Calculation of Electron Density Profiles from Topside Sounder Records" Journal of Geophysical Research, 68, 10, 15 May, p. 3237. Sec. II-2

Lusignan, B. - "Cosmic Noise Absorption Measurements at Stanford, California and Pullman, Washington" Journal of Geophysical Research, 65, 12, Dec 1960, pp. 3895-3902. Sec. II-3

Lyon, A. J. - "Diffusion of Ionization in a Dipole Field" Journal of Geophysical Research, 68, 9, 1 May 1963, pp. 2531-2540. Sec. III-5

Lyon, A. J., et al - "Diffusion in the Equatorial F Layer" Journal of Geophysical Research, 68, 9, 1 May 1963, pp. 2559-2569. Sec. IV-3

Lyon, A. J. and L. Thomas - "The F2-Region Equatorial Anomaly in the African, American and East Asian Sectors during Sunspot Maximum" Journal of Atmospheric and Terrestrial Physics, 25, 7, Jul 1963, pp. 373-386. Sec. IV-3

Maeda, K. and T. Sato - "The F Region during Magnetic Storms" Proc. IRE, 47, 1959, pp. 232-239. Sec. VII-3

Mange, P. "The Distribution of Minor Ions in Electrostatic Equilibrium in the High Atmosphere" Journal of Geophysical Research, 65, 11, Nov 1960, p. 3833. Sec. III-5

Mange, P. - "The Theory of Molecular Diffusion in the Atmosphere" Journal of Geophysical Research, 62, 2, Jun 1957, p. 279. Sec. I-4

Mange, P. and M. Nicolet - "The Dissociation of Oxygen in the High Atmosphere" Journal of Geophysical Research, 59, 1, Mar 1954, pp. 15-45. Sec. I-4

Mariani, F. - "Sulla Diffusione Degli Elettroni Nella Ionosfera" Ann. Geofis, 9, 1956, pp. 219-231. Sec. III-5

Martin, H. A. and W. Priester - "Earth Satellite Observations and the Upper Atmosphere" Nature, 188, 15 Oct 1960, pp. 200-202. Sec. I-5

Martyn, D. F. - "Processes Controlling Ionization Distribution in the F2 Region of the Ionosphere" Aust. J. Phys., 9, 1956, pp. 161-165. Sec. III-6

Martyn, D. F. - "The Normal F Region of the Ionosphere" Proc. IRE, 47, 1959, pp. 147-155. Sec. IV-6

Martyn, D. F. - "Electric Currents in the Ionosphere. III. Ionization Drift due to Winds and Electric Fields" Phil. Trans. Roy. Soc., 246, 1953z, pp. 306-320. Sec. VI-2

Martyn, D. F. - "Atmospheric Tides in the Ionosphere. I. Solar Tides in the F2 Region" Proc. Roy. Soc., A189, 1947, pp. 241-260. Sec. VI-3

Martyn, D. F. - "Geo-Morphology of F2-Region Ionospheric Storms" Nature, 171, 1953x, p. 14. Sec. VII-3

Martyn, D. F. - "The Morphology of the Ionospheric Variations Associated with Magnetic Disturbance. I. Variations at Moderately Low Latitudes" Proc. Roy. Soc., 218, 1953y, pp. 1-18. Sec. VII-3

Matsushita, S. - "Lunar Effects on the Equatorial Es" Journal of Atmospheric and Terrestrial Physics, 10, 3, Mar 1957. pp. 163-165. Sec. IV-7

Matsushita, S. - "A Study of the Morphology of Ionospheric Storms" J. Geophys. Res., 64, 1959, pp. 305-321. Sec. VII-3 Fig. 2

Matsushita & Smith - "Ionospheric Sporadic E" Macmillan, New York, 1962. Sec. IV-7

Matuura, N. - "Thermal Effect on the Ionospheric F Region Disturbance" J. Radio Research Laboratories, 10, 47, 1963, pp. 1-35. Sec. VII-3

Meadows, Edith B. and J. W. Townsend, Jr. - "Diffusive Separation in the Winter Night Time Arctic Upper Atmosphere 112 to 150 Km" Ann. Geophys. 14N1, 1958, pp. 80-93. Sec. I-4

Millington, G. - "Ionization Charts of the Upper Atmosphere" Proc. Phys. Soc., 44, 1932, pp. 580-593. Sec. III-6

Minnis, C. M. - "Ionospheric Behaviour at Khartoum during the Eclipse of 25th February 1952" Journal of Atmospheric and Terrestrial Physics, 6, 2/3, Mar 1955, pp. 91-112. Sec. IV-5

Mitra, S. N. - "Geomagnetic Control of Region F2 of the Ionosphere" Nature, 158, 1946, pp. 668-669. Sec. IV-3

Moler, W. F. - "VLF Propagation Effects of a D-Region Layer Produced by Cosmic Rays" Journal of Geophysical Research, 65, 5, May 1960, p. 1459. Sec. IV-1

Moorcroft, D. R. - "On the Determination of Temperature and Ionic Composition by Electron Backscattering from the Ionosphere and Magnetosphere" Journal of Geophysical Research, 69(5), 1964, pp. 955-970. Sec. II-5

Muldrew, D. B. - "Radio Propagation along Magnetic Field-Aligned Sheets of Ionization Observed by the Alouette Topside Sounder" J. of Geophys. Res., 68, 19, 1 Oct 1963, pp. 5355-5370. Sec. IV-6

Munro, G. H. - "Anomalies on Ionosonde Records due to Traveling Ionospheric Disturbances" Journal of Geophysical Research, 62, 2, Jun 1957, p. 325. Sec. IV-6

Nagata, Takesi - "Polar Geomagnetic Disturbances" Planetary and Space Sci., 11, 12, Dec 1963, pp. 1395-1429. Sec. VII-4

Nagy, et al - "Direct Measurements Bearing on the Extent of Thermal Nonequilibrium in the Ionosphere" Journal of Geophysical Research, 68, 24, Dec 1963, pp. 6401-6412. Sec. II-4

Naismith, R. - "A Subsidiary Layer in the E Region of the Ionosphere" J. Atmos. Terr. Phys., 5, 1954, pp. 73-82. Sec. IV-7

Nawrocki and Papa - "Atmospheric Processes" Published by Geophysics Corp. of America, Aug 1961. Sec. III-4

Nelms, G. L. - "Scale Heights of the Upper Ionosphere from Top-Side Soundings" Canadian Journal of Physics, 41, 1, Jan 1963, pp. 202-206. Sec. II-2

Nicolet, Marcel - "Structure of the Thermosphere" Planetary and Space Science, 5, 1961, pp. 1-32. Sec. I-3 Sec. I-5 Sec. IV-1

Nicolet, Marcel and William Swider, Jr. - "Ionospheric Conditions" Planetary and Space Science, 11, 12, Dec 1963, pp. 1459-1482. Sec. III-4

Nier, Alfred O., et al - "Neutral Composition of the Atmosphere in the 100- to 200- Kilometer Range" J. Geophys. Res., 69(5), 1964, pp. 979-989. Sec. I-4 Fig. 4

Nikol'skiy, A. P. - "Geomagnetic Time as a Controlling Factor in the Development of Magnetic Disturbances" Geomagnetism & Aeronomy, 1, 6, 1961, pp. 830-832. Sec. VII-2

Nisbet, John S. - "Factors Controlling the Shape of the Upper F Region under Daytime Equilibrium Conditions" Journal of Geophysical Research, 68, 22, Nov 1963, pp. 6099-6112. Sec. III-6

Nisbet, John S. - "The Recombination Coefficient of the Nighttime F Layer" Journal of Geophysical Research, 68, 4, Feb 1963, pp. 1031-1038. Sec. IV-4 Fig. 23a,& b

Norton, R. B., et al - "A Model of the Atmosphere and Ionosphere in the E and F1 Regions" Proc. Int. Conf. on the Ionosphere; Inst. of Phys, and Phys. Soc. London, 1963, p. 26. Sec. IV Fig. 23a

Norton, R. B., et al - "Photochemical Rates in the Equatorial F_2 Region from the 1958 Eclipse" J. of Geophys. Research, 65, 7, Jul 1960, pp. 2003-2009. Sec. IV-5

Obayashi, T. - "Entry of High Energy Particles into the Polar Ionosphere" Rep. Ionosph. Res. Japan, 13, 1959, pp. 201-219. Sec. VII-2

Paul A. K. and J. W. Wright - "Some Results of a New Method for Obtaining Ionospheric N(h) Profiles and Their Bearing on the Structure of the Lower F Region" Journal of Geophysical Research, 68, 19, 1 Oct 1963, p. 5413. Sec. II-2

Pfister, W. and J. C. Ulwick - "The Analysis of Rocket Experiments in Terms of Electron Density Distributions" J. Geophys. Res., 63, 1958, pp. 315-333; Gringauz Dokl. Akad Nauk SSSR, 120, 1958, p. 1234. Sec. IV-7

Phillips, G. J. and M. Spencer - "The Effects of Anisometric Amplitude Patterns in the Measurement of Ionospheric Drifts" Proc. Phys. Soc, 68, 1955, pp. 481-492. Sec. IV-6

Piddington, J. H. - "Recurrent Geomagnetic Storms, Solar M-Regions and the Solar Wind" Planet. Space Sci., 12, 1964, pp. 113-118. Sec. VII-1

Piddington, J. H. - "Geomagnetic Storm Theory" J. of Geophys. Res., 65, 1, Jan 1960, pp. 93-106. Sec. VII-4

Pineo, V. C. - "Oblique-Incidence Measurements of the Heights at which Ionospheric Scattering of VHF Radio Waves Occurs" J. Geophys. Res. 61, 1956, pp. 165-169. Sec. IV-6

Pokhunkov, A. A. - "On the Variation in the Mean Molecular Weight of Air in the Night Atmosphere at Altitudes of 100 to 210 km from Mass Spectrometer Measurements" Planetary and Space Science, 11, 3, Mar 1963, pp. 297-304. Sec. I-4

Poppoff, I. G. and R. C. Whitten - "Associative Detachment in the D Region" Journal of Geophysical Research, 67, 3, Mar 1962, p. 1183. Sec. III-4

Poppoff, I. G. and R. C. Whitten - "Ion Kinetics in the Lower Ionosphere" J. Atmos, Sci., 21, 1964, p. 117. Sec. III-4

Purcell, J. D. - "The Profile of Solar Hydrogen-Lyman α" Journal of Geophysical Research, 65, 1, Jan 1960, pp. 370-372. Sec. I-6

Rabinowitch, E. I. - "Photo Synthesis & Related Processes" Interscience Publishers, Inc., N. Y., 1951. Sec. I-2

Rastogi, R. G. - "Thunderstorms and Sporadic E Layer Ionization" Indian J. Met. Geophys., 8, 1957, pp. 43-54. Sec. IV-7

Ratcliffe, J. A. - "The Magneto-Ionic Theory and its Applications to the Ionosphere" Cambridge University Press, 1959. Sec. II-2

Ratcliffe, J. A. - "Solar Eclipses and the Ionosphere" Spec. Suppl. to J. Atmospheric and Terrestrial Physics, 6, 1956, pp. 1-13. Sec. IV-5

Ratcliffe, J. A. - "The Formation of the Ionospheric Layers F-1 and F-2" Journal of Atmospheric and Terrestrial Physics, 8, 4/5, May 1956, pp. 260-269. Sec. III-4

Ratcliffe, J. A. - "The Magneto-Ionic Theory" Wireless Engr., 10, Cambridge University Press, 1959, pp. 354-363. Sec. II-2

Ratcliffe, J. A., et al - "The Rates of Production and Loss of Electrons in the F Region of the Ionosphere" Phil. Trans. Roy. Soc., 248, 1956, pp. 621-642. Sec. IV-4 Sec. IV-5

Ratcliffe, J. A. and K. Weekes - "The Upper Atmosphere" Ed. Ratcliffe, Academic Press, Ch. 9, 1960, p. 454.	Sec. IV-2 Sec. VII-2
Rees, Manfred H. - "Auroral Ionization and Excitation by Incident Energetic Electrons" Planetary and Space Science, 11, 10, Oct. 1963, pp. 1209-1218.	Sec. III-3 Sec. IV-1
Reid, G. C. - "A Study of the Enchanced Ionization Produced by Solar Protons during a Polar Cap Absorption Event" Journal of Geophysical Research, 66, 12, Dec. 1961, pp. 4071-4085.	Sec. III-4 Sec. IV-1
Rishbeth, H. - "Ionospheric Storms and the Morphology of Magnetic Disturbances" Planet. Space Sci., 11, 1963, pp. 31-43.	Sec. VII-3
Rishbeth, H. - "Further Analogue Studies of the Ionospheric F Layer" Proc. Phys. Soc., 81, 1963, pp. 65-77.	Sec. III-6
Rishbeth, H. - "A Time-Varying Model of the Ionospheric F2-Layer" Journal of Atmospheric & Terrestrial Physics, 26, 6, Jun 1964, pp. 657-685.	Sec. IV-3 Sec. IV-4 Sec. III-6 Table III
Rishbeth, H. and C. S. G. K. Setty - "The F-Layer at Sunrise" Journal of Atmospheric and Terrestrial Physics, 20, 4, Apr 1961, pp. 263-276.	Sec. III-2 Sec. IV-3 Sec. IV-4
Roach, F. E. and J. R. Roach - "Stable 6300 Å Auroral Arcs in Mid-Latitudes" Planet. Space Sci., 11, 1963, pp. 523-545.	Sec. VII-1
Roberts, J. A. and J. P. Wild - "Regions in the Ionosphere Responsible for Radio Star Scintillations" Nature, 178, 1956, pp. 377-378.	Sec. IV-6
Robbins, Audrey and J. O. Thomas - "The Electron Distribution in the Ionosphere over Slough. II. Disturbed Days" J. Atmos. Terr. Phys., 13, 1958, pp. 131-139.	Sec. VII-3
Robinson, B. J. - "Experimental Investigation of the Ionospheric E-Layer" Rep. Progr. Phys., 22, 1959, pp. 241-279.	Sec. IV-2
Rosenburg, N. W. - "Chemical Releases in the Upper Atmosphere (Project Firefly), A Summary Report" Journal of Geophysical Research, 68, 10, 15 May 1963, p. 3057.	Sec. I-4

Rothwell, P., et al - "Field Aligned Strata in the Ionization above the Ionospheric F_2 Layer" Nature, 198, 20 Apr 1963, pp. 230-233. — Sec. IV-3

Salpeter, E. E. - "Density Fluctuations in a Non-equilibrium Plasma" Journal of Geophysical Research, 68, 5, 1 Mar 1963, p. 1321. — Sec. II-5

Salpeter, E. E. - "Scattering of Radio Waves by Electrons above the Ionosphere" Journal of Geophysical Research, 65, 6, Jun 1960, p. 1851. — Sec. II-5

Sato, T. - "Disturbances in the F1 and E Regions of the Ionosphere Associated with Geomagnetic Storms" J. Geomag. Geoelect. (Kyoto), 9, 1957, pp. 57-60. — Sec. VII-2, Sec. VII-3

Sato, T. - "Disturbances in the Ionospheric F2 Region Associated with Geomagnetic Storms. II. Middle Latitudes" J. Geomag. Geoelect. (Kyoto), 9, 1957, p. 1-22. — Sec. VII-2, Sec. VII-3

Schmerling, E. R. - "An Easily Applied Method for the Reduction of h'-f Records to N-h Profiles Including the Effects of the Earth's Magnetic Field" Journal of Atmospheric and Terrestrial Physics, 12, 1958, pp. 8-16. — Sec. II-2

Seaton, M. J. - "A Possible Explanation of the Drop in F-Region Critical Densities Accompanying Major Ionospheric Storms" J. Atmos. Terr. Phys., 8, 1956, pp. 122-124. — Sec. VII-3

Seddon, J. C. - "Propagation Measurements in the Ionosphere with the Aid of Rockets" Journal of Geophysical Research, 58, 1953, pp. 323-335. — Sec. II-3

Shimazaki, T. - "Nighttime Variations of F-Region Electron Density Profiles at Puerto Rico" Journal of Geophysical Research, 69, 13, 1 Jul 1964, pp. 2781-2797. — Sec. IV-4

Shimazaki, T. - "World-Wide Measurements of Horizontal Ionospheric Drifts" Rep. Ionosph. Res. Japan, 13, 1959, pp. 21-47. — Sec. IV-6, Sec. VI-4

Shimazaki, T. - "Dynamical Structure of the Ionospheric F2 Layer" Journal Radio Res. Labs., 4, 1957, pp. 309-332. — Sec. III-5, Sec. III-6

Shimazaki, T. - "A Statistical Study of World-Wide Occurrence Probability of Spread-F" J. Radio Res. Labs., 6, 1959, pp. 669-704. — Sec. IV-7

Singleton, D. G. - "Spread-F and the Parameters of the F-Layer of the Ionosphere-I" J. of Atmos. and Terrest. Physics, 24, 1962, pp. 871-884. Sec. IV-6

Singleton, D. G. - "The Geomorphology of Spread F" J. of Geophys. Res., 65, 11, Nov 1960, pp. 3615-3624. Sec. IV-6

Skinner, N. J. and R. W. Wright - "The Effect of the Equatorial Electrojet on the Ionospheric E_s and F_2 Layers" Proc. Phys. Soc., B70, 1957, pp. 833-839. Sec. IV-8

Smith, L. G. - Abstract on "Rocket Measurements of Electron Density and Temperature in the Nighttime Ionosphere" J. Geophys. Res., 67, 1962, p. 1658. Sec. IV-7

Smith, E. K. and J. A. Thomas - "A Survey of the Present Knowledge of Sporadic E Ionization" J. Atmos. Terr. Phys., 13, 1959, pp. 295-314. Sec. IV-7

Spencer, et al - "Electron Temperature Evidence for Nonthermal Equilibrium in the Ionosphere" Journal of Geophysical Research, 67, 1, Jan 1962, p. 157. Sec. II-4

Sterne, T. E. - "High Altitude Atmospheric Density" Phys. Fluids, 1(3), 1958, pp. 165-170. Sec. I-7

Stewart, Balfour - In "Encyclopedia Britannica" 9th Ed. 1882, 36 pp. Sec. VI-1

Stormer, Carl - "Corpuscular Theory of the Aurora Borealis" Terrestrial Magnetism & Atmospheric Electricity, 22, 1917, pp. 23-97. Sec. VII-2

Stroud, W. G., et al - "Rocket-Grenade Measurements of Temperatures and Winds in the Mesosphere over Carchill, Canada" Journal of Geophysical Research, 65(8), 1960, pp. 2307-2323. Sec. I-7

Swenson, G. W., Jr. and K. C. Yeh - "The Scintillation of Radio Signals from Satellites " J. Geophys. Res., 64, 1959, pp. 2281-2286. Sec. IV-6

Takahashi, H. and T. Yonezawa - "On the Electron and Ion Density Distributions from the Lower Up to the Uppermost Part of thc F Region" Journal of the Radio Research Laboratories, 7, 32, Jul 1960, pp. 335-378. Sec. III-4 Fig. 23a

Taubenheim, J. - "On the Influence of Solar Flares on thc Ionospheric E-Layer" J. Atmos. Terr. Phys., 11, 1957, pp. 14-22. Sec. VII-2

Taylor, G. N. - "The Total Electron Content of the Ionosphere during the Magnetic Disturbance of November 12-13, 1960" Nature, 189, 4 Mar 1961, pp. 740-741. Sec. VII-3

Thomas, J. O. - "The Electron Density Distribution in the F_2 Layer of the Ionosphere in Winter" Journal of Geophysical Research, 68, 9, May 1963, pp. 2707-2718. Sec. IV-3

Thomas, J. O. - "The Distribution of Electrons in the Ionosphere" Proc. IRE, 47, 1959, pp. 162-175. Sec. II-2

Thomas, L. - "The Winter Anomaly in Ionospheric Absorption" Journal of Atmospheric and Terrestrial Physics, 23, Dec 1961, pp. 301-317. Sec. IV-1

Thomas, L. - "The Distribution of Dense E_S Ionization at High Latitudes" J. Atmos. & Terrestrial Physics, 24, Jul 1962b, pp. 643-658. Sec. IV-7 Sec. VII-2

Titheridge, J. E. - "Ionization Below the Night-Time F-Layer" Journal of Atmospheric and Terrestrial Physics, 17, 1/2, Dec 1959, pp. 126-133. Sec. IV-2

Titheridge, J. E. - "The Use of the Extraordinary Ray in the Analysis of Ionospheric Records" Journal of Atmospheric & Terrestrial Physics, 17, 1959, p. 110. Sec. II-2

Titheridge, J. E. - "A New Method for the Analysis of Ionospheric h'(f) Records" Journal of Atmospheric & Terrestrial Physics, 21, 1961, p. 1. Sec. II-2

Van Zandt, T. E., et al - "Photochemical Rates in the Equatorial F_2 Region from the 1958 Eclipse" Journal of Geophysical Research, 65, 7, Jul 1960, p. 2003. Sec. IV-4 Sec. IV-5

Vestine, E. H., et al - Carnegie Inst. Wash. Publ., 580, 1947. Sec. V-3

Warren, E. S. - "Some Preliminary Results of Sounding of the Top Side of the Ionosphere by Radio Pulses from a Satellite" Nature, 197, 16 Feb 1963, pp. 636-639. Sec. IV-3

Watts, J. M. - "Complete Night of Vertical-Incidence Ionosphere Soundings Covering Frequency Range from 50 Kc/s to 25 Mc/s" Journal of Geophysical Research, 62, 3, Sep 1957, p. 484. Sec. II-2

Webber, William - "The Production of Free Electrons in the Ionospheric D Layer by Solar and Galactic Cosmic Rays and the Resultant Absorption of Radio Waves" Journal of Geophysical Research, 67, 13, Dec 1962, pp. 5091-5106. — Sec. III-4, Sec. IV-1

Weekes, K. - "The Drift of an Ionized Layer in the Presence of the Geomagnetic Field" J. Atmos. Terr. Phys. Spec., Suppl. II, 1957, pp. 12-19. — Sec. VI-2

Weekes, K. and M. V. Wilkes - "Atmospheric Oscillations and the Resonance Theory" Proc. Roy. Soc., A192, pp. 80-99. — Sec. VI-1, Fig. 28

Whitehead, J. D. - "The Formation of the Sporadic-E Layer in the Temperate Zones" Journal of Atmospheric and Terrestrial Physics, 20, 1, Feb 1961, pp. 49-58. — Sec. IV-7

Wright, J. W. - "Diurnal and Seasonal Variations of the Atmosphere near the 100-Kilometer Level" J. of Geophys. Res., 69, 13, 1 Jul 1964, pp. 2851-2853. — Sec. IV-3

Wright, J. W. - "The F-Region Seasonal Anomaly" J. of Geophys. Res., 68, 14, 15 Jul 1963, pp. 4379-4381. — Sec. IV-3

Wright, J. W. - "Diurnal and Seasonal Changes in Structure of the Mid-Latitude Quiet Ionosphere" J. of Research of the National Bureau of Standards, 66D, 3, 1962, pp. 297-312. — Sec. IV-3

Wright, J. W. - "Ionosonde Studies of Some Chemical Releases in the Ionosphere" Radio Science J. of Research NBS/ USNC - URSI, 68D, 2, Feb 1964, pp. 189-204. — Sec. IV-8

Yerg, D. G. - "Notes on Correlation Methods for Evaluating Ionospheric Winds from Radio Fading Records" Journal of Geophysical Research, 60, 2, Jun 1955, pp. 173-185. — Sec. IV-5

Yerg, D. G. - "Observations and Analysis of Ionospheric Drift" J. Atmospheric and Terrestrial Physics, 8, 1956, pp. 247-259. — Sec. IV-6

Yonezawa, T. - "A New Theory of Formation of the F2 Layer" J. Radio Res. Labs., 3, 1956, pp. 1-16. — Sec. III-5, Sec. III-6

Yonezawa, T. - "On the Influence of Electron-Ion Diffusion Exerted upon the Formation of the F2 Layer" J. Radio Res. Labs., 5, 1958, pp. 165-187. — Sec. III-6

Yonezawa, T. - "On the Seasonal and Non-Seasonal Annual Variations and the Semi-Annual Variation in the Noon and Midnight Electron Densities of the F2 Layer in Middle Latitudes. II" J. Radio Res. Labs., 6, 1959, pp. 651-668. Sec. IV-3

Yonezawa, T. - "On the Physical Properties and Composition of the Upper Atmosphere between 100 and 400 Kilometers above Ground in Middle Latitudes" J. Radio Res. Labs., 7N30, 1960, pp. 69-84. Sec. I-3 Fig. 23a & b